

# Astronomical Detectors

supervisor ING: *Simon Tulloch, head of CCD group, optical detector specialist*  
professor: *Jan Kuijpers, Astrophysics Nijmegen*

Author: *Richard A. Hijmering*

September 18, 2002

# Chapter 1

## Preface

For my graduation in applied physics at the catholic university Nijmegen (KUN) I performed a 9 months student project under professor J. Kuijpers at the astrophysics department Nijmegen. This student project was divided into two parts. The first part, which lasted for 6 months, I perform a student project at the Isaac Newton Group of telescopes in La Palma. Here I was part of the detector group with Simon Tulloch as my supervisor. Under him I performed different quality control measurements to the CCD detectors for the telescopes. These quality control measurements involved linearity of the detectors, quantum efficiency of the detectors, the hold time of the cryostat and some properties of individual detectors. The second part I performed a 3 months project at ESTEC's STJ project with Jos de Bruijne as my supervisor. Here I have written a Quick Look Analytic Tool for the scam3 data in the IDL programming language. This tool is to be used with the next observing runs to look at the quality of the received data on site. For each experiment a report has been written. All these reports are combined in this paper as a total report of this project. The second part, which lasted for 3 months, I performed at ESTEC. I was part of the

In this document all the experiments I performed at Isaac Newton Group are discussed. Each chapter of this report is about one project performed by me. Each has its own theory, procedure, results and reference list. The references are labeled in the following manner [*first three letters of the authors name and the last two figures of the year it was published*] and can be found at the end of the chapter. All of the experiments discussed in the chapters are performed by me unless stated otherwise. For the theory of the detectors I used different references to obtain the information. The information from different references together with custom made images have been combined to produce the theory sections. Both the two parts of the paper begin with a theory about how the detector works. For the quality control measurements at the CCD detectors I used some custom written IRAF programs. The programming code can be found in the appendices. The reports are written for people who are not experts in astronomical detectors but do have a background in physics.

I want to express special tanks to professor Jan Kuijpers for the possibility of graduating under him, Danny Lennon for making it possible for me to come to ING in La Palma, Simon Tulloch for the great guidance and all the red ink and Jos de Bruijne for making it possible to come to ESTEC and answering all my thorough questions. At last I want to thank Celesta v. Os for standing behind me and tangling along to all the places I had to be, the same goes for Merak (El cato monstrouso).

# Contents

<b>1</b>	<b>Preface</b>	<b>1</b>
<b>2</b>	<b>The CCD</b>	<b>8</b>
2.1	Introduction . . . . .	8
2.2	How does it work . . . . .	9
2.2.1	Simple analogy . . . . .	9
2.2.2	The real stuff . . . . .	9
2.2.3	Photoelectric effect . . . . .	10
2.2.4	Electric field . . . . .	10
2.2.5	Transport of the charges . . . . .	11
2.2.6	Electronics . . . . .	12
2.3	CCD structure . . . . .	14
2.3.1	Back- and frontside CCD's . . . . .	16
2.3.2	Frame transfer chips . . . . .	17
2.3.3	Camera construction . . . . .	17
2.3.4	The controller . . . . .	18
2.3.5	The Data Acquisition System (DAS) . . . . .	18
2.3.6	IRAF . . . . .	19
2.4	Using the CCD . . . . .	19
2.4.1	Noise on the CCD . . . . .	19
2.4.2	Imaging . . . . .	20
2.4.3	Image defects . . . . .	21
2.5	The detectors of the Isaac Newton group . . . . .	23
2.6	References . . . . .	24
<b>3</b>	<b>Mapping of the defects in the SITe2 detector</b>	<b>25</b>
3.1	Summary . . . . .	25
3.2	Results . . . . .	26
<b>4</b>	<b>Dark current measurements on the Wide Field Camera after a 1 minute light flood</b>	<b>27</b>
4.1	Summary . . . . .	27
4.2	Theoretical background . . . . .	28
4.3	Procedure . . . . .	28
4.3.1	Script . . . . .	28
4.3.2	Measurement . . . . .	28
4.4	Results . . . . .	28
4.4.1	Script . . . . .	28
4.4.2	Measurement . . . . .	29
4.5	References . . . . .	29

<b>5</b>	<b>Linearity measurements of all the detectors at the Isaac Newton Group</b>	<b>30</b>
5.1	Summary . . . . .	30
5.2	Procedure . . . . .	31
5.2.1	Non-linearities . . . . .	31
5.2.2	Filters . . . . .	31
5.2.3	LED . . . . .	31
5.2.4	Linearity measurements . . . . .	31
5.3	Theoretical background . . . . .	32
5.4	Results . . . . .	33
5.4.1	Scripts . . . . .	33
5.4.2	Filters . . . . .	34
5.4.3	LED . . . . .	34
5.4.4	Linearity measurements [engw] . . . . .	35
5.4.5	Linearity of the detectors . . . . .	37
5.5	References . . . . .	38
<b>6</b>	<b>Quantum efficiency measurements of detectors at Isaac Newton Group</b>	<b>44</b>
6.1	Summary . . . . .	44
6.2	Theoretical background . . . . .	45
6.3	Procedure . . . . .	45
6.3.1	Stability measurement of the tungsten lamp source . . . . .	45
6.3.2	Quantum efficiency measurements . . . . .	46
6.4	Results [engw] . . . . .	46
6.4.1	The tungsten lamp . . . . .	46
6.4.2	SITe1 . . . . .	46
6.4.3	SITe2 . . . . .	47
6.4.4	TEK1 . . . . .	47
6.4.5	TEK5 . . . . .	47
6.5	References . . . . .	47
<b>7</b>	<b>Measuring the influence of the shutter at short exposures on the Jacobus Kapteyn Telescope</b>	<b>50</b>
7.1	Summary . . . . .	50
7.2	Procedure . . . . .	51
7.3	Results . . . . .	51
<b>8</b>	<b>Monitoring the bias level of several detectors</b>	<b>54</b>
8.1	Summary . . . . .	54
8.2	Procedure . . . . .	55
8.3	Results . . . . .	55
8.3.1	IRAF script . . . . .	55
8.3.2	Short term measurements . . . . .	55
8.3.3	Long term measurements . . . . .	56
8.3.4	Problems which came up during the measurements . . . . .	61
<b>9</b>	<b>Wide Field Camera control on the Isaac Newton Telescope</b>	<b>63</b>
9.1	Summary . . . . .	63
9.2	Theory . . . . .	64
9.2.1	Quantum efficiency . . . . .	64
9.3	Procedure . . . . .	64
9.3.1	Quantum efficiency Wide Field Camera autoguider . . . . .	64
9.3.2	Pressure . . . . .	65
9.4	Results . . . . .	65
9.4.1	Quantum Efficiency Measurements . . . . .	65
9.4.2	Pressure . . . . .	65

9.5	References . . . . .	67
<b>10</b>	<b>Temperature survey on the detectors of Isaac Newton Group</b>	<b>68</b>
10.1	Summary . . . . .	68
10.2	Electronics . . . . .	69
10.2.1	Temperature electronics within the detector . . . . .	69
10.3	Procedure . . . . .	69
10.3.1	Calibrating the platinum resistor . . . . .	69
10.3.2	Temperature measurement with the DVM . . . . .	69
10.3.3	Temperature test box . . . . .	69
10.4	Results . . . . .	70
10.4.1	Calibrating the platinum resistor . . . . .	70
10.4.2	Temperature measurements . . . . .	70
10.5	Consequences . . . . .	71
10.6	References . . . . .	71
<b>A</b>	<b>Useful reading</b>	<b>72</b>
A.1	Documents . . . . .	72
A.2	Weblinks . . . . .	72
<b>B</b>	<b>IRAF scripts</b>	<b>73</b>
B.1	IRAF script to find the defect on the SITe2 detector . . . . .	73
B.2	IRAF script to measure the darkcurrent . . . . .	75
B.3	IRAF script to find the maximum . . . . .	77
B.4	IRAF script to find the SUI value with a electron count nearest to 1000 electrons .	81
B.5	IRAF script to measure the linearity . . . . .	82
B.6	IRAF script for the linearity measurements . . . . .	84
B.7	An IRAF script to measure the biaslevels from the detectors. . . . .	86
B.8	IRAF script to measure the quantum efficiency of the auto guider of the wide field camera. . . . .	88
<b>C</b>	<b>Autoguider coating</b>	<b>92</b>
C.1	Thinning process . . . . .	92
C.2	References . . . . .	93
<b>D</b>	<b>Temperature circuitry</b>	<b>94</b>
D.1	Wire diagram of the temperature measurement circuitry . . . . .	94
D.1.1	Temperature electronics inside the detector . . . . .	94
D.1.2	Temperature electronics inside the controller . . . . .	94

# List of Figures

2.1	Simple analogy of a CCD matrix ( <i>image from: Introduction to CCD's, by Simon Tulloch</i> )	9
2.2	The CCD array configuration . . . . .	10
2.3	Electric potential inside a CCD chip . . . . .	11
2.4	MOS capacitor . . . . .	11
2.5	Row of pixels . . . . .	11
2.6	Transport mechanism of a three phase transfer. . . . .	12
2.7	The on-chip amplifier of the CCD chip. . . . .	12
2.8	Typicle video waveform (one period shown). . . . .	13
2.9	The Correlated Double Sampler. . . . .	13
2.10	General construction of a CCD chip. . . . .	14
2.11	Typical graph of the reflectivity with an optimum at 400 nm. . . . .	15
2.12	On the left hand side a frontside CCD is shown; on the right hand side a backside CCD is shown. In both figures the light comes from above. . . . .	16
2.13	A schematic figure of a frame transfer chip. The upper region is used to collect the image and the lower region, which is covered from light, is used as memory. . . . .	17
2.14	A CCD detector as used at Isaac Newton Group . . . . .	18
2.15	Procedure to combine the science image with the flatfield, biasframe and darkframe to get the best result. . . . .	22
3.1	Map of the defects on the SITe2 detector. . . . .	26
4.1	Darkcurrent decay in a period of 250 minutes. . . . .	29
5.1	Measurement rig used to measure the linearity of the different detectors (picture by <i>Simon Tulloch</i> ) . . . . .	32
5.2	Measurement rig used to measure the linearity of the LED source . . . . .	35
5.3	Error in linearity versus the flashtime in ms . . . . .	36
5.4	Linearity measurement of EEV11 in fast readout speed . . . . .	36
5.5	a) Linearity measurement of EEV10 in the fast readout speed. b) Linearity measurement of EEV10 in the slow readout speed . . . . .	37
5.6	a) Linearity measurement of EEV12 in the fast readout speed. b) Linearity measurement of EEV12 in the slow readout speed . . . . .	38
5.7	a) Linearity measurement of EEV13 in the fast readout speed. b) Linearity measurement of EEV13 in the slow readout speed. . . . .	39
5.8	a) Linearity measurement of wide field camera chip 1 in the fast readout speed. b) Linearity measurement of wide field camera chip 1 in the slow readout speed . . . . .	39
5.9	a) Linearity measurement of wide field camera chip 2 in the fast readout speed. b) Linearity measurement of wide field camera chip 2 in the slow readout speed . . . . .	40
5.10	a) Linearity measurement of SITe1 in the fast readout speed. b) Linearity measurement of SITe1 in the slow readout speed . . . . .	40
5.11	a) Linearity measurement of SITe2 in the fast readout speed. b) Linearity measurement of SITe2 in the slow readout speed . . . . .	41
5.12	a) Linearity measurement of TEK1 in the fast readout speed. b) Linearity measurement of TEK1 in the slow readout speed . . . . .	41

5.13	a) Linearity measurement of TEK2 in the fast readout speed. b) Linearity measurement of TEK2 in the slow readout speed, both measured by Simon Tyllöch . . . . .	42
5.14	a) Linearity measurement of TEK4 in the fast readout speed. b) Linearity measurement of TEK4 in the slow readout speed . . . . .	42
5.15	a) Linearity measurement of TEK5 in the fast readout speed. b) Linearity measurement of TEK5 in the slow readout speed . . . . .	43
5.16	Linearity measurement of TEK6 . . . . .	43
6.1	Quantum Efficiency rig in the detector lab located in the William Herschel Telescope	46
6.2	Stability of the QE source at a wavelength of 400 nm. . . . .	47
6.3	QE of the SITe1 detector. . . . .	48
6.4	QE of the SITe2 detector measured at 28-1-2002. . . . .	48
6.5	QE of the TEK1 detector. . . . .	49
6.6	QE of the TEK5 detector. . . . .	49
7.1	The jammed shutter on the Jacobus Kapteyn Telescope . . . . .	51
7.2	0.06 sec exposure . . . . .	52
7.3	0.08 sec exposure . . . . .	52
7.4	0.10 sec exposure . . . . .	52
7.5	0.51 sec exposure . . . . .	53
7.6	1.01 sec exposure . . . . .	53
8.1	a) bias level fluctuations of the wide field camera of the Isaac Newton Telescope over a period of 3 days. b) bias level fluctuations of the TEK4 detector over a period of 3 days. . . . .	56
8.2	a) bias level fluctuations of the SITe2 detector in fast readoutspeed over a period of 30 days. b) bias level fluctuations of the SITe2 detector in slow readout speed over a period of 5 days . . . . .	57
8.3	Bias level fluctuations of the wide field camera in fast readout speed over a period of 37 days. a) of chip 1. b) of chip 3. c) of chip 4. . . . .	58
8.4	The bias level data of the chip 2 of the wide field camera of the Isaac Newton Telescope. Lots of spikes are seen which are too high. This indicates there is something not correct. . . . .	59
8.5	Bias level and temperature fluctuations of the TEK6 detector in fast readout speed over a period of 32 days. . . . .	59
8.6	Bias level fluctuations of the TEK4 detector in fast readout speed over a period of 30 days. . . . .	60
8.7	Bias level fluctuations of the EEV12 detector in fast readout speed over a period of 35 days. . . . .	60
8.8	Bias level fluctuations of the SITe2 detector in fast readout speed over a period of 30 days without filtering out the problem images. . . . .	61
8.9	A saturated star which is close to the biasregion. It is seen that the charge also leaks into the bias regions causing an increase in the average biassignal of this region. 62	
9.1	Quantum efficiency decay of the autoguider on the Wide Field Camera over a period of 42 days. . . . .	66
9.2	Pressure decay of the Wide Field Camera cryostat over a period of 45 days. . . . .	67
10.1	Temperature test box. . . . .	70
10.2	Changed temperature measurement circuitry inside the controller. . . . .	71
C.1	Backside well induced by positive charge at the Si-SiO <sub>2</sub> interface. . . . .	92
D.1	Temperature measurement circuitry inside the cryostat. . . . .	94
D.2	Temperature measurement circuitry inside the controller. . . . .	95

# List of Tables

2.1	Important IRAF commands . . . . .	19
5.1	Results of linearity measurement . . . . .	30
5.2	The reduction factor of the ND filters over a wavelength band from 400 to 500 nm	34
5.3	Table of commanded and real flashtimes . . . . .	35
9.1	Filters with the quantum efficiency of the science chip and the output used by the script. . . . .	65
10.1	Offset between the real operating temperature and indicated temperature by the DAS.	70
10.2	Equations used by the DAS to calculate the temperature of the CCD. . . . .	71



# Chapter 2

## The CCD

### 2.1 Introduction

The Charge Coupled Device, or CCD, was developed in 1970 by Boyle and Smith at Bell Laboratories. The original device was designed to store analogue information in the form of packages of electric charges within a semiconductor structure. The light sensitive properties were quickly discovered and put into use for imaging application especially for use in astronomy. The CCD improves the light gathering power of a telescope by almost two orders of magnitude in comparison to conventional means or the naked eye. The CCD can have various uses like; memory, delay lines, correlators and optical detectors. The last application is of most interest to us. The charge in a photosensitive CCD is created by the photoelectric effect. The charge storage sites are photo elements (elements that are sensitive to light) within the CCD. When the CCD is exposed to light, charge builds up in the photo elements. After the integration time (time the CCD is exposed to light) the charges are transferred one after each other to the output stage. The electrical signal delivered at the output stage is proportional to the incident illumination on the photo element. At the output of the chip we read an electrical signal that varies synchronously with the readout rhythm of the chip. This pattern of charge is converted into a video waveform which is digitized and stored as an image file on the computer. The photo elements can be oriented in lines like one can see in photocopiers or in a matrix like in digital cameras.

## 2.2 How does it work

### 2.2.1 Simple analogy

The simplest analogy of the working principle of a CCD is a set of vertical conveyor belts with buckets that catch raindrops and one horizontal conveyor belt with buckets and at the end a reservoir. The raindrops represent the descending photons that fall onto the pixels. These pixels are represented by the buckets. The conveyor belts represent the shift registers that transport the charge to the output stage (see fig. (2.1)).

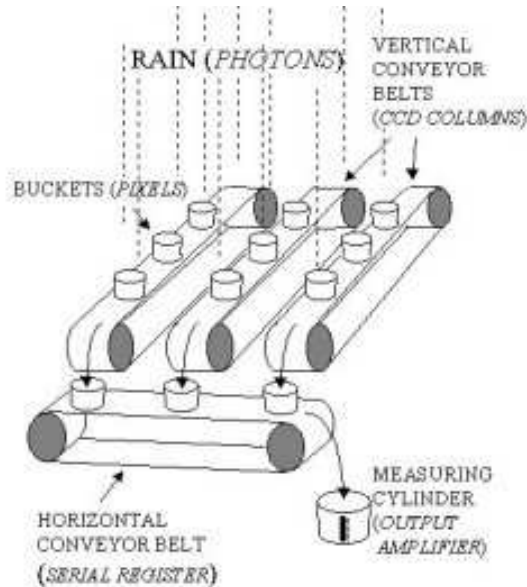


Figure 2.1: Simple analogy of a CCD matrix ( image from: *Introduction to CCD's*, by Simon Tulloch)

During the integration time the buckets catch the fallen raindrops. After the integration time all of the buckets contain a sample of the rain that has fallen down. The vertical conveyor belts will then move down one line. The rain inside the buckets of the first line is dropped into the buckets on the horizontal conveyor belt, which is then moved sideways. This way the different rainsamples are transported to the reservoir one by one. There the water level is measured and after the value is sent to the computer the sample is thrown away so the next sample can be measured. This way the water level of each of the buckets is measured in the reservoir. When the horizontal conveyor belt is read out the vertical conveyor belts move down another line to drop the next row of samples on the horizontal conveyor belt, which moves it to the reservoir to be read out. This procedure is continued until all the buckets of the matrix are read out.

### 2.2.2 The real stuff

[Tull1] In the CCD it basically goes the same way as described above. The CCD is configured into several thousand vertical shift registers and usually one horizontal shift register (see fig. (2.2)). Both registers need their own clock pattern (voltage pattern which is used to move the charges during readout). It all works in the following way. First the pixels collect the incident photons. These are converted into an electric charge by the photoelectric effect. After the integration time the charge is transported in a conveyor belt fashion by the vertical shift registers to the horizontal shift register. This register transports the pixel charges, one pixel at a time, to the output stage. Here the charge is converted into a voltage which is then available as a typical CCD wave pattern.

**Under- and overscan regions** In many professional CCDs an over- and underscan region exists. This is a region of the image that receives no light and thus only carries a charge produced

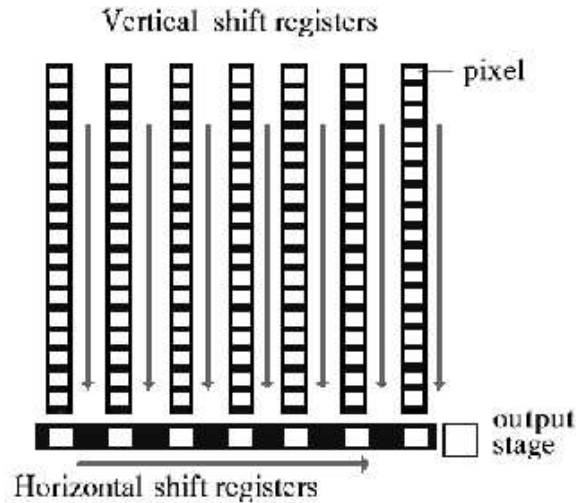


Figure 2.2: The CCD array configuration

by the detector itself. This bias region can be produced by reading out the pixel of the horizontal shift register without it receiving the charge from the vertical shift registers or after it read all of the charges in the horizontal register. These are called the under- and overscan region. The other way is to continue reading out the chip after all the charges have been dumped into the output stage. This is also called the overscan region.

### 2.2.3 Photoelectric effect

[Tull1] A CCD chip is constructed out of an N and P silicon layer. This silicon crystal contains discrete energy bands that can be occupied by electrons. The higher energy band is called the conduction band and the lower energy band is called the valence band. Most of the electrons occupy the valence band and can be excited to the conduction band by absorbing energy. This energy can come from heating the crystal or absorption of a photon. The energy difference between the two bands is 1.26 eV. When an electron is in the conduction band it is free to move around in the crystal. At the same time the electron leaves a *hole* which acts like a positive charge carrier inside the crystal. Normally the electron and the hole recombine quickly, but in a CCD an electric field is induced to prevent this from happening easily. This effect is of fundamental importance for the CCD.

### 2.2.4 Electric field

[Tull1] The CCD chip consists of an N and a P-layer silicon junction similar to a diode junction. The P-layer has an excess of holes which flow into the N-layer, and the N-layer an excess of electrons which flow into the P-layer. This way an electric field is built up inside the chip. The electric potential has its maximum just near the N-P border inside the N-layer (see fig. (2.3)). Because of this maximum the generated electrons will be collected at the N-P surface. This structure is called the buried channel which has the advantage that all of the generated electrons are confined away from the surface where they could be trapped. A nice side effect is that this structure also reduces the thermal noise (dark current) in the CCD.

### Trapping electrons in pixels

Commonly each pixel on the CCD chip consists of three MOS capacitors which are called shift registers. MOS capacitors consist of a semiconducting substrate which is covered by an insulating layer (see fig. (2.4)). These can build up charge to produce a potential well or barrier.

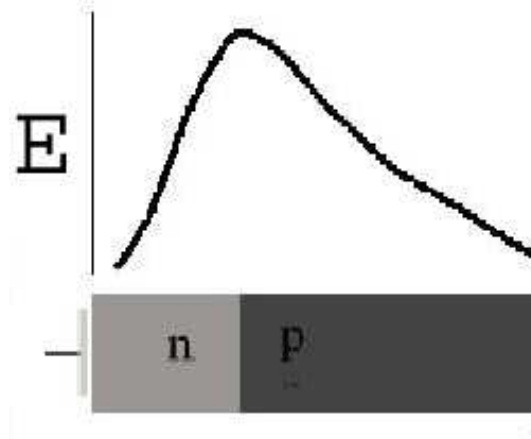


Figure 2.3: Electric potential inside a CCD chip

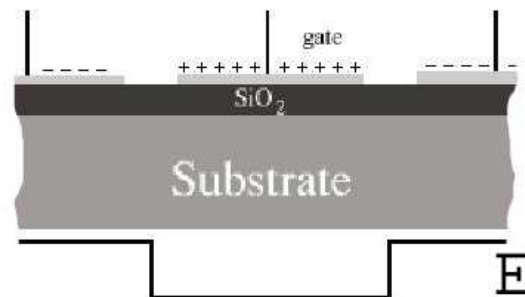


Figure 2.4: MOS capacitor

During integration one of the shift registers is held at a positive potential. This way it attracts all the freed electrons and captures them inside its potential well. The neighboring capacitors are kept at a lower potential, so these function as potential barriers in the vertical direction to trap the electrons. In the horizontal direction channel stops prevents the electrons from escaping the pixel (see fig. (2.5)).

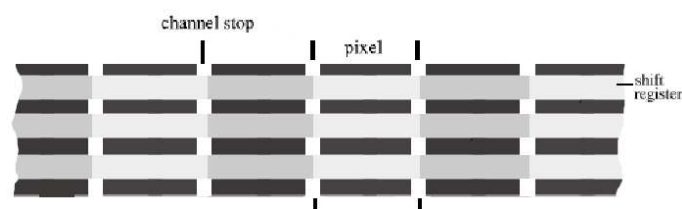


Figure 2.5: Row of pixels

### 2.2.5 Transport of the charges

[Buil] There are three ways that are used to transfer the charge inside a CCD chip. They all make use of shifting the potential on the different segments of the shift register but do this in a different clock pattern. The three ways are the two, three and four phase transfer. We will only discuss the three phase transfer here because it is mostly used and the other transfer methods work fundamentally with the same mechanism. In fig. (2.6) the method explained is schematically shown.

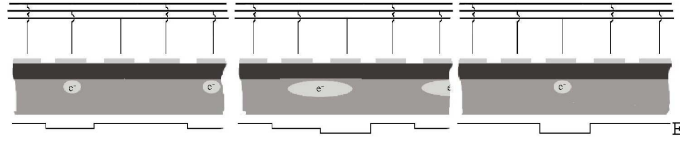


Figure 2.6: Transport mechanism of a three phase transfer.

With this method every pixel consists of three registers. On the left hand side of fig. (2.6) a charged trapped inside a potential well is shown. The potential of the right hand side register is lowered below the energy of the potential well, as seen in the middle panel of fig. (2.6). Because the charge will seek the lowest energy state possible the charge will move to this register. The potential of the previously occupied register is then raised to form a potential barrier so the charge cannot return. This is shown in the last panel of fig. (2.6). As the last action in this process the potential inside the formed well is raised to the level of the former potential well so the process can restart to move the charge one step further. As seen in the figure every third register is held at the same potential level at every step to prevent the different charge to mix. The shifting of these levels is done in a special order which are called clocks. By going to a series of these clocks the charges are transported to the place they need to be. This can be the horizontal shift register or the output stage.

## 2.2.6 Electronics

### On-chip amplifier

[Buil][Tull1] The basic electronics within a CCD chip are rather simple. The whole chip itself consists of a N-P junction. This construction generates the charges when it is illuminated. The shift registers are simple MOS-FET's. These can be positively or negatively charged which induces a field in the silicon which attracts or repels the freed electrons. These MOS-FETs are connected to the controller which produces the clock signal to transfer the charges to the output stage. (For further information about MOS-FETs see *The art of electronics*[2.6]). The transported charge is collected in the summing well. The charge is read out by measuring the voltage inside the well. This is done with the circuit shown in fig. (2.7) called the on-chip amplifier.

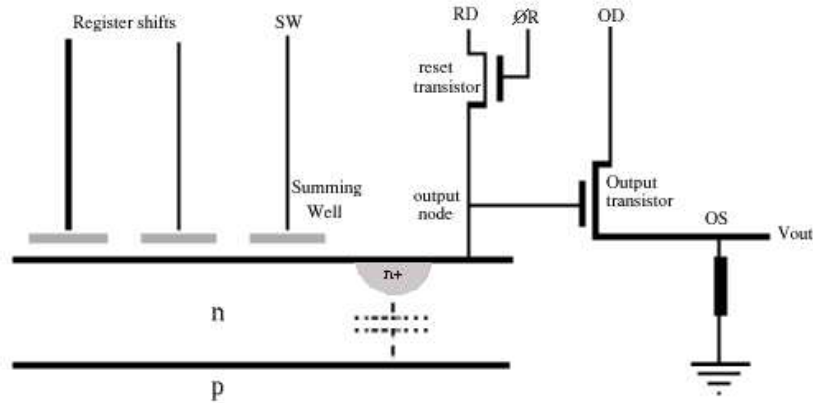


Figure 2.7: The on-chip amplifier of the CCD chip.

The cycle to read the charge begins with resetting the summing well by firing the  $\phi_R$ . This opens the transistor so the charge inside the summing well can escape through the RD (*resetdrain*) pin. The charge is then dropped into the summing well. This induces a voltage over the gate of the output transistor which opens the gate so a voltage proportional to the charge package is measured

as  $V_{out}$ . This happens since OD is kept on a constant voltage. When the summing well is filled with charge it acts as a conductor with the P-layer.

### Correlated Double Sampler (CDS)

[Horro][Tull3] The voltage waveform produced by the chip is at a very low level (few microVolts per photo-electron), so care should be taken in the amplification. To do this precise timing is essential. For a one pixel measurement the waveform is shown in figure (2.8)

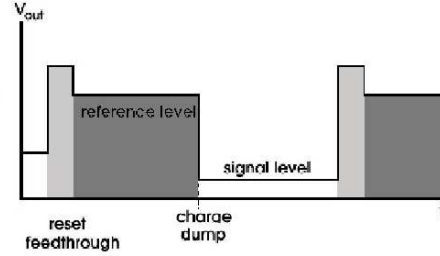


Figure 2.8: Typical video waveform (one period shown).

The first spike is called the reset feedthrough. This signal comes from the R connection (see fig. (2.7)) which charges the reset transistor. The reset transistor opens and the charge left from the previous readout is sent to the reset drain. The plateau that comes next is the reference level. Then the charge is dumped into the summing well (SW) to have its value measured. This is done by lowering the signal on the SW node to collect the charge packages and then raising it again so the charge package goes straight on the output node. This signal is then subtracted from the reference level. Is through as the output. If the level of the output shifts, the reference level shifts in the same way so the difference is still the same. So interference will be less of a problem during readout.

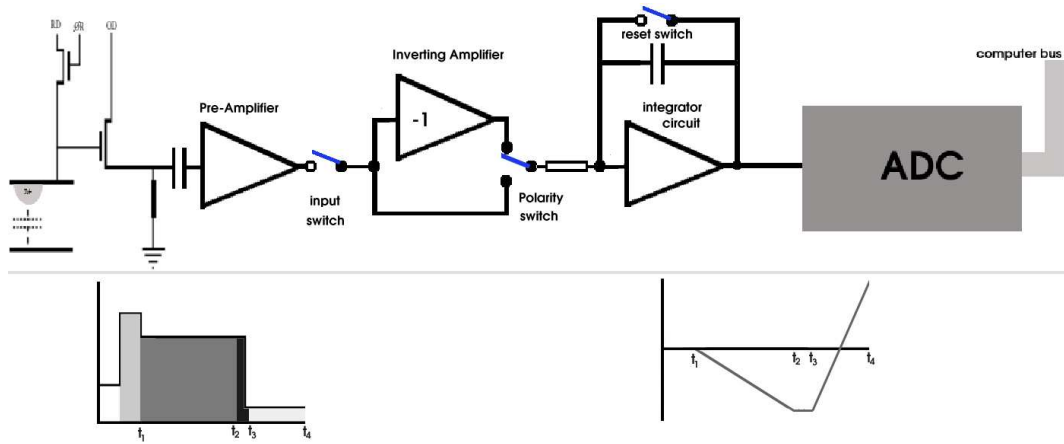


Figure 2.9: The Correlated Double Sampler.

The subtraction is performed using a 'Correlated Double Sampler' (CDS, see fig. (2.9)). To minimize the read noise the reset signal is eliminated by the CDS by means of a switch. This switch opens when the reset feedthrough arrives and closes when it has passed. First the reference signal is fed into the CDS. At this point the inverter is connected so the signal is changed from positive to negative. The output signal of the CDS is going downwards during this time. When the voltage is changed to the signal level the first switch is opened to avoid any noise coming through. The output of the CDS stays constant during this time. When the pixel-signal is read out the switch just after the inverter is changed to the other side so this signal does not pass through the

inverter. At the output the signal goes up. For this to work the sampling and signal window must be the same. Otherwise signal gets lost and the output of the CDS does not reach the correct height. This time is typically between 1 and 20 microseconds. When the entire signal is read out the voltage that is on the output is sent to the ADC and digitized (between 0 and 65535). The digitized data is stored into the computer memory. The CDS is reset and ready to measure the next pixel.

## 2.3 CCD structure

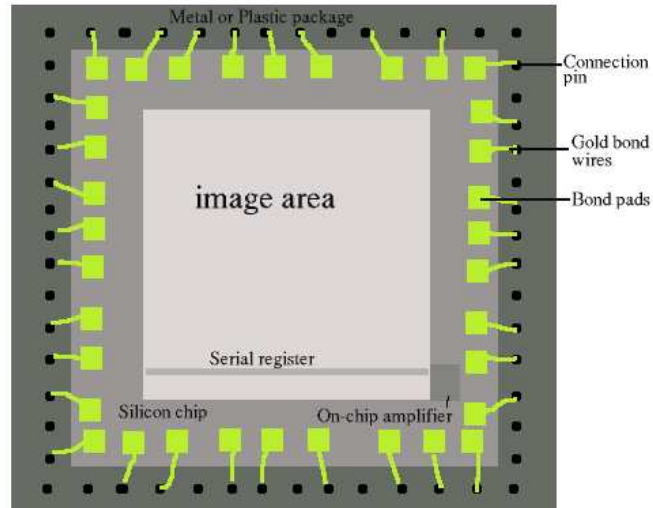


Figure 2.10: General construction of a CCD chip.

[Tull1] In fig. (2.10) the general structure of a CCD chip is shown. In this figure the different components of the chip can be seen. The whole chip is mounted on a metal, ceramic or plastic package. This package contains different connection pins to connect the outputs or clock connections of the CCD. These connections are made with gold bond wires to the connection pads on the silicon chip. On this chip the on-chip amplifier is seen in the right bottom of the figure. This is the circuit described in the previous section which is used for measuring the signal produced by the chip. In the middle of the chip photons are collected to produce the CCD image. This image area is placed in the focal plane of the telescope to capture the image produced by the telescope.

### Large CCDs

[Tull1] The whole chip itself is made of silicon wafers using lithographic techniques. These wafers have a maximum size of 6" in diameter so only a few (or even only one) CCD chips can be placed on a wafer which makes the process expensive. Another problem with manufacturing large CCD chips is that there is a bigger chance for errors or defects on the chip which make large CCD chips very rare and more expensive. A way to produce a large image area is to make mosaic cameras. This is done by placing several "small" CCD chips next to each other with only a small gap in between. For this technique the CCDs must be placed on the same plane. Only an error region of a few tens of a micron is allowed. Another thing is the physical construction of the chip itself. The gap between the chips is generally only a few hundred microns wide. This leaves no space for

connections. Chips with connections on only one side is used so three sides are available to place other chips. The next step is to make chips with the connections on the back side so all four sides are available.

### Antireflection coatings

[Tull2] The reflection index of silicon is 3.6. In comparison to water (=1.33) and air/vacuum (=1.0) this is very high. Because of this high refractive index most of the photons that reach the surface are reflected. The fraction of photons that are reflected can be calculated using equation (2.1).

$$\text{photons}_{\text{reflected}} = \left( \frac{n_t - n_i}{n_t + n_i} \right)^2 \quad (2.1)$$

In this equation  $n_i$  is the reflective index of the incident medium and  $n_t$  of the transmitting medium. From this equation it is easily calculated that the number of reflected photons when light passes from air to silicon will be in the order of 50 %. This phenomenon must be counteracted. The solution is to put an antireflection coating on the silicon chip. This coating has a thickness of 1/4 the wavelength of the light that should be transmitted. This is why this layer is called a quarter wave layer. Typically the wavelength of 550 nm is chosen for this wavelength because it lies close to the middle of the optical spectrum. The reflective index of the layer should lie in between the indices of the two surrounding media and can be calculated by equation (2.2).

$$n_{\text{AR}} = \sqrt{n_i * n_t} \quad (2.2)$$

In this equation  $n_{\text{AR}}$  is the index of the anti reflection coating. The index necessary is 1.9. Fortunately a material with such a reflective index exists and is called Hafnium Dioxide. This is regularly used to coat CCD detectors. The resulting number of reflected photons can be calculated with equation (2.3) which is for this configuration about 30 % in general. At the centre wavelength it can reach 0 % reflectivity.

$$\text{photons}_{\text{reflected}} = \frac{n_t * n_i^2 - n_{\text{AR}}^2}{n_t * n_i^2 + n_{\text{AR}}^2} \quad (2.3)$$

In fig. (2.11) a typical graph is shown of the reflectivity against wavelength with an optimum at 400 nm.

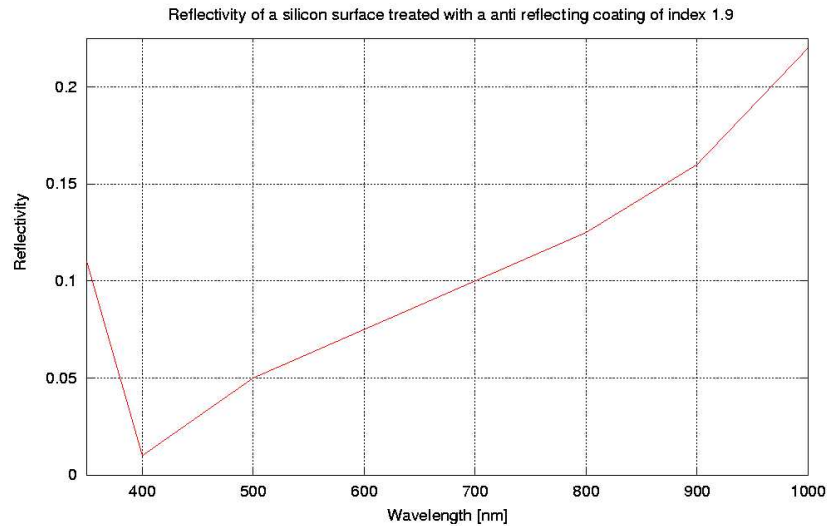


Figure 2.11: Typical graph of the reflectivity with an optimum at 400 nm.

In this graph it is seen that below the optimum wavelength the reflectivity increases rapidly. Above the optimum wavelength the curve also increases but with a more slowly pace.



### 2.3.1 Back- and frontside CCD's

[Tull2] There are two kinds of CCDs: back- and frontside CCDs. The main difference is the direction the CCD is illuminated from. In fig. (2.12) both types of CCDs are schematically shown.

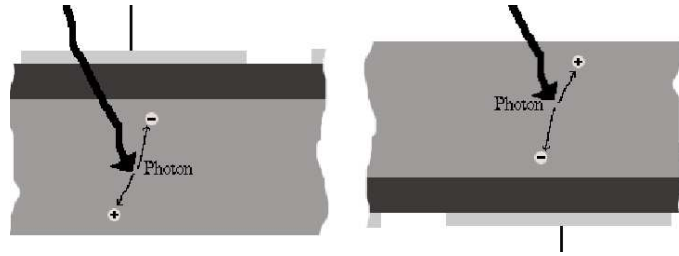


Figure 2.12: On the left hand side a frontside CCD is shown; on the right hand side a backside CCD is shown. In both figures the light comes from above.

**Frontside CCDs** [Buil] With a frontside CCD the chip is illuminated through the side with the electrodes. This way the light has to cross the electrodes and the insulating layer to reach the silicon. The frontside CCD is easy to make and, not of slight importance, low in costs. It usually consists out of an epitaxial substrate with a thick layer of silicon, from 5 to several 10's of micrometers thick. An epitaxial layer is used because of the possibility to control the thickness of the charge collecting zone which optimizes certain parameters such as spatial resolution. Light crossing several layers can produce interference phenomena that are revealed by a variation of the transmission as a function of wavelength. Also the different layers are not 100 % transparent to the light detected which is why these kind of CCDs do not have a higher efficiency than 50 %. Especially for wavelengths shorter than 400 nm the layers become opaque. The red sensitivity of a thick frontside CCD on the other hand is satisfactory. It allows one to reach the theoretical limit in the infrared. The thicker the substrate the better the sensitivity in the red region of the spectrum. There are limits on the thickness of the chip because of thermal induced currents and loss of spatial resolution. There are ways to make a frontside CCD sensitive in the blue region of the spectrum. One technique used is using a thin layer of fluorescent material that is deposited on the silicon layer. This way this layer emits light of a longer wavelength when blue light falls upon it. This light can then be detected by the CCD.

**Backside CCDs** [Buil] With a backside CCD chip the light comes from the opposite direction compared to the frontside CCD. This chip is high in cost to manufacture and can only be made in small quantities. But their performances make them almost perfect detectors when used properly. These CCDs should theoretically reach the maximum efficiency because the photons do not cross any intermediary layers. But for the blue photons to be collected these should be generated near the depletion zone. This zone is very thin and since the rest of the silicon is very opaque the substrate should be considerably thinned. This is usually done chemically with a strong acid. The thinned CCD chip is very efficient but limited by the reflection coefficient. This is why the chips have an antireflection treatment applied so the efficiency increases drastically. The thinned layer is the cause of interference fringes of equal thickness which strongly modulate the sensitivity across the detector's surface. Another consequence of thinning a CCD is that it will be less sensitive to the red region of the spectrum but they are perfect in the blue region of the spectrum. This is because thinning allows short wavelengths to interact with the silicon efficiently. The sensitivity for UV light depends on many things. One is the small variations in the substrate thickness which is usually controlled to within a micron. As a result the local variations in sensitivity can be of importance. Another thing that affects the sensitivity in this region is the presence of a thin layer of silicon dioxide on the silicon surface. This produces a potential well which traps the electrons generated within a few hundred Angströms. These are mostly electrons generated by the UV light since these are absorbed near the surface of the chip. There are several ways to counter this effect.

One is a UV flood. This generates enough electrons to fill the potential well and thereby produce an electric field which counteracts the effect. This treatment can last for months. Another way is to deposit a very fine metal layer on the surface. The metal mostly used is platinum or gold. This metal acts as a catalyst for oxygen ions to stick to the silicon surface. The negative charge of the oxygen ions produces an electrical field. This field is negative and repels the generated electrons away from the potential well.

### 2.3.2 Frame transfer chips

[Buil][Tull3] The frame transfer chip is mostly used inside 'quick-look' imaging systems like auto-guiders or commercially available digital cameras. This is because the high readout speed of the chips. The disadvantage is that you can only use half the chip for light gathering.



Figure 2.13: A schematic figure of a frame transfer chip. The upper region is used to collect the image and the lower region, which is covered from light, is used as memory.

With a frame transfer chip there are two distinct active regions. One region is the image zone which is sensitive to light. The other region is the same in structure as the image region but shielded so it cannot receive any light. This region is the store area. After integration the charges in the image zone are transferred to the store area just by clocking the chip in the vertical direction. This way the whole image is put in the store area at once. This memory zone is then read out in a normal fashion. During readout of the store area the image zone is available for integration. This way the integration and readout of the chip can be done at the same time to speed up the process. In most applications these chips do not have a shutter. The integration time is just the time between two transfers to the store area. During the transfer the image zone is still exposed to light but because of the speed of the transfer this will not affect the transferred image. A typical transfer time is in the order of several hundred microseconds. A typical integration time is from about a second to several minutes.

### 2.3.3 Camera construction

[Tull3] A normal professional CCD detector is located inside a cryostat to keep it cold. The detectors used at Isaac Newton Group are about 50 cm long and 10 kg in weight (see fig (2.14)).

Within the cryostat a vacuum of about  $10^{-6}$  mbar is kept for isolation purposes. To keep this vacuum the detector has a vacuum chamber made of 3 mm aluminum. Inside this vacuum chamber a copper chamber is located where the liquid nitrogen goes in to keep the detector cold. This chamber is connected to the outside by a tube through which the liquid nitrogen is put into the cryostat. While the nitrogen boils off the gas can escape through the same tube. The

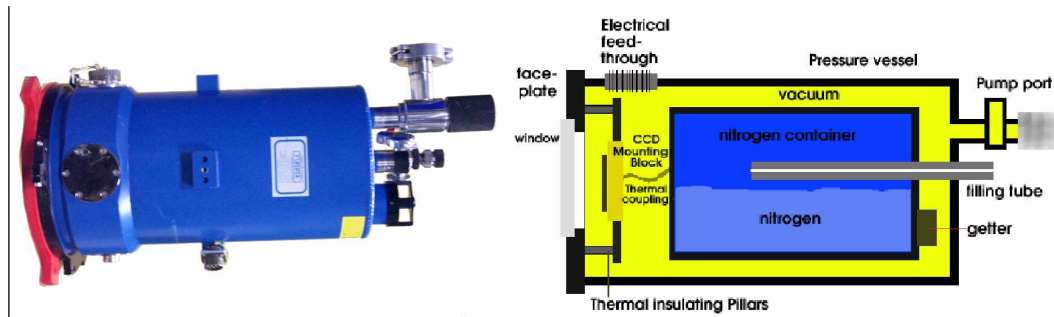


Figure 2.14: A CCD detector as used at Isaac Newton Group

surfaces inside the vacuum chamber are covered with aluminized mylar film to improve the thermal isolation. At the end of the vacuum chamber a piece of activated charcoal known as a 'getter' is located. This acts as a sponge and collects all the residual gases inside the vacuum chamber. The getter contains a heater to release all the absorbed gases when it is being pumped.

The CCD chip is mounted on a copper block which is thermally isolated from the outer pressure vessel. A flexible copper braid connects the chip thermally to the liquid nitrogen. The thickness of the braid is adjusted so that the temperature of the chip is 10 degrees below the optimum operating temperature. A platinum resistor to measure the temperature and a heater to regulate the chip's temperature are mounted on the copper block. In front of the chip a removable endplate is located which is sealed with a synthetic rubber 'o' ring. In the center of this plate a fused silica window is located. To prevent condensation it is necessary to blow dry air across the outside.

Over the CCD mounting block a radiation shield is mounted. It is placed in such a manner that it covers all of the components but does not obscure the line of sight of the CCD. This shield is highly polished and cooled by the braid to shield the detector from radiation as much as possible.

### 2.3.4 The controller

[Tull2] The CCD needs a computer to operate. This system is embedded inside what is called the controller. The controller will basically contain a low noise analog section for application and filter of the CCD video waveform, an analog to digital converter, a high-speed processor for clock waveform generation and a fiber optic transceiver for receipt of commands and transmission of pixel data.

The clock signals are generated by Digital Signal Processing (DSP) chips running at 50 MHz. The clock sequences are generated in software and output through on-chip parallel ports by the DSP. DSPs come with a small on-chip memory for the storage of waveform generation tables and software. Small codes can be stored in a few kB of external RAM. So the computer inside the controller is fast and simple in design. A poorly performing processor can result in long readout times and poor use of telescope resources.

### 2.3.5 The Data Acquisition System (DAS)

[Tull2] The DAS system is the system which collects the data on the computer. This is normally a SUN SPARC workstation. The data will be transferred to the computer by means of fibre optics from the controller. The hardware inside the SUN will be 'off the shelf' with only one addition: a fibre optic transceiver card. A DAT drive is normally also included to store the large amounts of data on DAT's just as a high speed Ethernet card to connect to the observatory local area network. The software required to carry out the data acquisition task is typically in-house developed. This software can be complex if it needs to talk with other telescope systems. The DAS receives the data and stores the images inside an automatically made directory. At the Isaac Newton Group these directories are named in the manner yyyyymmdd (yyyy=year mm=month dd=day). This changes every day at noon. This change happens during daytime to make sure all the images

taken on one night will be in the same directory. The images are stored with a header. In this header all the information about the images is stored. This can be information as the coordinates were the telescope is pointing at, temperature of the CCD, name of the observer, biassections of CCD, etc.

### 2.3.6 IRAF

[Barn] IRAF (Imaging Reduction and Analysis Facility) is an image processing tool. It is developed by the National Optical Astronomy Observatories (NOAO) for the astronomical community. IRAF has found a wider range of use within science nowadays.

IRAF provides the user with a wide range of image processing tools using a command line interface. The commands that can be given in IRAF are called tasks. Tasks are executed to perform various functions. Each task has a parameter file which can be modified by the user to change the outcome. It is also possible to execute some of the shell commands from within IRAF, it depends on the version is used if a ! sign has to be put in front of the shell command. Important commands which are used are:

Table 2.1: Important IRAF commands

command	outcome
<b>display</b>	Displays a given image into an image display tool like XIMTOOL.
<b>imstatistics</b>	measures the mean, median, standard deviation inside a given region.
<b>imexam</b>	is mouse interactive, plots the pixel values of a row, column, small area etc..
<b>imarith</b>	can do simple calculations between images like adding, subtracting, dividing. It does this pixel by pixel.

To extend the use of IRAF the program can be enlarged with additional packages. These packages are available from a variety of sources and can be installed to run under the IRAF environment. Another way to extend the use of the IRAF program is by programming a task oneself. This can be done in a couple of ways. Through IRAF scripts (these are much like UNIX shell scripts or VMS command procedures), through Fortran or C programs (these are written at the host level that are interfaced with the IMFORT library routines) and through programming in IRAF's own SPP/VOS programming environment.

## 2.4 Using the CCD

### 2.4.1 Noise on the CCD

[Buil][Tull3] There are four main sources of noise for a CCD detector. These are: Read noise, Photon noise, Darkcurrent and Pixel response non-uniformity.

**Read noise** This is caused by the electronic noise produced in the output transistor of the CCD. It is mainly produced by thermally induced motions of electrons in the output amplifier. The noise can be reduced by cooling the output amplifier or decreasing its electronic bandwidth. The last means an increase in readout time because it takes longer to measure each pixel. This kind of read noise is called Johnson noise and is always present to some degree. It places a fundamental limit on the performance of the CCD detector. It is also possible that readout noise is produced by external electronics. The system can pick up interference from other circuitry in the observatory

which can contribute to the read noise. Scientific CCD detectors have a typical readout noise of about 2-3 electrons.

**Photon noise** This is the statistical noise of the detected photons. Photons arrive in an unpredictable manner which is described by Poissonian statistics. This unpredictability produces noise. When an image of a uniform field is taken the photons that fall on the detector will not be distributed in a uniform way. When the detector is exposed long enough all pixels will read the same value. But with short a exposure this will not be the case. There will be a non-uniformity within the field: some of the pixels will measure higher counts and some will measure lower counts. This is due to the unpredictable manner in which the photons arrive. Poisson statistics tells us the root mean square uncertainty (RMS noise) in the number of photons per second detected by a pixel is equal to the square root of the mean photon flux, which is the average number of photons detected per second. By making the exposure longer the signal to noise ratio will increase because the photon noise increases with the square root of the exposure time.

**Darkcurrent** Because of thermal energy electrons will be excited from the valence band to the conduction band. After a period of time an equilibrium is reached. This period is called the 'thermal relaxation time'. This time can vary between one and several dozen seconds. The electrons on the surface cannot be distinguished from the electrons that are freed by incident photons, so they will act as a noise in the images. This phenomenon is known as dark current and it depends on the type of silicon used, on the state of the surface between the silicon and the oxide and on the temperature of the chip. The first two are characteristics of the chip and can only be controlled when it is manufactured. To counter the last the CCD chip has to be cooled drastically to reduce the effects of dark current inside it. The temperature cannot be too cold because the sensitivity of the chip will reduce because of lack of thermal energy. Typical operating temperatures from professional CCD's are 150 K which normally provides a dark current of about 1 electron per hour. Dark current is also governed by Poissonian statistics.

**Pixel response non-uniformity** Small defects in the silicon crystal and manufacturing errors can result in the fact that some pixels are less sensitive than others. These variations can be as big as 4 %. It is also possible that dust and other obstacles are blocking the photons from arriving at the chip and causing local insensitivity. When the dust is on the filter and the telescope is of a cassegrain type the dust particles can be recognized by the donut shape on the image. These variations can be easily removed by dividing by a flat field image (discussed later).

**Combining the noise sources** The sources of noise are combined to one by the following equation:

$$N_{tot} = \sqrt{N_{PRNU}^2 + N_{readout}^2 + N_{darkcurrent}^2 + N_{photon}^2} \quad (2.4)$$

In this equation is  $N_{tot}$  the total noise in the image,  $N_{PRNU}$  the noise implied by the pixel response non-uniformity,  $N_{readout}$  the readout noise,  $N_{darkcurrent}$  the dark current and  $N_{photon}$  the photon noise. Some of the noise sources can be excluded from the equation by some of the procedures which are executed on the images. The Pixel Response Non-Uniformity can be excluded by deviding the image with a flat field. The darkcurrent tends to zero when the detector is sufficiently cooled. With high signal levels readnoise is small compared to the photon noise and only of importance when one does low signal level applications such as spectroscopy.

## 2.4.2 Imaging

[Buil][Tull2] There are three kinds of calibration images that are of importance for doing science with a CCD detector. These images are taken to process the raw images. It is of great importance that these images are taken with care since if they are of low quality they can degrade the science

images instead of improving them. Preferably the calibration images should be taken before and after each night.

**Biasframe** A biasframe is taken to measure the zero point of the pixels. It is done by taking a zero second exposure with the shutter closed. The chip will always give a signal; this signal is the biaslevel and should be subtracted from the images. A biasframe can contain structures or a gradient which is produced by limitations in the signal processing electronics of the camera. The normal procedure with biasframes is that a large number of biasframes are taken and then averaged pixel by pixel, rejecting any pixel values that vary much from the other 4. This way any cosmetic defects caused by cosmic rays will be excluded from the resulting biasframe. By averaging the 5 frames the readout noise will be reduced by a factor of  $\sqrt{5}$ . The resulting biasframe should be subtracted from all the images taken with the detector.

There are also bias areas on the sides of the chip. These give an accurate assumption about the height of the biaslevel. But it does not include the pixel response non-uniformity. These regions make it possible to subtract the biaslevel without having to take a biasframe. This should only be done if the accuracy in which the observation has to be done allows it.

**Flat field** The surface of the CCD chip may vary in sensitivity to light. This can be caused by several reasons. One is that the pixels can vary in sensitivity from pixel to pixel. Another is that there can be dust on the chip, cryostat window or filter which blocks the light from reaching the sensitive part of the chip. This causes an object to appear brighter on one part of the chip than on another part. To filter out this difference in sensitivity a flat field is used. This is an image which is evenly illuminated. This can be from the twilight or the inside of the dome using special flat field lamps located in the telescope dome. The first is strongly recommended because of the better quality in evenly illumination. The science image is then divided pixel by pixel by this image to get a normalized signal without the effects of variations in sensitivity. Because the variations can be caused by dust particles it is wise to take flat field just before and after the science images. Averaging several flat fields to reduce the photon noise is normal procedure.

**Dark frame** A CCD chip produces darkcurrent which are self generated charges that increase with time. To counter this in the science images a dark frame has to be taken. A dark frame is an exposure in complete darkness with the same integrationtime as the science image. The image contains only the darkcurrent and the bias signal of the chip. This darkframe should then be subtracted from the science image. Again it is wise to average several images to filter out any defects caused by cosmic rays. Since the procedure is rather time consuming it is not used in professional observatories. This can be done because the detectors are effectively cooled with liquid nitrogen and do not contain high darkcurrents (5 electrons per hour).

**Combining the images** In figure (2.15) the way to combine the described images is explained. If this procedure is followed the detector is used at its best. First the darkframe (or biasframe if the darkcurrent is sufficiently low) should be subtracted from the science image to get all the values at the reference level. The same has to be done with the flatfield. For this the biasframe is used. Then the science image is divided by the new flatfield to get rid of the pixel to pixel difference in sensitivity.

### 2.4.3 Image defects

[Tull2] Many of the used CCD chips show defects. This is because the chips are made from huge silicon wafers which are almost impossible to make without defects. This makes CCD chips without defects rare and therefore very expensive. For science applications these defects do not cause any real problems. This is because most of the defects are small so very large areas of the chip are still useful. For pretty pictures a bit more effort has to be taken to filter the defects out. There are several kinds of defects known.

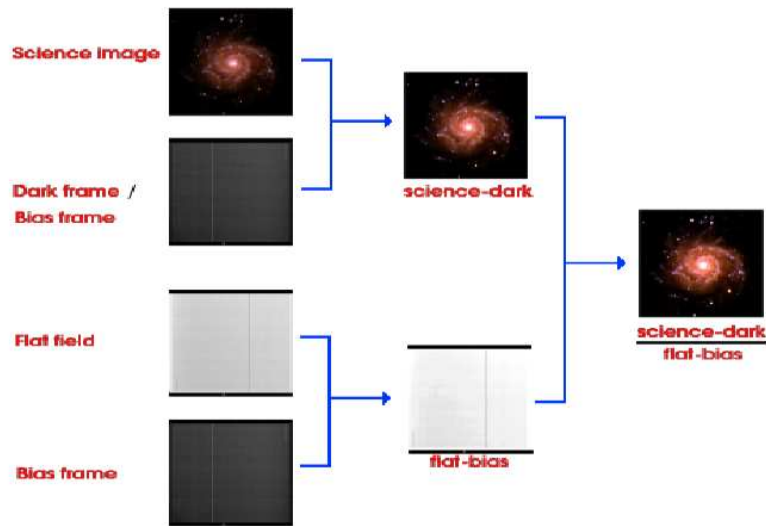


Figure 2.15: Procedure to combine the science image with the flatfield, biasframe and darkframe to get the best result.

**Dark columns** Some of the pixels inside the CCD chip are so called traps. These are defective pixels that trap all the charge that falls into them. These defects are caused by boundaries in the crystal or just by manufacturing defects. The defect means that during readout all the charge which is put into these pixels is lost. This will cause a column above the defective pixel in the directions opposite to the readout direction. In the image this can be seen as a dark column, a column that contains no data. The best way to spot the dark columns is by taking a flat field.

**Bright columns** Just like the darkcolumns these defects are produced by traps. These traps leak out charge during readout. This leaves a bright column above the defective pixel. These traps can be seen with a dark exposure.

**Hot spots** Hot spots are pixels which have a higher darkcurrent then the rest of the pixels. This way it contains more charge then the rest of the pixels. Hot spots can be located with a dark exposure. A rare kind of hot spot is the one that emits light by itself. Roughly speaking the silicon of the chip with the substrate is similar to the P-N junction of a LED. This way a LED can be produced on the surface of the CCD chip. This defect will cause a halo of light on the chip.

**Cosmic rays** Cosmic rays are not just like a defect in the chip but are cosmetic defects in the image itself. Charged particles from outer space fall to the Earth with a flux of 2 per  $\text{cm}^2$  per minute. These also fall on the CCD chip. When a ray hits the silicon chip it ionizes the silicon and produces electrons. These electrons cannot be distinguished from the photogenerated electrons and will be read out in the same way. A single cosmic ray will produce several thousand electrons that will be spread out over a couple of pixels.

**Electronic defects** It is also possible the signal of the processing electronics is not operated correctly. This will produce a bright line at the beginning of the image.

**Difference in pixel sensitivity** Although the whole chip is manufactured in the same way there are slight differences on the pixel level. This means that the pixel to pixel sensitivity will vary, which can be up to 10 %. So with every incident photon the charge produced in one pixel can be

different from the charge produced if the photon would have hit another pixel. These differences are tiny but noticable. The remedy is to divide the image by a flatfield (discussed earlier).

**Blooming** When blooming occurs the image, of e.g. a star, appears to be smeared out in vertical direction. It is caused by saturating the pixels. A pixel is a potential well which can collect charge inside the chip. This well does not have an infinite depth and has a limit to the amount of charge it can contain. When too much charge is produced the excess charge will flow into the adjacent pixels. The charge confinement capacity of the channel stops is bigger than that of the electrodes. So the excess charge will spread in vertical direction. This effect is mostly seen on nights with good seeing conditions when star images are confined to small areas of the chip. To counter this problem one can put electrodes on the edges of the pixel. The potential barrier to these anti-blooming devices is lower than the barrier to the other pixels so the excess charge will flow away through these channels. The disadvantage of these anti-blooming devices is that it will produce an area that is light sensitively 'dead' in the middle of the image zone. This will decrease the sensitivity of the chip by 10 %.

## 2.5 The detectors of the Isaac Newton group

In this section a brief description of the detectors used at the Isaac Newton Group is provided.

**EEV10** EEV10 is a detector on the Isaac Newton Telescope. It is on a spectrograph together with TEK5. The size of the chip is 2048 x 4100 pixels with a pixel size of 13.5 x 13.5  $\mu\text{m}$ . The maximum QE (quantum efficiency) is 85 % at 450 nm.

**EEV12** EEV12 is the ISIS blue detector. ISIS is a highly efficient spectrograph on the William Herschel Telescope which is double armed. This means it has two detectors, one which is sensitive in the red and one which is sensitive in the blue region of the spectrum. EEV12 is sensitive in the blue region of the spectrum. The size of the chip is 2048 x 4100 pixels with a pixel size of 13.5 x 13.5  $\mu\text{m}$ . The maximum QE is 85 % at 450 nm.

**EEV13** EEV13 is a spare detector which is also used on the planetary nebula spectrograph (PNS) of the William Herschel. The size of the chip is 2048 x 4100 pixels with a pixel size of 13.5 x 13.5  $\mu\text{m}$ . The maximum QE 85 % at 450 nm.

**Wide Field Camera of the William Herschel Telescope** The Wide Field Camera (2EEV on the William Herschel Telescope) is the detector to UES. UES is a spectrograph on the William Herschel Telescope which optically aligns the spectra to fit on the Echelle spectrograph. The detector contains two closely placed eev chips to create a large image area. The size of each chip is 2048 x 4100 pixels with a pixel size of 13.5 x 13.5  $\mu\text{m}$ . The maximum QE of chip 1 is 78 % at 400 nm and of chip 2 81% at 400 nm.

**Wide Field Camera on the Isaac Newton Telescope** This is a 4 EEV chip CCD detector on the Isaac Newton Telescope. It is connected on the prime focus of the telescope. The detector contains four closely placed eev chips to create a large image area. The size of each chip is 2048 x 4100 pixels with a pixel size of 13.5 x 13.5  $\mu\text{m}$ . The maximum QE of chip 1 is 80 %, of chip 2 87%, of chip 3 80 % and of chip 4 78 % at 400 nm.

**SITe1** The SITe1 detector is just as the Wide Field Camera (2EEV) a detector on UES. The size of the chip is 2048 x 2048 pixels with a pixel size of 24 x 24  $\mu\text{m}$ . The maximum QE is 80 % at 650 nm.



**SITe2** SITe2 is the only detector commissioned on the Jacobus Kapteyn Telescope. It is mounted on the direct image port of the telescope. The size of the chip is 2048 x 2048 pixels with a pixel size of 24 x 24  $\mu\text{m}$ . The maximum QE is 60 % at 700 nm.

**TEK1** The TEK1 detector is a detector which is used with NAOMI, the adaptive optics system, it is also a spare detector. The size of the chip is 1024 x 1024 pixels with a pixel size of 24 x 24  $\mu\text{m}$ . The maximum QE is 65 % at 700 nm.

**TEK2** The TEK2 CCD detector is on the AUX port on the William Herschel Telescope. This is a direct imaging port which can be used to make direct images from the sky when other instruments are used. The size of the chip is 1024 x 1024 pixels with a pixel size of 24 x 24  $\mu\text{m}$ . The maximum QE is 70 % at 700 nm.

**TEK4** The TEK4 detector is the ISIS red detector. It is sensitive in the red region of the spectrum. The size of the chip is 1024 x 1024 pixels with a pixel size of 24 x 24  $\mu\text{m}$ . The maximum QE 65 % at 700 nm.

**TEK5** TEK5 is a detector which is operated on the Isaac Newton Telescope spectrograph together with EEV10. The size of the chip is 1024 x 1024 pixels with a pixel size of 24 x 24  $\mu\text{m}$ . The maximum QE is 70 % at 700 nm.

**TEK6** TEK6 is the detector for WYFFOS which is a multi object fibre-fed spectrograph. This detector has only one readout speed. The size of the chip is 1024 x 1024 pixels with a pixel size of 24 x 24  $\mu\text{m}$ . Information about the maximum QE of this detector was not available at this point.

## 2.6 References

- [Buil] CCD Astronomy, Construction and Use of an Astronomical CCD Camera, by Christian Buil
- [Tull1] Activity 1: Introduction to CCDs, by Simon Tulloch
- [Tull2] Activity 2: Use of CCD cameras, by Simon Tulloch
- [Tull3] Activity 3: Advanced CCD techniques, by Simon Tulloch
- [Baie] CCD Imaging system, by Stephan Baier
- [Horo] The art of electronics, Horowitz and Hill
- [Barn] A beginner's guide to using IRAF, Jeanette Barnes
- For more information about the detectors see the detectorspage of ING  
([www.ing.iac.es/Engineering/engweb6a.htm](http://www.ing.iac.es/Engineering/engweb6a.htm) )

## Chapter 3

# Mapping of the defects in the SITe2 detector

### 3.1 Summary

According to a fault report which has been sent in it seemed that there are small defects on the SITe2 CCD chip. In this experiment the defective pixels from the SITe2 detector on the Jacobus Kapteyn Telescope have been mapped. This is done with a custom written script in IRAF. This script examines every pixel separately. The script is first used on a flatfield image that was taken recently. The chip was mainly affected on the lower half. This script was then used on an old flatfield image from a previous year. This was done to verify whether the defect had increased over the last year, which was not the case.

## 3.2 Results

To find the defects a script has been written that examines all the pixels, one pixel at a time. This script measures the value of the pixel and the average value of the pixels in a 10 by 10 pixel box surrounding the examined pixel. The two values are then compared and if the pixel value is 10% less then the average value of the 10 by 10 box, its coordinates and depth as a percentage are saved to a file. When the pixel is at the edge of the image field then the pixel box is shifted so that the bias region of the image is not included. After the script had finished the following map of the defects was produced (see figure (3.1)).

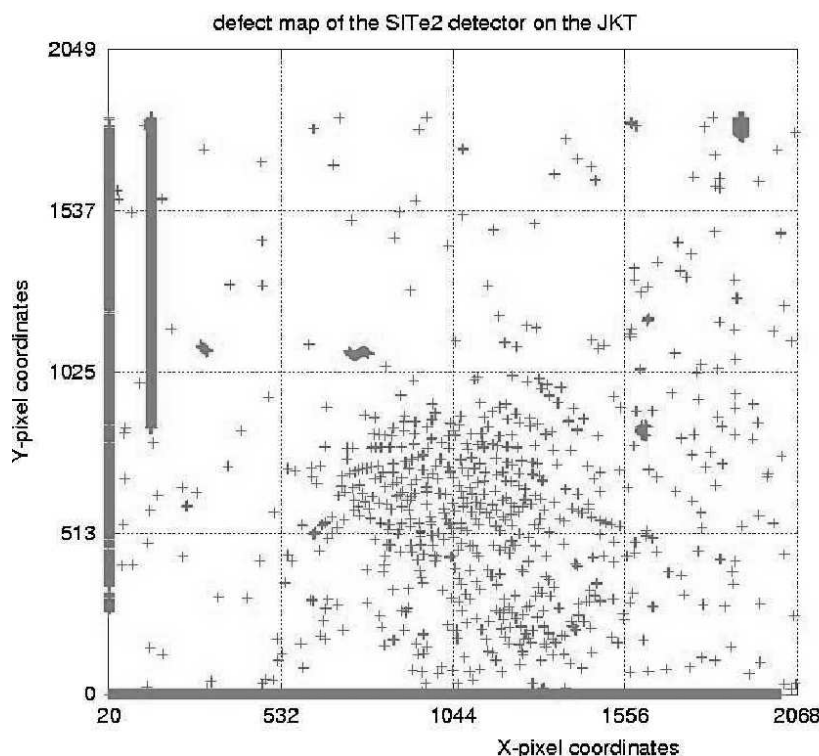


Figure 3.1: Map of the defects on the SITe2 detector.

In this map it is shown that the defects are mostly concentrated in the lower half of the chip. The dark spots can be flat fielded out with normal flat field images. Despite of this it means that if an observer wants to do photometry, it is wise to choose the higher part of the chip because of the lower photon noise due to the higher signal. The defect pattern on the image taken a year ago looks the same as the pattern on the image taken recently. It is concluded that the defects did not increase over the last year. The reason for the radial pattern, which is not clearly visible in the map but is so on the flat field images, and the cause of the defects are not known. It is our believe that it is due to an error in the manufacturing of the SITe2-chip. The defects are present in the anti reflecting coating. In the map also some bands are visible. These are bad columns in the chip. These can occur in every chip (see paragraph (2.4.3)).

## Chapter 4

# Dark current measurements on the Wide Field Camera after a 1 minute light flood

### 4.1 Summary

In this experiment the remnant image of the four Wide Field Camera CCD chips after a domeflood through a V filter is measured. The wide field camera has an autoguider which is located next to the science chips. This autoguider has to be exposed to the star light to let the telescope track. Therefore the shutter is programmed to open after an exposure has been taken. This also happens during the daytime leaving the science chips exposed for long times to bright lights. Therefore the time that is required to lower the dark current to acceptable levels has to be known. It took 150 minutes for chip 1 and 3 to reach the tolerated dark current value of 5 electrons per hour. Chip 2 and especially chip 4 do not reach the lower threshold of 5 electrons per hour. Chip 4 reaches 25 electrons per hour after 200 minutes. The goal was to do this for more filters to investigate whether if the remnant image was wavelength dependent. Due to lack of operating time because of the daily maintenance and repairs on the Isaac Newton Telescope this was not possible.

## 4.2 Theoretical background

[Jane] There are two kinds of residual images known. These are the *Residual Surface Image* (RSI) and *Residual Bulk Image* (RBI).

**Residual Surface Image** is charge that is trapped within forbidden states between the conduction band and the valence band caused by impurities and crystal defects. They are only detected when full well is reached. The lifetimes of these states are in the order of hours. The lifetime is estimated by eq. (4.1).

$$E_e = kT \ln(t_d v_{th} \sigma_n N_C) \quad (4.1)$$

In this equation  $E_e$  is the energy level discharged from the conductance band (eV),  $t_d$  the time given to discharge the trap (s),  $V_{th}$  the thermal velocity of an electron (cm/s),  $\sigma_n$  the electron cross-section (cm<sup>2</sup>), and  $N_C$  the effective number of states in the conduction band. Because the lifetimes from these forbidden bands are in the order of hours the charges can be seen in images that are taken at a later time.

**Residual Bulk Image** are created because charge is trapped inside the epitaxial-substrate interface between the Si – SiO<sub>2</sub> and the substrate. This can only be caused by photons that penetrate the chip deeply enough. RBI is seen mostly at wavelengths  $\geq 700$  nm. Unlike RSI it is also detected below full well. RBI is not detected in CCDs that don't have an epitaxial-substrate interface like backside CCD's or CCDs grown on bulk silicon.

## 4.3 Procedure

### 4.3.1 Script

For this experiment an IRAF script to measure the darkcurrent had to be written. This script has to contain the following features: The script should do an **imstatistics** on the given image region and on a given bias region to get the average value of these regions. And then it must get the values of the time the dark frame is taken after the flood, the exposure time and the gain of the chip. This information is located in the header of the image. With all this information it can begin its calculations. After the calculations the values are plotted in a time vs. dark current plot.

### 4.3.2 Measurement

This experiment is done with the Wide Field Camera (WFC) on the Isaac Newton Telescope. To saturate the detector the number of electrons necessary to reach saturation has to be known. This can be looked up on the Isaac Newton Group website [engw], which is  $20000e^-$  for the wide field camera. Then a short exposure of 4 seconds is taken with the dome lights on. The number of counts per pixel of that image is measured. With this information the exposure time necessary to saturate the CCD is calculated by simple multiplication. The detector is saturated by taking images with the dome lights on for a period of time longer than the required time to saturate the detector. After this a series of dark frames is taken where the dark current is measured using the custom written IRAF script.

## 4.4 Results

### 4.4.1 Script

The IRAF uses as input a file with a list of images that are taken for the measurement, number of chips in the detector and a name which is used for the output files. The first image in the list must be the image with which the CCD is flooded. This to get the precise time the experiment

is started. From the other images it also gets the time that the examined image was taken to calculate the expired time since the dome flood. The script executes an **imstatistics** command on each of the images of each chip to measure the mean of the pixel value in the image region and in the underscan region. These two values are subtracted from each other to get the signal. From the image header it gets the gain of the chip to convert the measured value from ADUs into electrons. Together with the exposure time it calculates the number of electrons per hour measured. All of this is saved to file. Every chip has its own file where the calculated data is stored. At the end it plots a graph on the screen of the last chip examined for a quick look to check that no problems have occurred during the measurement.

#### 4.4.2 Measurement

The measurements were done when the wide field camera was attached to the Isaac Newton Telescope. The detector needs a minimum exposure of 40 seconds to saturate.

A 60 seconds exposure was taken as a flood to be sure that the CCD was fully saturated. In fig. (4.1) the final graph is shown.

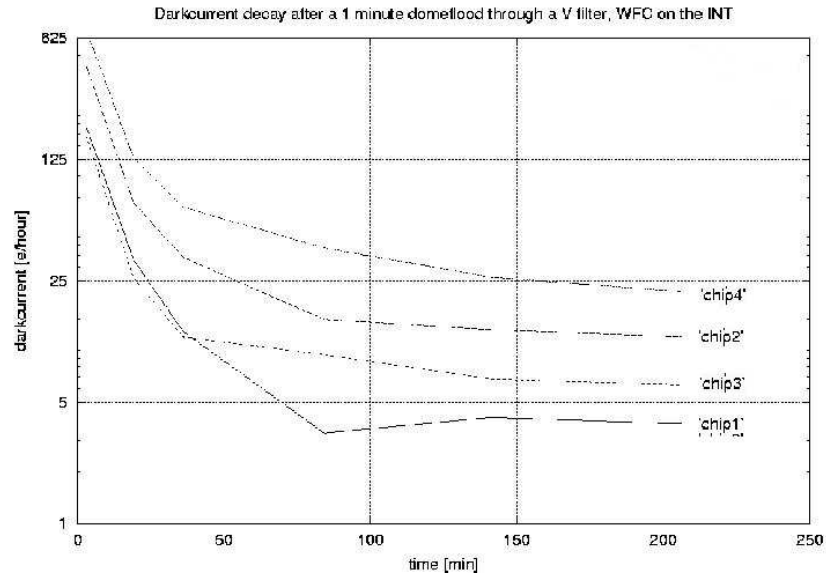


Figure 4.1: Darkcurrent decay in a period of 250 minutes.

This graph shows that the darkcurrents from chip #1 and #3 go to an equilibrium of about 5 electrons per hour after 150 minutes. Only chip #2 and especially chip #4 stay at a high dark current. This phenomenon was seen in every region of the chip. Even after 5 hours this darkcurrent was still at a value higher than 5 electron per hour.

## 4.5 References

- [engw] <http://vela.ing.iac.es/Engineering/engweb6a.htm>
- [foib] <http://www.ast.cam.ac.uk/~wfcsur/foibles.html>
- [Jane] Scientific Charge-Coupled Devices, James R. Janesick

## Chapter 5

# Linearity measurements of all the detectors at the Isaac Newton Group

### 5.1 Summary

In this experiment the linearity of the detectors at the Isaac Newton Group were measured. The goal is to measure the linearity of all the detectors, update the astronomers information pages and automate this measurement for future use. First the linearity of the used LED source is measured. For this neutral density filters are used. The LED source is linear to 1 %. Except under a flash time duration of 0.1 seconds the non linearity increases to 5 %. This is probably due to the fact that there is a difference in the requested flash time and the actual on time of the LED noticeable with the short flash times, which is a software problem. With this LED source the linearity of the different detectors is measured. The linearity is measured as a percentage of the SUI (Signal per Unit Illumination) value at 1000 electrons. This value is chosen because the nonlinearity of the electronics will be negligible. The deviation of total linearity is plotted versus the flash time. A summary of the results is shown in table (5.1).

Table 5.1: Results of linearity measurement

Detector	Fast readout speed	Slow readout speed
EEV11	1 %	
EEV10	0.5 %	0.25 %
EEV12	2 %	1 %
EEV13	1.5 %	0.7 %
EEV2 chip 1	3.5 %	3 %
EEV2 chip 2	2 %	4 %
SIT1	7 %	2.5%
SIT2	8 %	3 %
TEK1	0.25 %	0.3 %
TEK2	0.2 %	0.4 %
TEK4	1 %	0.5 %
TEK5	0.9 %	0.5 %
TEK6	0.5 %	

## 5.2 Procedure

### 5.2.1 Non-linearities

Over a given period of time the absorption of photons within the silicon layer can be considered an ideal linear function. The possible nonlinearity of a detector is introduced by existence of an electronic exposure control circuit adjacent to the photosensitive sites. It is possible that these electronics allow small quantities of charge to remain isolated in unwanted potential wells. Whether or not any potential wells exist depends on the design and manufacturing of the particular image sensor. It is also possible charge packages are lost during transport. This CCD charge transfer inefficiency will reduce the amplitude. This effect is rather small and will only be noticeable with small signal levels. The largest contribute to the nonlinearity will be the output amplifier. When biased properly, the output amplifier will yield a nonlinearity of typically less than 2 %.

### 5.2.2 Filters

The transmissions of the used neutral density filters are known for the wavelength of 544 nm. For the linearity measurements the used neutral density must be known precisely at the used wavelength. The transmittance is measured with use of a well known photodiode which is linear to 1 %. An LED is placed before the photodiode which is attached to a multimeter. In between the LED and the photodiode the filters can be put in a filter holder. The amount of light that goes through each filter separately is measured with the photodiode. This is done several times with each filter to reduce the statistical error. With this information the factor at which the light is reduced is calculated.

### 5.2.3 LED

[Tull4] The flashes in this measurement are produced with the *flash*-command on the ULTRADAS system. This command lets the controller produce a pulse to the LED which then flashes for the time that is put in with the flash command. But the real on time of the LED is not consistent with the flashtime entered with the command. This is not negligible for flashtimes under 0.1 seconds. The actual pulse width of the signal sent from the controller to the LED is therefore to be measured with an oscilloscope and tabulated. These flashtimes are still used in this experiment because we need to get enough measurement points and stay under the saturation limit of the detectors.

It is possible that the LED is not linear in the region it is used. This nonlinearity can be caused by warming up of the LED when it is switched on. The linearity of the LED is measured by shining the LED for 0.01s on a CCD detector. Then the LED light is sent through each of the filters for an exposure time of 0.01 s multiplied with the light reduction factor of the filter. This way the same amount of light will fall onto the CCD detector with each filter. The images are then examined with a custom written script that measures the pixel value and plots the deviation in counts as a percentage versus the actual flashtime. This way the linearity of the detector does not have to be known because the same amount of light falls on the CCD with every measurement.

### 5.2.4 Linearity measurements

[Tull5][INGinst] In figure (5.1) the linearity rig is shown. On the left the whole rig with a detector and controller is seen. In the middle of this figure the source under the detector is clearly visible. And on the right the mount, source and cable are visible.

The linearity measurements are done by using the flash command in the data acquisition system. The names of the images are recorded in a file that later on will be used by an IRAF script. The images will not be taken in a descending order of flashtime but first a high flashtime, then a low flashtime and so on. This is done so that any changes, in time, of the measurement rig will be noticeable in the graph. This is because the points will spread out in case of changes. After the images are taken these are examined with a selfwritten IRAF script. This script measures the mean pixelvalue in the image region and the mean pixelvalue in the bias region. These are subtracted





Figure 5.1: Measurement rig used to measure the linearity of the different detectors (picture by *Simon Tulloch*)

to get the real signal value. Then it calculates the SUI signal and produces a graph where the deviation from  $\text{SUI}_{1000e^-}$  as a percentage is plotted versus the signal value in ADUs.

### 5.3 Theoretical background

The neutral density filters are characterized by their ND number which is calculated by equation (5.1).

$$ND = \log^{10} \frac{1}{T} \quad (5.1)$$

In this formula  $T$  is the transmittance of the filter. The transmittance from each filter used to measure the linearity of the source is calculated with equation (5.2).

$$\text{LRF} = \frac{S_{\text{diode}}}{S_{\text{diode\_filter}}} \quad (5.2)$$

LRF is the light reduction factor,  $S_{\text{diode}}$  is the signal of the photodiode and  $S_{\text{diode\_filter}}$  the signal of the photodiode with a filter placed in front of it. The linearity is measured in SUI (Signal per Unit Illumination). This is calculated with equation (5.3).

$$\text{SUI} = \frac{P_{\text{mean}}}{t} \quad (5.3)$$

In this equation  $P_{\text{mean}}$  is the mean pixel value and  $t$  is the exposure time of the image. The final result is then expressed in a percentage of the difference between SUI ( $\text{SUI}_{\%}$  and the SUI-value at approximately 1000 electrons ( $\text{SUI}_{e^-}$ ).

$$\text{SUI}_{\%} = \frac{\text{SUI} - \text{SUI}_{1000e^-}}{\text{SUI}_{1000e^-}} \quad (5.4)$$

The choice of the SUI-value at  $1000 e^-$  is an arbitrary one. At a value like this the electronics will be linear, so that the only nonlinearity comes from the CCD chip itself, which is a linear element by design. In this way the deviation of linearity will be plotted with respect to the value at approximately  $1000 e^-$ . The choice of the unit of  $e^-$  implies that the gain of the CCD is excluded from the equation. This way the detectors can be compared with each other since the gain is a characteristic of the CCD chip itself and can differ between detectors.

## 5.4 Results

### 5.4.1 Scripts

#### **fm.cl**

Since the LED produces a sharp spot instead of a uniformly illuminated area a script had to be written to find the area which is illuminated the most. It needs 1 image from the list of images taken for the linearity measurement. The search is done with two search patterns. The first cuts the chip area in half and looks in which half the maximum is located by measuring the average ADU count. Then it cuts that part in half again and does the same. In the resulting quarter of the image area the second search pattern is executed. This one takes a band of 10 pixels wide in which it calculates the average signal. This band is swept over the image area in the x direction to find the band with the highest ADU count. The same is done in the y direction. The cross-section of the two bands with the highest ADU count is taken as the 10 by 10 area that has the highest illumination. The LED has a very sharp peak of illumination which makes this method possible. The region that is found is printed on the screen as a string.

#### **fsui1000.cl**

This script searches for the flash image which has an electron count of 1000 electrons. The input of the script is the region in which the signal is measured and a list with all the images taken for the linearity measurement with their actual flash times in descending order of the flash times. The search is done by measuring the signal in the given region. From this signal the bias is subtracted which is measured in the bias region taken from the image header. The signal with the bias subtracted is divided by the gain which produces the signal in electrons. From this electron count the value of 1000 is subtracted to get the difference of the electron count and 1000 electrons. This value is squared, to remove negative values, and compared with the value `electron_old`. If it is smaller than `electron_old`, `electron_old` gets the squared value. SUI1000 gets the SUI value which is calculated with eq. (5.3) and belongs to that electron count. If the value is smaller it is thrown away to move on to the next image. To start the whole cycle `electron_old` has the large value of 1000000000000000. At the end the SUI value closest to 1000 electrons is saved in the variable SUI1000. This is printed to the screen and put in the string SUI1000a.

#### **linearity.cl**

In this script the actual linearity measurement is taking place. It uses a region to measure the signal from and a value for the SUI at 1000 electrons. In the region it measures the signal. The bias is subtracted from this value which is measured in the region which is taken from the image header. The signal with the bias subtracted is then used together with the flash times provided by the list to calculate the SUI using eq. (5.3). Then the percentage is calculated with eq. (5.4) and SUI at 1000 electrons. Also the error is calculated. This is the statistical error which is produced by the Poisson distribution with which the signal is measured. All this is then written to a file in the following order: Signal in ADU, percentage from signal in SUI with SUI at 1000 electrons, error, flash time, bias and image. This file can then be used by a plotting program such as *gnuplot* to produce a linearity graph. For this graph only the first two or three columns are used. The rest is information for the user. The name of the file is automatically generated with information which is obtained from the header. It is named in the following format to assure a unique name for every measurement:

$$\text{detector\_chipname\_speed\_date}$$

The program also produces a graph on its own. This graph is made with raw data and not ment for publication. It is produced for the user so he/she can quickly check the graph for any strange behavior that would indicate a problem in the measurement.

### autolin.cl

This script calls all the different scripts described above and takes the last string called in the script as a result and passes it on to the next. This is why all scripts declare their result as a string in the end. In this way the whole measurement can be done with just one command which takes a list of the images with their flash times as a input. First it calls upon fm.cl to find the maximum. It gives the first image in the list and gets the region as a string out of it. This region is then passed on to fsui1000.cl together with the list of images with their flash times. From this it gets the value of SUI at 1000 electrons. The list, region and SUI at 1000 electrons is then given to linearity.cl to measure the linearity of the detector. In between the different scripts the program write information about the task it is executing at that point and the results to the screen. For instance if it begins its search for the maximum it prints the following message on the screen:

*finding 10X10 area where the intensity is the highest*

After finding the region it prints:

*this area is: [x<sub>1</sub>:x<sub>2</sub>,y<sub>1</sub>:y<sub>2</sub>]*

with  $x_1$ ,  $x_2$ ,  $y_1$  and  $y_2$  the boundary coordinates of the region. At the end of the calculations it gives the user information about the output file and thanks the user for using the script.

### 5.4.2 Filters

All filters were measured in the way discribed in section (5.2.4). The results are tabulated in table (5.2).

Table 5.2: The reduction factor of the ND filters over a wavelength band from 400 to 500 nm

ND(544nm)	ratio	ND(400-500 nm)
0.15	$1.396 \pm 0.001$	$0.1450 \pm 0.0003$
0.3	$1.94 \pm 0.06$	$0.289 \pm 0.01$
0.6	$3.82 \pm 0.02$	$0.583 \pm 0.002$
1.0	$9.43 \pm 0.04$	$0.974 \pm 0.001$
1.3	$21.1 \pm 0.3$	$1.324 \pm 0.005$
1.6	$36.6 \pm 0.3$	$1.563 \pm 0.003$
2.0	$107 \pm 1$	$2.031 \pm 0.004$
2.3	$204.7 \pm 0.7$	$2.311 \pm 0.002$
2.6	$376 \pm 1$	$2.576 \pm 0.001$
3.0	$1138 \pm 2$	$3.0562 \pm 0.0008$
3.3	$2066 \pm 3$	$3.3152 \pm 0.0005$
3.6	$4298 \pm 70$	$3.633 \pm 0.008$

Filter 0.3 has a big error but because we are using all of the filters in the measurement this is no problem.

### 5.4.3 LED

[Tull4] The ontimes of the LED corresponding to the given flashtimes are measured with an oscilloscope. The results are tabulated in table (5.3):

With these flashtimes the linearity of the LED is measured with the EEV11 engineering CCD detector. For this measurement the rig shown in fig. (5.2) is used.

Table 5.3: Table of commanded and real flashtimes

demanded flashtime [s]	actual flashtime [s]
0.001	0.000828
0.002	0.00163
0.004	0.00403
0.007	0.0064
0.01	0.00964
0.02	0.02
0.03	0.0297
0.05	0.0498
0.08	0.0802
0.1	0.0996
0.12	0.1204
0.15	0.1496
0.3	0.3
0.5	0.5
1	1

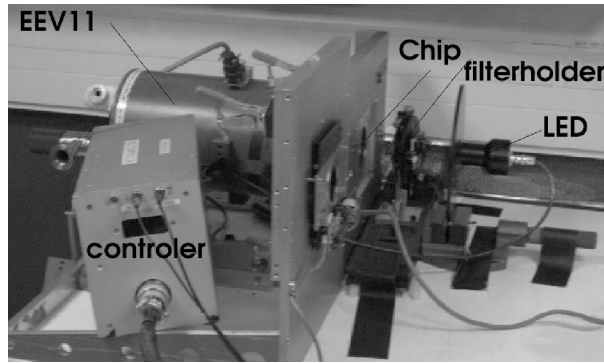


Figure 5.2: Measurement rig used to measure the linearity of the LED source

In this figure you see the EEV11 detector on the left with the controller in front of it. On the right the source is shown and in between the source and the CCD the filter holder is visible. In fig. (5.3) the graph of the measured error in linearity of the LED is shown.

In this graph it is visible that the LED is linear to 1% for the greater part of the flashtimes. For flashtimes below 0.1 second the error goes up to 5 %. This is probably caused by the fact that the on times of the LED were not equal to the required ontimes.

#### 5.4.4 Linearity measurements [engw]

##### Spikes

In all of the graphs spikes are visible. These are located in the beginning of the graphs. These spikes are not the linearity of the detectors that vary at low exposure times. They exist because the nonlinearity of the source is higher at these low exposure times. This effect is increased by the SUI calculation in which the signal is divided by the exposure time through which these little variations are enlarged to this amount. The linearity in this region of the graph is in fact near perfection since the only nonlinearity can come from the chip itself. The rest of the graphs have an error of about 1 %. This is due to the nonlinearity of the LED which is greater than the overall statistical Poisson error. In the graphs there are no errorbars shown to improve their clarity.

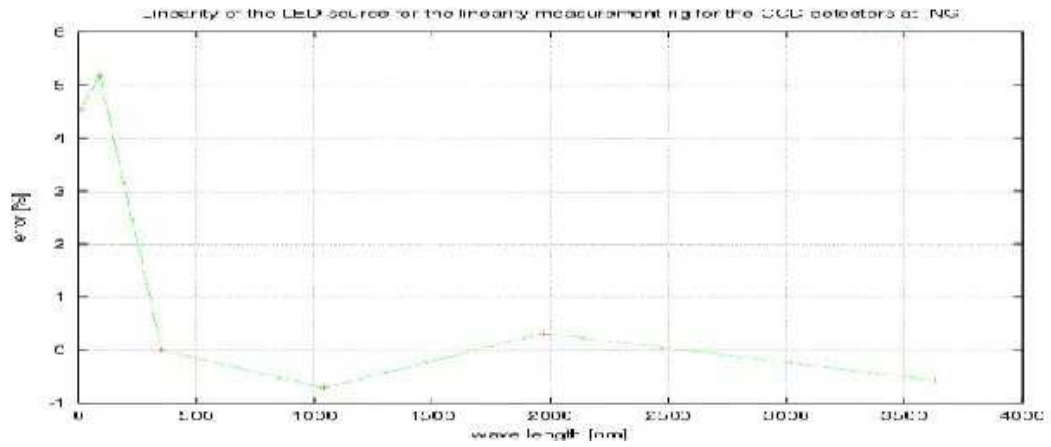


Figure 5.3: Error in linearity versus the flashtime in ms

### EEV11

The first detector to undergo the linearity measurements was EEV11. This is an engineering detector what means that it can only be used for tests because of malfunctions. With this detector the linearity rig is tested. Half of the CCD chip of EEV11 does not work. This will not interfere with the linearity test. The same rig as in the measurements for the linearity of the source was used. The results are shown in fig. (5.4).

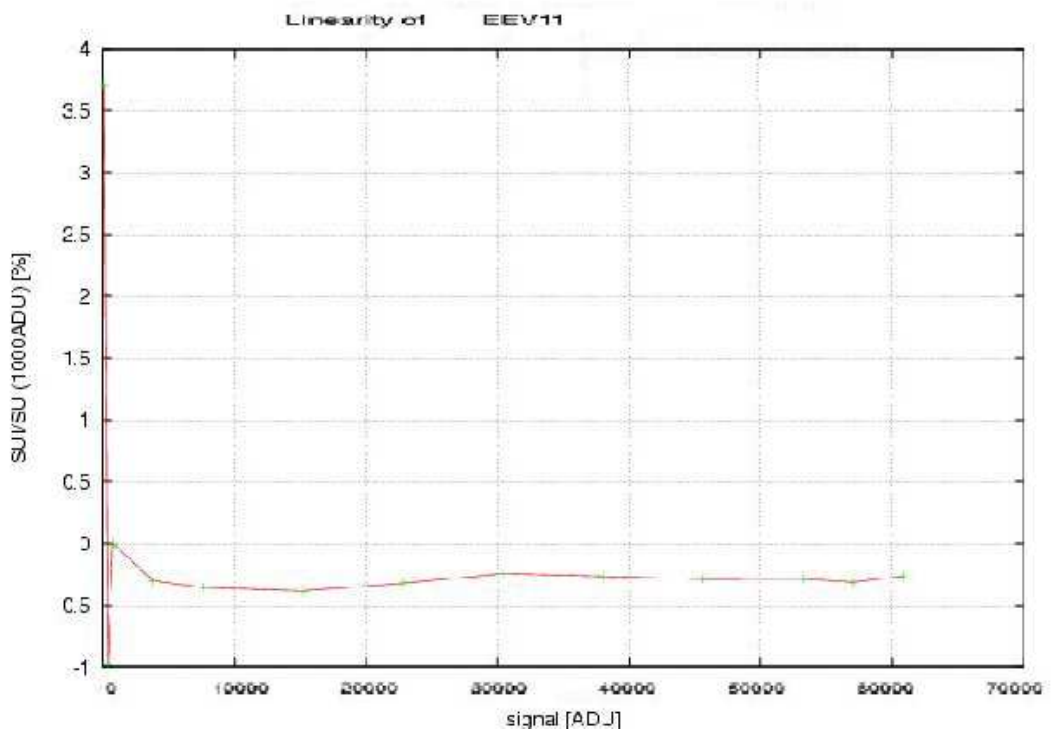


Figure 5.4: Linearity measurement of EEV11 in fast readout speed

The graph shows a nice linearity to 0.5%. This result is consistent with previous results which indicate the rig is performing acceptably.

### 5.4.5 Linearity of the detectors

All the linearity graphs of the detectors are shown in figures ((5.5)-(5.16)). Some of the detectors that are measured in a special way or show special features are handled in more detail.

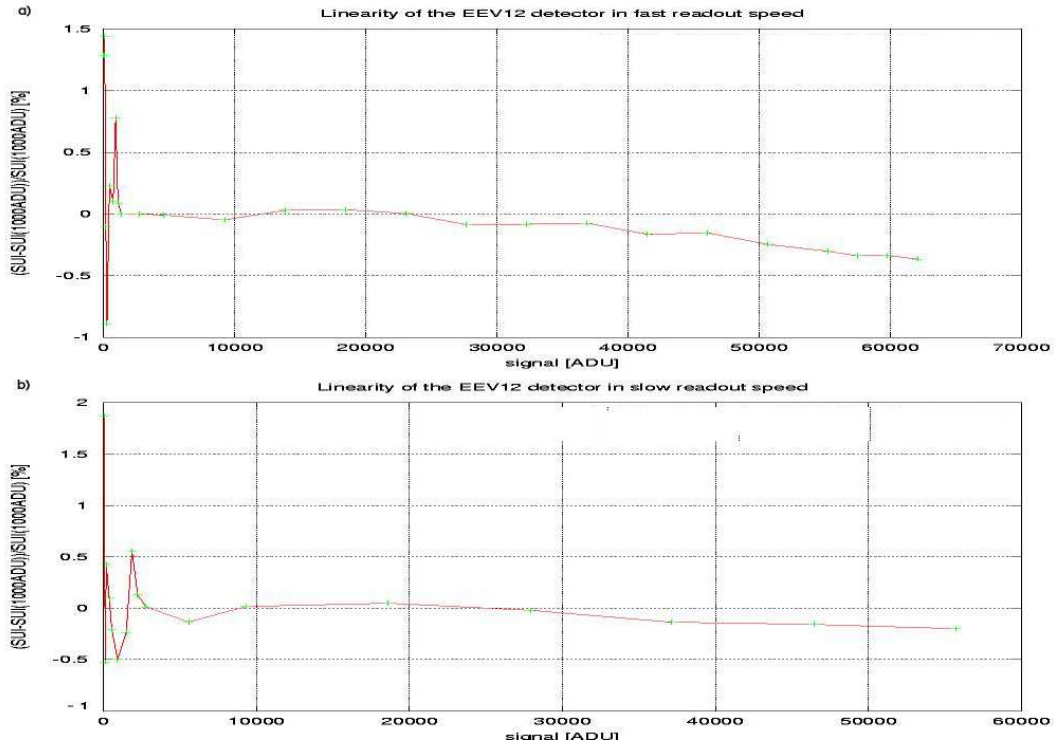


Figure 5.5: a) Linearity measurement of EEV10 in the fast readout speed. b) Linearity measurement of EEV10 in the slow readout speed

The linearity of EEV12, EEV13, SiTe1 TEK1 and TEK6 are measured on the linearity rig in the dome of the William Herschel Telescope with a black cloth around it to shield it from light. This is done because the controllers must be attached to the fibers that lead to the ULTRADAS system in the control room to operate the detector. These connections are not available in the detector lab. The only problem is that the lights in the dome could not be turned off because of other activities. To see if this causes any problems a darkframe with the dome lights on was taken before the linearity measurements. This did not show any interference of the dome lights.

Both the SiTe detectors are very nonlinear in contrast to the other detectors. The linearity graph of SiTe1 in fast readout speed is seen in fig. (5.10a). Here it is seen that the nonlinearity goes up until 7 %. To get a linearity within 2 % the user should stay under 35000 ADU to be on the safe side. The linearity in slow readout speed is shown in fig. (5.10b). In this readout speed the linearity stays within 2.5 %.

The SiTe2 detector measurement is done in the dome of the Jacobus Kapteyn Telescope because the detector controller must be connected to the ULTRADAS system in the Jacobus Kapteyn Telescope to operate. In fig. (5.11a) the linearity in fast readout speed is shown. Here it is clearly visible that the linearity goes up to 8%. To get a good result the images should remain below the 25000 ADU in this readout speed. This way the linearity stays within 2 %. In fig. (5.11b) the linearity on slow readout speed is shown. In this readout speed the linearity error stays within 3 %. For a linearity of 2 % the user should remain below 55000 ADU in slow readout speed.

The linearity of the TEK2 detector has been measured by *Simon Tulloch*.

The linearity of the Wide Field Camera on the Isaac Newton Telescope is not measured. This is not done because the detector is too big to fit in the measurement rig. The linearity of this detector is measured with use of standard stars by Mike Irwin.

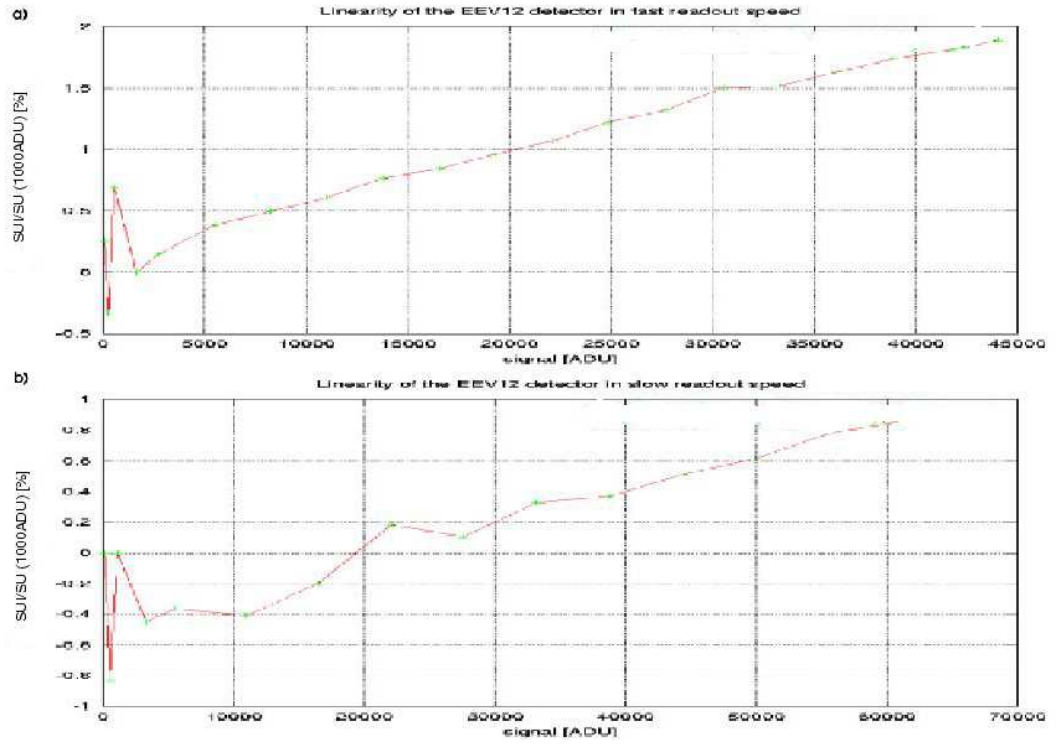


Figure 5.6: a) Linearity measurement of EEV12 in the fast readout speed. b) Linearity measurement of EEV12 in the slow readout speed

## 5.5 References

- [Tull4] [www.ing.iac.es/Engineering/detectors/Measuring\\_lin.htm](http://www.ing.iac.es/Engineering/detectors/Measuring_lin.htm), Simon Tulloch
- [Tull5] [www.ing.iac.es/~eng/detectors/QC/Linearity\\_Source.htm](http://www.ing.iac.es/~eng/detectors/QC/Linearity_Source.htm), Simon Tulloch
- For more information on the Isaac Newton Group detectors:  
[engw] [www.ing.iac.es/Engineering/engweb6a.htm](http://www.ing.iac.es/Engineering/engweb6a.htm)
- For more information on the Isaac Newton Group instruments:  
[INGinst] <http://www.ing.iac.es/Astronomy/instruments/index.html>

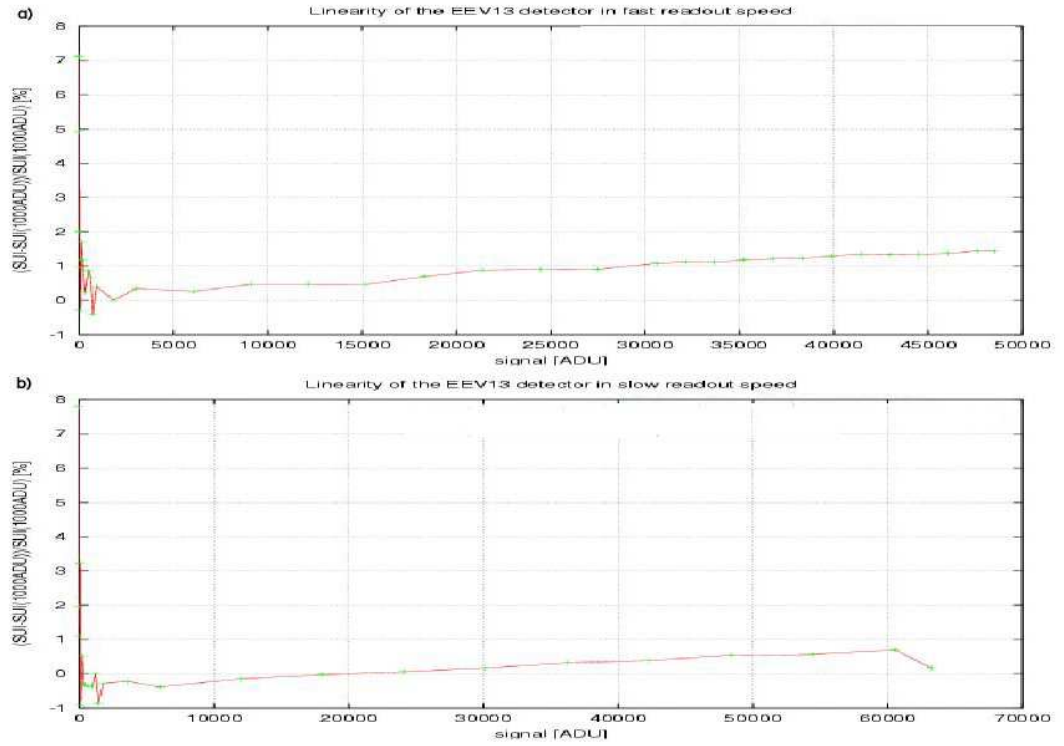


Figure 5.7: a) Linearity measurement of EEV13 in the fast readout speed. b) Linearity measurement of EEV13 in the slow readout speed.

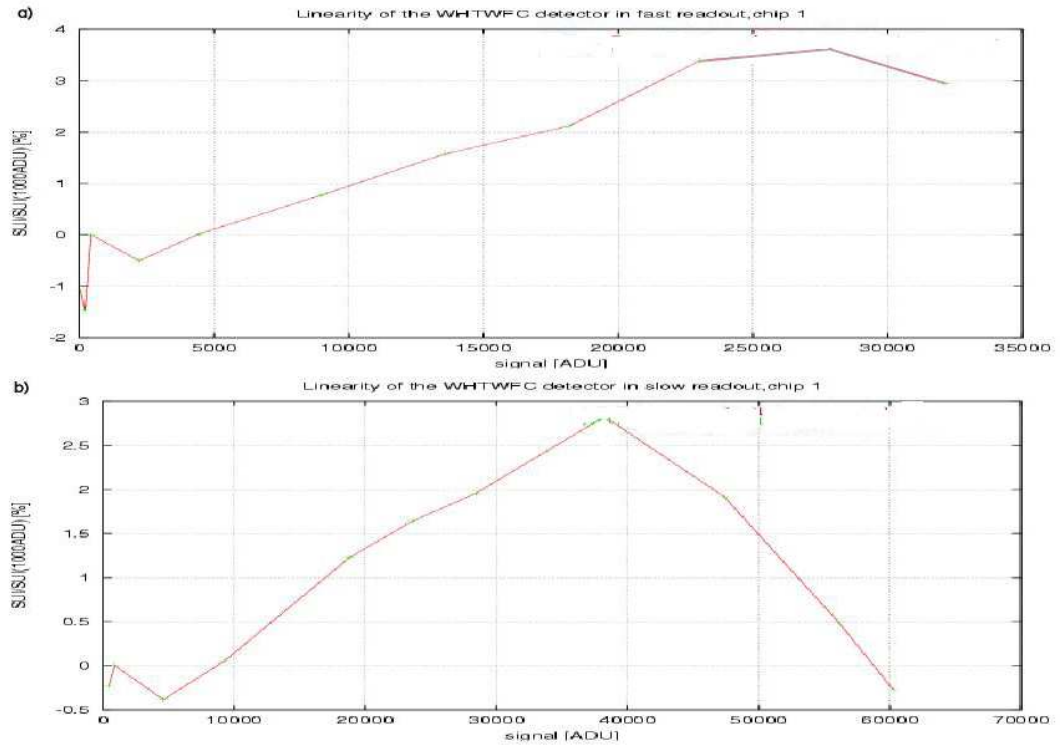


Figure 5.8: a) Linearity measurement of wide field camera chip 1 in the fast readout speed. b) Linearity measurement of wide field camera chip 1 in the slow readout speed



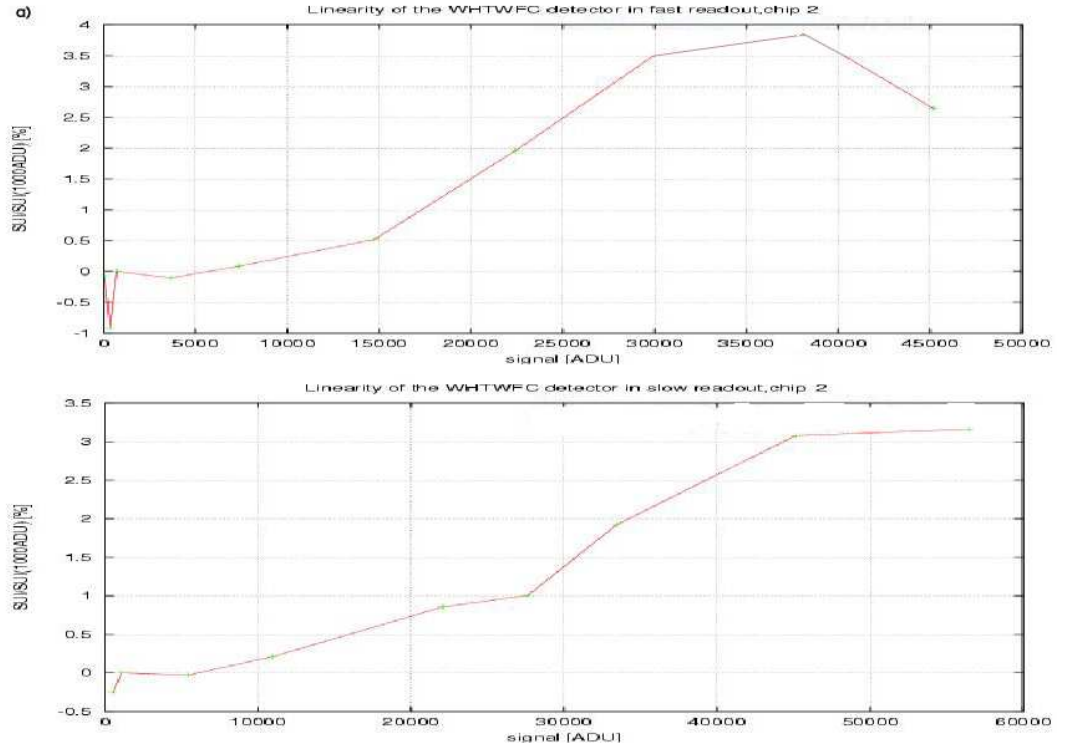


Figure 5.9: a) Linearity measurement of wide field camera chip 2 in the fast readout speed. b) Linearity measurement of wide field camera chip 2 in the slow readout speed

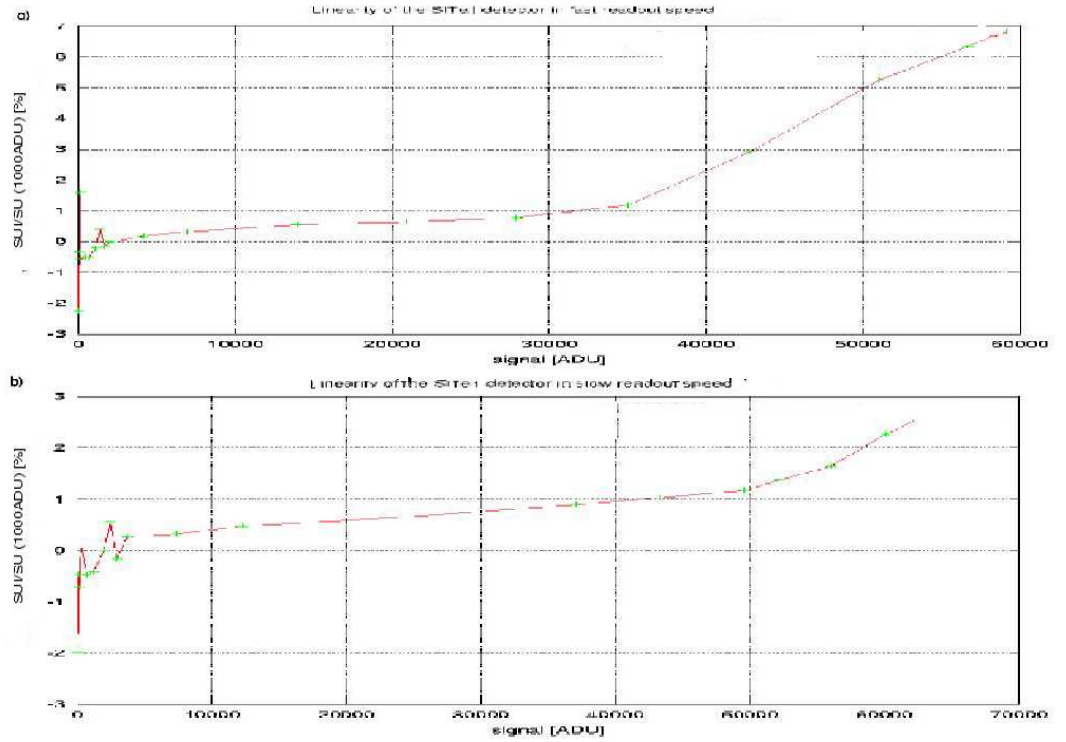


Figure 5.10: a) Linearity measurement of SITe1 in the fast readout speed. b) Linearity measurement of SITe1 in the slow readout speed

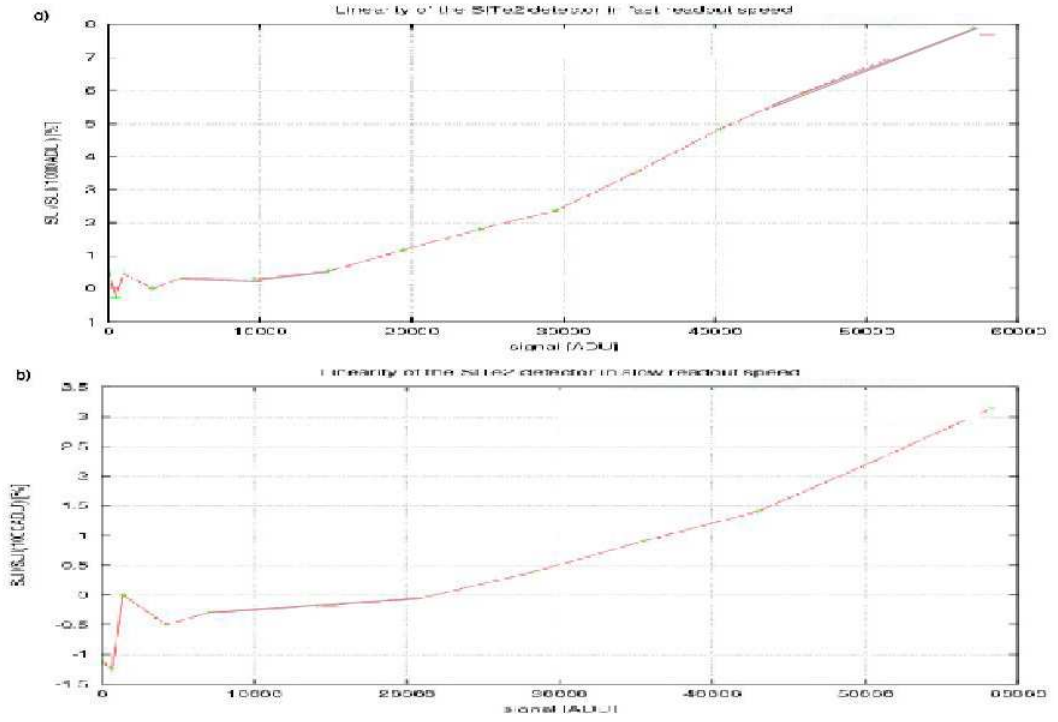


Figure 5.11: a) Linearity measurement of SITE2 in the fast readout speed. b) Linearity measurement of SITE2 in the slow readout speed

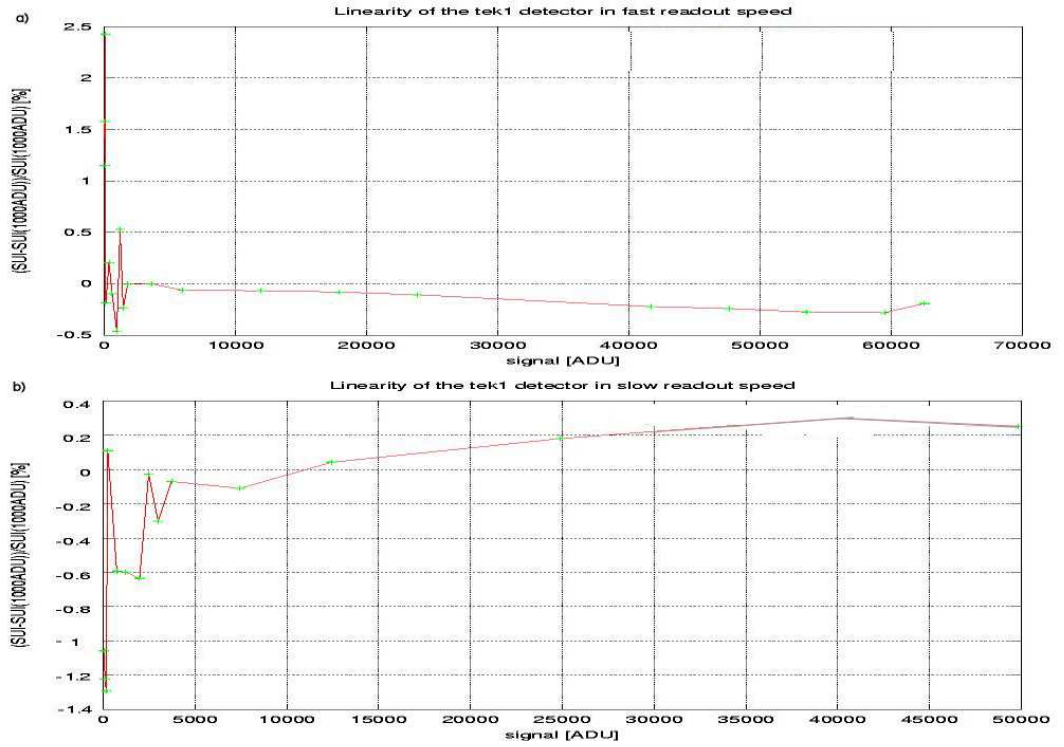


Figure 5.12: a) Linearity measurement of TEK1 in the fast readout speed. b) Linearity measurement of TEK1 in the slow readout speed

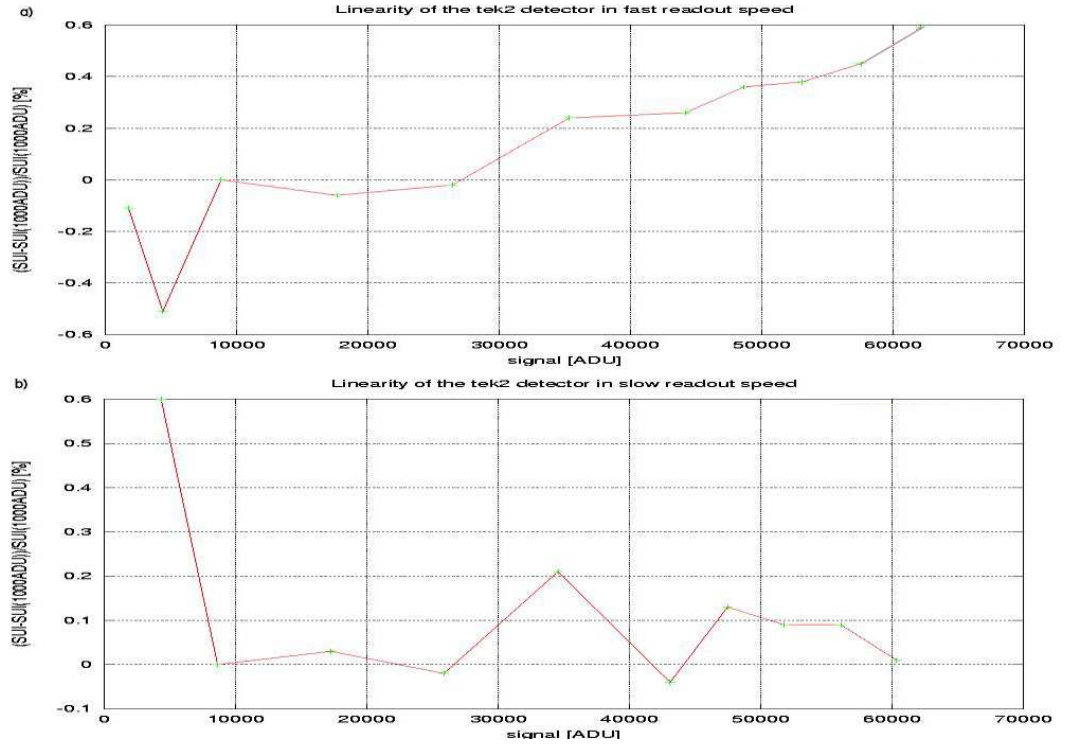


Figure 5.13: a) Linearity measurement of TEK2 in the fast readout speed. b) Linearity measurement of TEK2 in the slow readout speed, both measured by Simon Tylloch

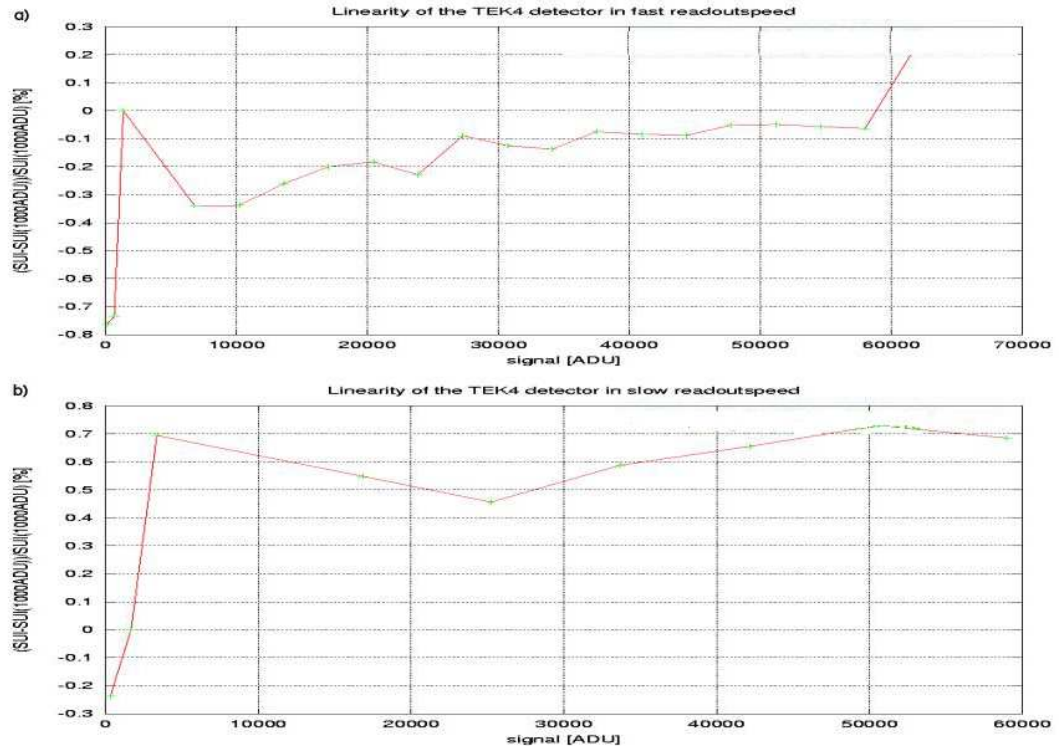


Figure 5.14: a) Linearity measurement of TEK4 in the fast readout speed. b) Linearity measurement of TEK4 in the slow readout speed

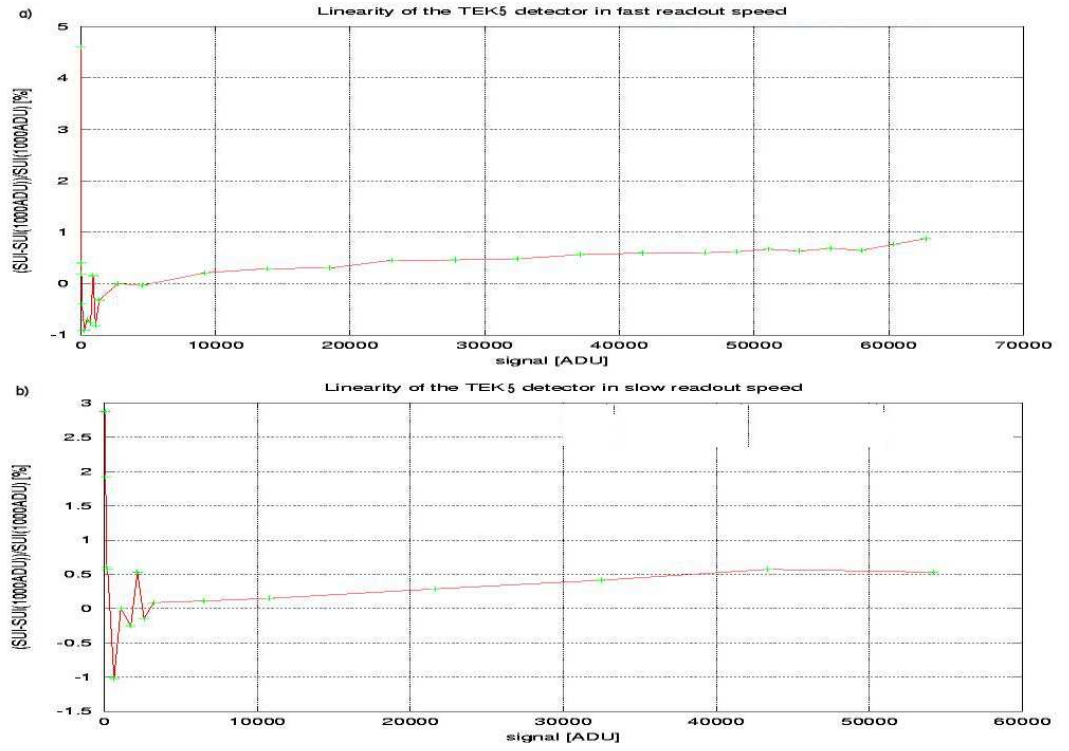


Figure 5.15: a) Linearity measurement of TEK5 in the fast readout speed. b) Linearity measurement of TEK5 in the slow readout speed

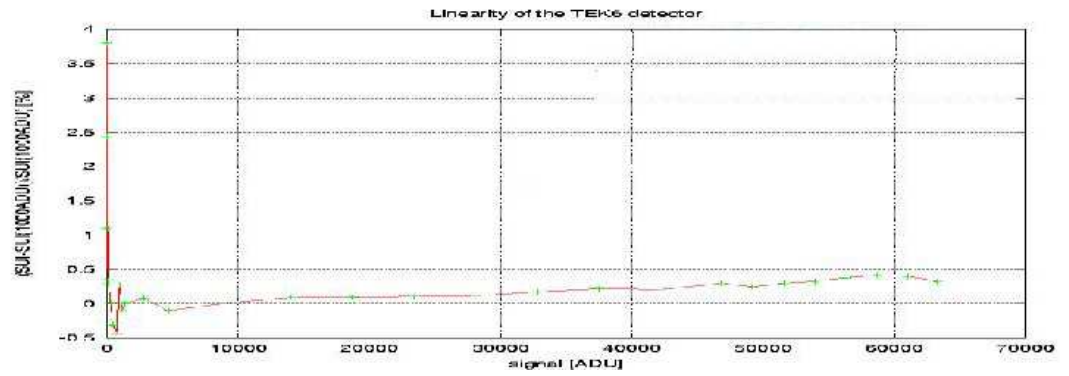


Figure 5.16: Linearity measurement of TEK6

## Chapter 6

# Quantum efficiency measurements of detectors at Isaac Newton Group

### 6.1 Summary

In this experiment the quantum efficiency (QE) of different detectors at Isaac Newton Group in La Palma is measured. This is done using the QE-rig in the detector lab located in the William Herschel Telescope. The QE is measured at 8 different wavelengths. First the light flux is measured with a photodiode through all of the filters and then the same is done with the detector. The data is then plotted in a wavelength versus QE, in percentage, graph. The detectors which were examined are: SITe1, SITe2, TEK1 and TEK5. During the test it was discovered that the quantum efficiency rig source was not bright enough. The current through the tungsten lamp was increased to counter this effect. After this change the time for the tungsten lamp to stabilize was measured. The time for the tungsten lamp to stabilise was 45 minutes.

## 6.2 Theoretical background

[Jane] The QE is measured by first measuring the output of the lamp at a certain wavelength with a well known photodiode. Then the output of the CCD is measured at the same wavelength using the same source. The QE can be calculated with equation (6.1).

$$QE = \frac{A_{\text{diode}} S_{\text{CCD}} QE_{\text{diode}}}{P_S S_{\text{diode}}} \quad (6.1)$$

In this equation  $A_{\text{diode}}$  is the active area of the diode ( $\text{cm}^2$ ),  $S_{\text{CCD}}$  the average signal generated by the CCD ( $e^-/\text{pixel}/\text{sec}$ ),  $P_S$  the active area of a pixel ( $\text{cm}^2$ ),  $S_{\text{diode}}$  the photo signal generated by the photodiode ( $e^-/\text{sec}$ ), and  $QE_{\text{diode}}$  the QE of the photodiode. The value of  $QE_{\text{diode}}$  is taken from the specifications of the used photodiode. The signal produced by the CCD is found by measuring the average signal from a small group of pixels through equation (6.2):

$$S_{\text{CCD}} = \frac{S_{\text{diode}} K}{t_E} \quad (6.2)$$

Here is  $t_E$  the exposure time of the CCD.  $S_D$  is defined by (6.3):

$$S_{\text{diode}} = \frac{I_{\text{diode}}}{q} \quad (6.3)$$

Here is  $I_{\text{diode}}$  the photo current measured with an amp/ere meter (A). Note; here the CCD is shuttered while the photodiode is illuminated constantly by the light source.

The detector can also be configured as a photodiode. This is done by connecting an amp/ere meter to the substrate and the RD pin. For this another way to measure the quantum efficiency is developed. With this the quantum efficiency can be calculated with:

$$QE_{\text{CCD}} = QE_{\text{diode}} \frac{I_{\text{CCD}}}{I_{\text{diode}}} \quad (6.4)$$

With  $QE_{\text{CCD}}$  is the quantum efficiency of the CCD detector,  $QE_{\text{diode}}$  is the quantum efficiency of the photodiode,  $I_{\text{CCD}}$  is the current generated by the detector and  $I_{\text{diode}}$  is the current generated by the photodiode.

## 6.3 Procedure

### 6.3.1 Stability measurement of the tungsten lamp source

[Tull6] While doing the quantum efficiency measurements it was found that the source of the QE-rig was not bright enough to let light pass through the nr. 1 filter which has its peak at 350 nm. To make it possible to also measure this datapoint the current to the tungsten lamp was increased. With this minor change most of the specifications of the QE-rig will stay the same. The only thing one has to take into account is a change in warm-up time of the tungsten lamp. This is the time necessary for the tungsten lamp to stabilize its output. This warm-up time is measured by mounting a photodiode in front of the QE-rig connected to the multimeter. It is known that the source has the longest stabilisation time in the blue region of the spectrum. For this reason the filter with its peak at 400 nm is put in front of the source. At time  $t=0$  the tungsten lamp is switched on and the current that comes out of the photodiode is measured. The current is then measured after 1 minute and again after 2 minutes. From that point on the current is measured every 5 minutes. When the lamp has reached a stable current the data is plotted into a graph time vs. current.

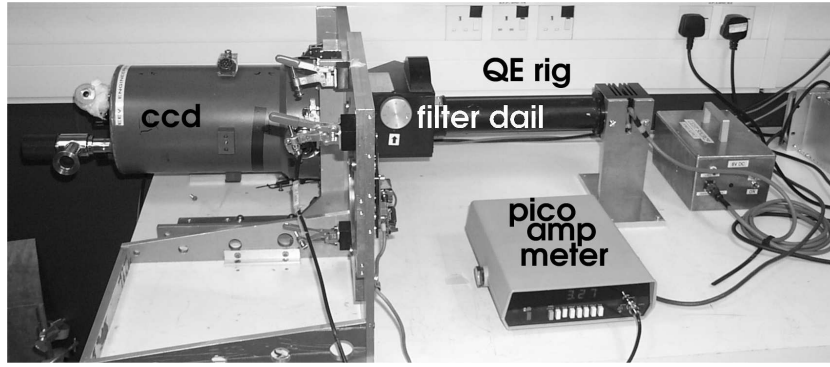


Figure 6.1: Quantum Efficiency rig in the detector lab located in the William Herschel Telescope

### 6.3.2 Quantum efficiency measurements

[Tull6] In this experiment the quantum efficiency rig located in the detector lab in the William Herschel Telescope is used (see fig. (6.1)). This rig is equipped with a 6V tungsten halogen lamp. A filter wheel is positioned in front of it which contains 8 different filters. Two apertures collimate the beam. One is positioned in front of the beam and one close to the CCD. This way a collimated beam is produced by the rig. At the CCD front the diameter of the beam is about 5.5 mm. 150 mm further downstream the beam has diverged to only 7 mm. The outer regions of the beam contain almost no signal at all. Because the beam has a very tight geometry there is much room for error in positioning a large photodiode in front of the beam. This should be placed at the same place the CCD is positioned while measuring the QE.

The QE measurement consists of firstly measuring the output of the rig through the different filters on the filter wheel with a well known photodiode which is connected to a pico-amp meter. Then the CCD is positioned at the same position in front of the QE rig. Again the output of each filter on the filter wheel is measured this time using the CCD. All CCDs can be configured as a photodiode by attaching a pico-ammeter between the substrate and the reset drain pin.

The darkcurrent is measured by attaching the pico-amp meter to the CCD and measuring the signal when there is no light coming out of the QE rig. The obtained signal is the darkcurrent of the CCD. This value should be subtracted from the signals measured by the CCD.

## 6.4 Results [engw]

### 6.4.1 The tungsten lamp

The relaxation time of the tungsten lamp used has been measured. The output current of the photodiode has been plotted against time while the tungsten lamp was shining on it through a narrow band filter of 400 nm. This graph is displayed in fig. (6.2).

At time  $t=0$  the source is switched on and shone on the photodiode. First a big spike is seen after which the current goes down in a rapid movement. After this the current goes up to 5.96 nA. It takes about 45 minutes to reach this stable level. To be on the safe side it is recommended to leave the source to warm up for one hour before beginning the quantum efficiency measurements.

### 6.4.2 SITE1

The quantum efficiency of the SITE1 detector has been measured inside the QE-rig in the detectors lab. The resulting graph is shown in fig. (6.3). The point of 350 nm is taken as the biaslevel since there is no light from the tungsten lamp that passes through the filter.

The quantum efficiency is high at the red end of the spectrum and becomes lower in the blue end.

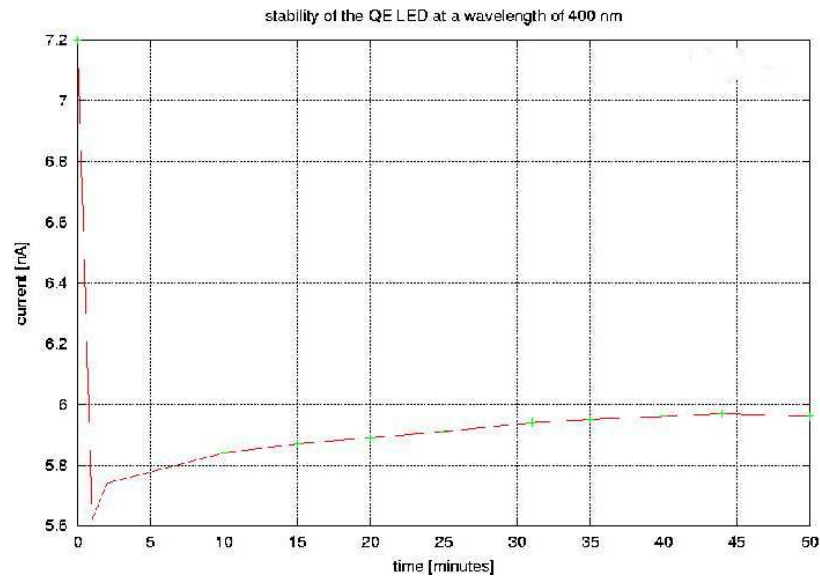


Figure 6.2: Stability of the QE source at a wavelength of 400 nm.

### 6.4.3 SITE2

The QE of the SITE2 detector has been measured in the QE rig at the detector lab located in the William Herschel Telescope. The problem with this detector is that it will keep a high darkcurrent for a long time after it is exposed to light. For this reason the detector has been kept in the dark for several hours. The resulting graph of the SITE2 quantum efficiency is shown in fig. (6.4).

### 6.4.4 TEK1

Also the TEK 1 has been measured in the QE rig in the William Herschel Telescope lab. Its quantum efficiency is shown in fig. (6.5).

The peak is at a wavelength of about 700 nm with a value of 64 %.

### 6.4.5 TEK5

The quantum efficiency of the TEK5 detector has also been measured. It is shown in fig. (6.5).

## 6.5 References

- [Tull6] [http://www.ing.iac.es/~eng/detectors/QC/QE\\_rig.htm](http://www.ing.iac.es/~eng/detectors/QC/QE_rig.htm), Simon Tulloch
- [Jane] Scientific Charge-Couptungsten lamp Devices, by James R. Janesick
- For more information on the Isaac Newton Group detectors:  
[engw] [www.ing.iac.es/Engineering/engweb6a.htm](http://www.ing.iac.es/Engineering/engweb6a.htm)



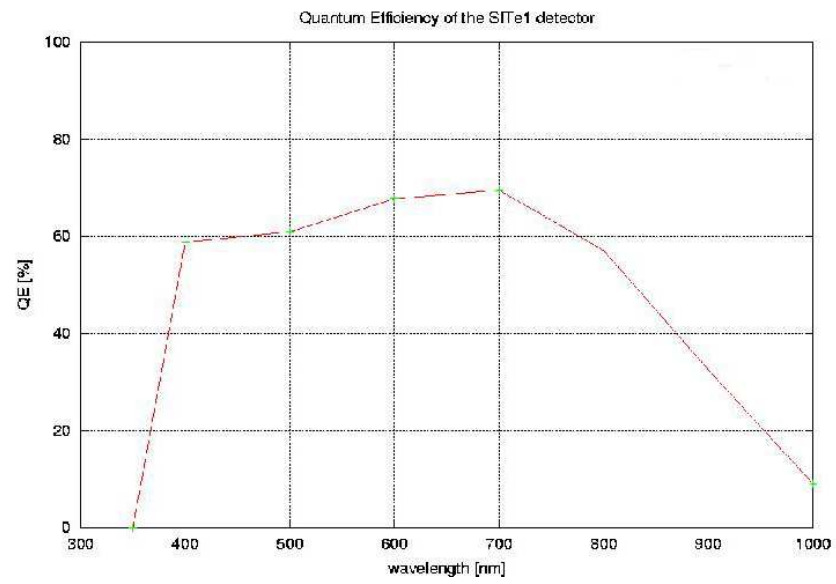


Figure 6.3: QE of the SITe1 detector.

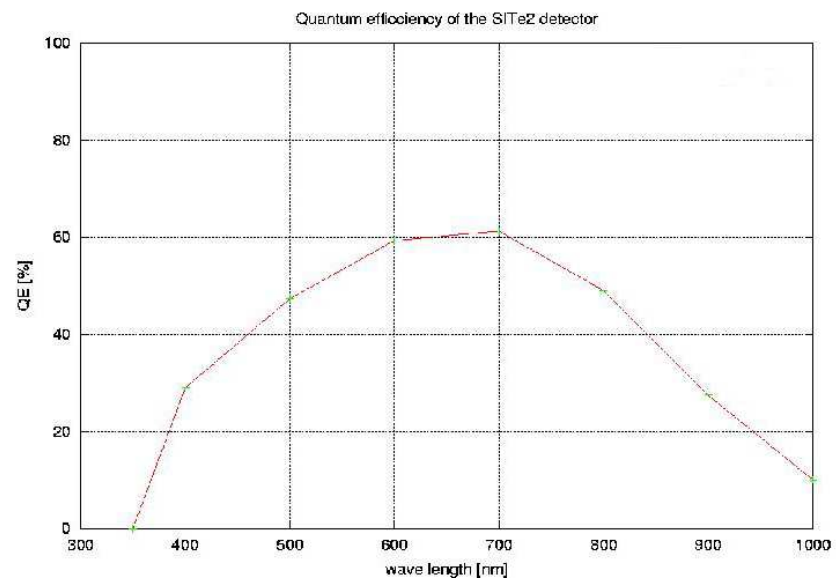


Figure 6.4: QE of the SITe2 detector measured at 28-1-2002.

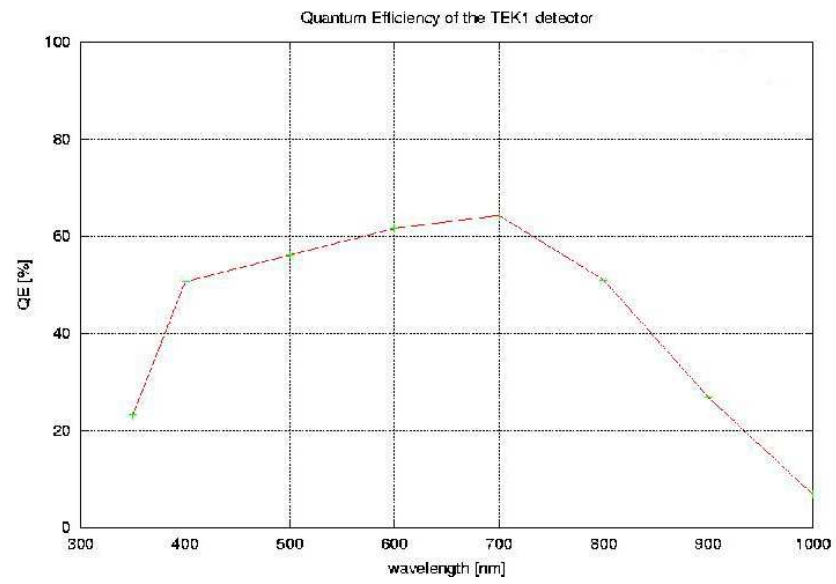


Figure 6.5: QE of the TEK1 detector.

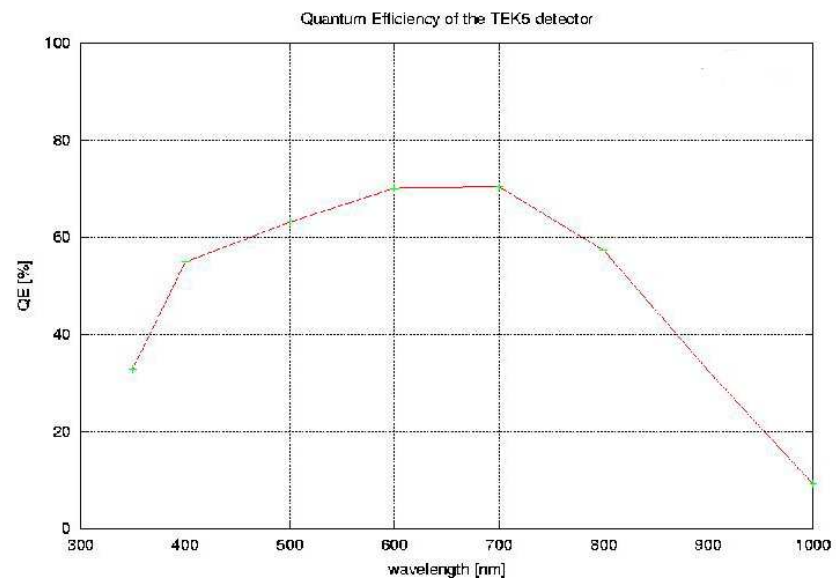


Figure 6.6: QE of the TEK5 detector.

## Chapter 7

# Measuring the influence of the shutter at short exposures on the Jacobus Kapteyn Telescope

### 7.1 Summary

The goal of this experiment is to see if there is any shadowing from the shutter in short exposures. Short exposures are necessary for photometric applications. An interference of the shutter can make images useless. On the Jacobus Kapteyn Telescope an iris type shutter with six blades is used. The shadowing which is produced by the shutter opening and closing will be a slight decrease of the light received on the edges of the CCD chip. The shutter speed is characterized with 22 ms to open and 33 ms to close. Expected is that this will give an interference with exposures under 1 second. The experiment is done by taking a 30 seconds exposure as a reference. A series of short exposures from 0.06 to 1 s are taken. These images are multiplied by  $(30/\text{exposure time})$  to get the same ADU count as the reference image. The image is then divided by the reference image. On several points on the resulting image the value is measured using IRAF. This data is put into a file which is plotted into a surface plot using *gnuplot*. On this surface plot the shadowing of the shutter can be detected as lower values at the edges. The shutter gives no noticeable interference for images with an exposure time longer than 1 second.

## 7.2 Procedure

Because in fast readout speed of the SITe2 detector is only linear to within 2 % for exposures below 25000 ADU, the images should stay under this limit. This is done by using the flatfield lamps with the correctly adjusted intensity and using a narrow band filter. The filter is only used to decrease the light intensity. The type of filter used is not of importance since the shutter behaviour is not wavelength dependent. At the Jacobus Kapteyn Telescope the flatfield lamps were set on level 10 and a NII filter was used to reduce the light intensity. A series of five 30 second exposures are taken and averaged to lower the noise. The resulting image will act as a reference image. Because the exposure time is much longer than the time required to open and close the shutter the effect of the shutter on the reference image is negligible. The reference image is followed by a series of images with short exposures. The exposure times will be around the exposure time for which the effect of the shutter will be detectable. These images are then multiplied by  $30/(\text{the exposure time})$  to get the same ADU count as in the reference image. They are then divided by the reference image. The signal of several points in the resulting image spread out into a  $20 \times 20$  matrix are measured and saved to a file. The resulting data is then plotted as a surface plot with x - pixelcoordinates in the x direction, y - pixelcoordinates in the y direction and the normalized signal is plotted in the z direction. If the shutter gives an even exposure the surface plot should be flat and normalized. If the shutter is interfering than this is seen as a decrease of in the z value at the edges of the surface plot.

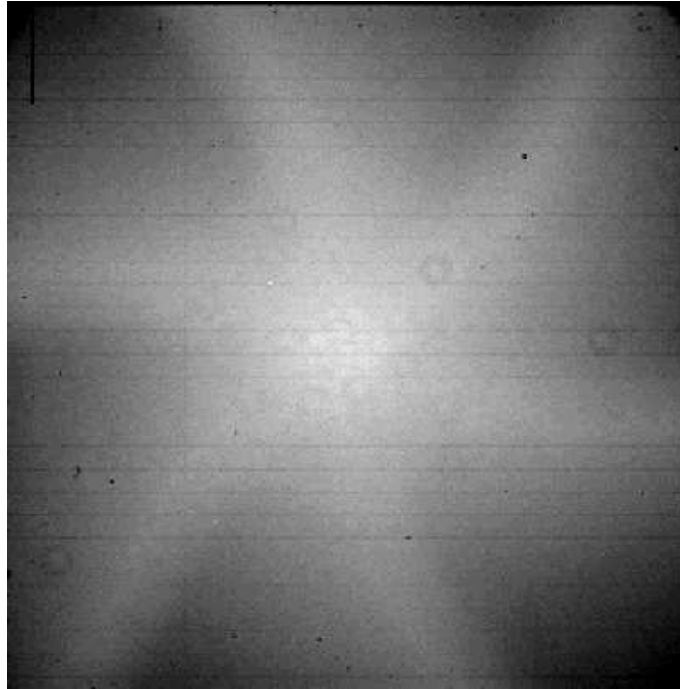


Figure 7.1: The jammed shutter on the Jacobus Kapteyn Telescope

In fig. (7.1) an image of the shutter on the Jacobus Kapteyn Telescope is seen. This image is taken as a normal flatfield when the shutter was jammed. The shape in which it opens is clearly visible as a star pattern. This star pattern is also the pattern that is expected to be visible in the surface plots due to the shadowing of the shutter.

## 7.3 Results

A series of 5 short exposures are taken. The exposure times used are: 0.06, 0.08, 0.11, 0.51 and 1.01 seconds. The surface plots are displayed in fig. ((7.2) - (7.6)).

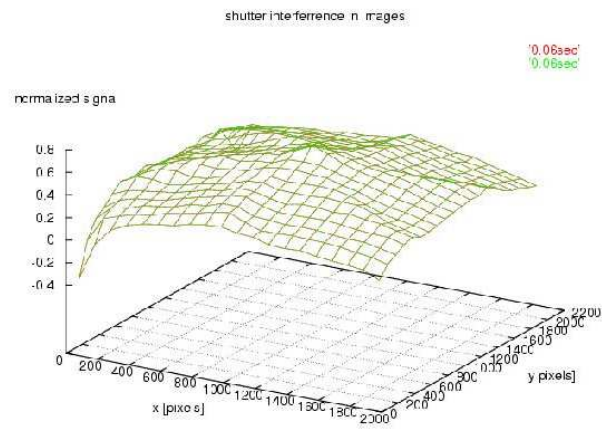


Figure 7.2: 0.06 sec exposure

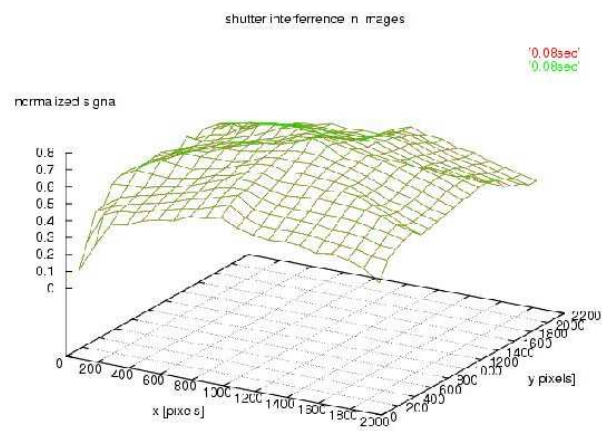


Figure 7.3: 0.08 sec exposure

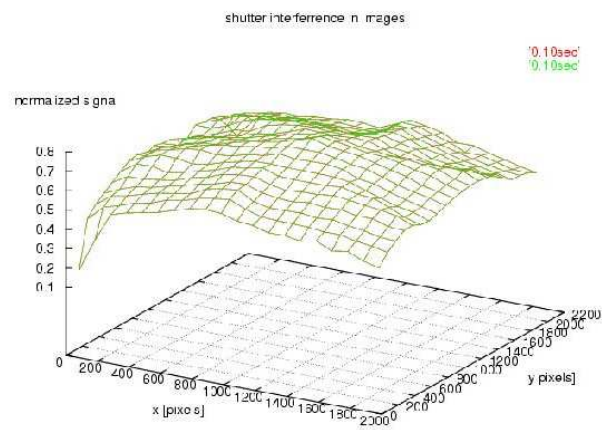


Figure 7.4: 0.10 sec exposure

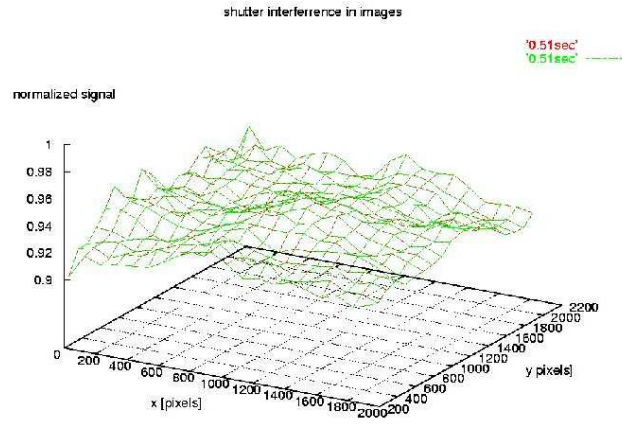


Figure 7.5: 0.51 sec exposure

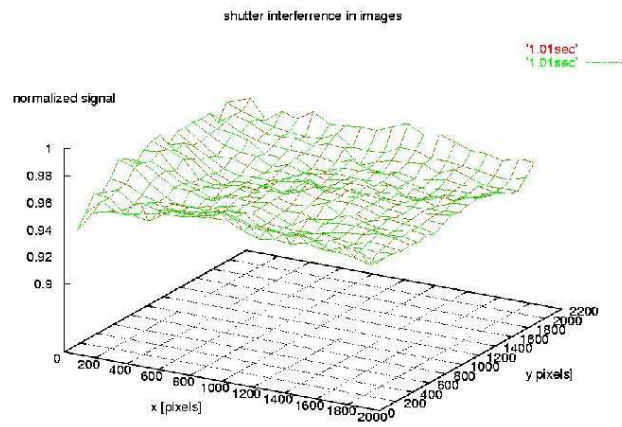


Figure 7.6: 1.01 sec exposure

The first three exposures show a star pattern in the surface. This is clearly due to the interference of the shutter. The edges are illuminated less than the center of the image. The star pattern shows the shape of the shutter when it opens as seen in fig. (7.1). In the 0.51 seconds exposure, the star pattern is still slightly visible. But the noise caused by it is within the noise level of the chip. In the 1 second exposure no interference of the shutter is visible. The fluctuations in the plotted surface are completely due to noise in the chip. The fact that the surface is not around unity indicates that a constant value is subtracted from the asked integration time to get the actual integration time. The surface of the 0.51 s exposure is 5 /

## Chapter 8

# Monitoring the bias level of several detectors

### 8.1 Summary

In this experiment the short- and long term fluctuations in the bias level of the different detectors is monitored. In December 2001 a detector report has been entered about the fact that the bias level of the detectors varies during the night. The detector report was about was the TEK4 on the William Herschel Telescope. The goal is to see if these problems persist and if yes to find the cause of these changes and to find out if this is a not known normal effect and how the bias changes over a period of time. The bias level is the amount of noise which is produced by the detector itself. This was thought to be stable. This is done by daily measurement of the bias levels in each of the images made in the previous nightly run. This is done for each detector which is used separately with a custom written IRAF script. The daily measurements are plotted into graphs for the short term fluctuations. After a period of 30 days the results are plotted into a graph to see the long term fluctuations. It seemed that the bias levels of all the detectors are not stable during the night. They can differ up to 5 % between exposures. This fluctuation is highly correlated with the temperature changes during night. This is probably because the electronics on the detector react to temperature changes.

## 8.2 Procedure

The procedure to measure the bias level is kept simple. First a short measurement has been done to look for certain causes for the change in bias level. One of the main factors is believed to be the temperature. So the temperature of the camera is also measured for each of the images. After the short term measurement a long term measurement is done on several detectors of the Isaac Newton Group. This is done to establish if the fluctuations are a normal phenomenon. And if they are how big the fluctuations normally are. For the long term measurement an IRAF script has been written that puts all the .fit files into a list. After this it reads all the images from that list, filters out the non science images like bias images. Then it measures the bias level from the bias region provided by the image header. This value is written to a file which has the name *detector\_chip\_readout\_speed*. In the beginning the script asks for the date (day of February since this experiment is executed in this month starting at the 1<sup>st</sup> of February) which is also written into the file. Every day of February all of the bias levels from all images taken the previous night are examined with this script. This way about 100-200 data points per night are gathered and a good database of the fluctuations in the bias level per detector is formed. After a month all the files that have been made are plotted with a plotting program. In these graphs the bias level is plotted against the day of the month so an accurate description of the fluctuations in the bias levels is provided.

## 8.3 Results

### 8.3.1 IRAF script

An IRAF script to measure the bias levels has been written. It asks the user only for the day of the month February to start. First through redirecting the UNIX `textbf` command to a file called `test` the program puts all the fits files into a list. Then this list is read and every image in that list is examined. First the program looks if it is a right kind of image. To avoid complications only the images which are taken from real objects are examined. It is possible that some flat field or dark frames affect their bias regions by e.g. saturation. This will result in a higher bias level. There are also images taken for test purposes which are also excluded just as images without bias regions. The filtering is done by looking into the image header and getting the type of the image. If it is the wrong type the program moves on to the next one. From the image header it also gets the time the image is taken. This value lies between -0.5 and 0.5. Negative before midnight and positive after. This value is added to the value entered at the beginning of the program. This is the value which is plotted on the time scale. With the bias region which is taken from the header the bias level is measured. A complication is that the bias regions provided by the header are not always correct which we assumed and checked for most cameras. Together with the time, temperature of the detector and the name of the image the bias value is put into a file which can be plotted.

### 8.3.2 Short term measurements

Two detectors have been monitored for the short term measurements. These are the TEK4 and the wide field camera of the Isaac Newton Telescope chip 1. The TEK4 detector and the wide field camera have been monitored for three days. The graphs of the measurements are shown in figures (8.1 a & b). In these graphs the bias level is plotted as a percentage of the average bias level from the whole period it is monitored. The temperature is plotted in the same way in the same graph. A strong correlation between the two graphs is visible. It is concluded that the temperature is the main cause of the fluctuations in the bias level; another cause can be interference of electronics but that is not explored further. There are differences on how the two detectors react to temperature changes. With the wide field camera when the temperature goes down the bias level goes down. With the TEK4 detector it is the other way around. When the temperature goes up the bias level goes down. Since they are different kinds of detectors with different electronics which have their own qualities this can be expected. The gaps between the areas of fluctuations are due to the fact



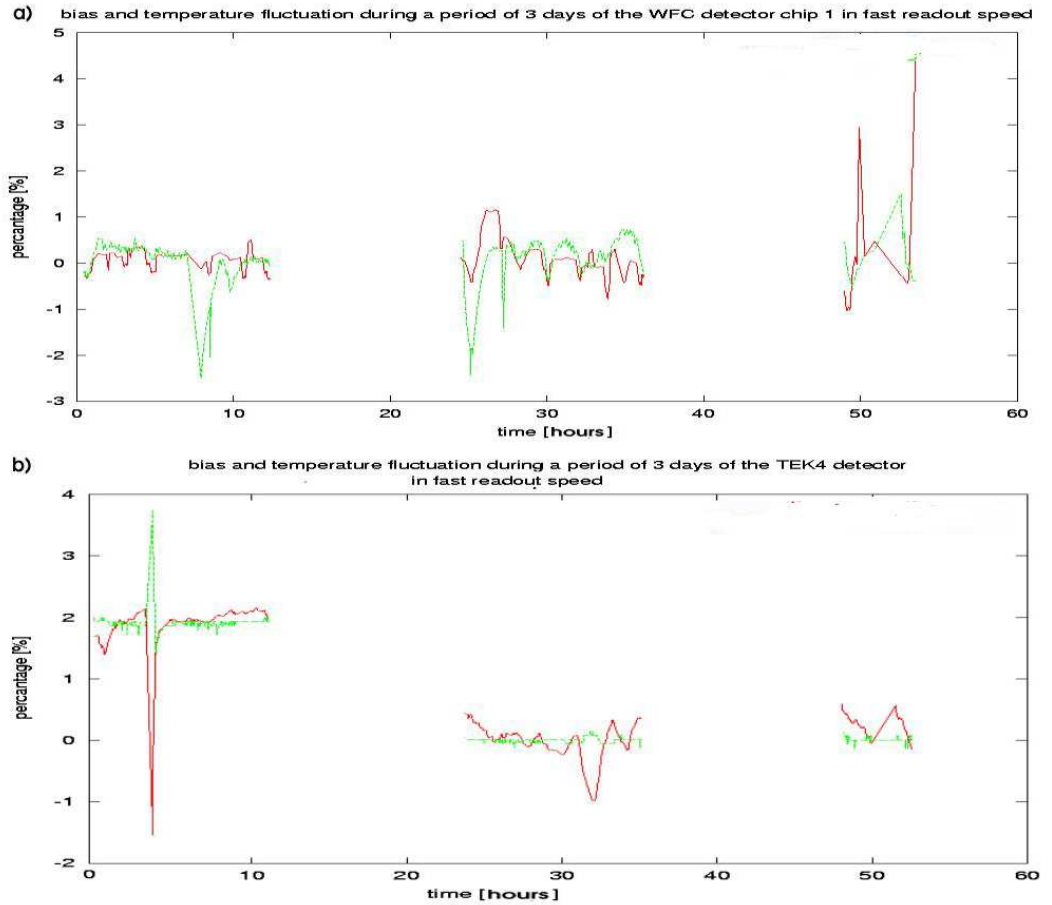


Figure 8.1: a) bias level fluctuations of the wide field camera of the Isaac Newton Telescope over a period of 3 days. b) bias level fluctuations of the TEK4 detector over a period of 3 days.

that it is daytime and no images are taken during this period of time. Since a lot of things happen with the telescope which can affect the bias levels no data is taken during these periods and the regions are excluded from the measurements.

### 8.3.3 Long term measurements

For this measurement several detectors have been monitored during a period of 30 days. Some of the detectors have been on the telescopes for the whole while others have been mounted for a shorter period. Since the images used were images taken that night by the observing astronomer there was no control over in which speed the images were taken or which detector was used that night. The cameras which have been used during the whole period are SITe2, TEK6 and the wide field camera on the Isaac Newton Telescope all in fast readout speed. The others have gaps in between because they were not used or were off the telescope.

The bias level fluctuations of the SITe2 detector are plotted in fig. (8.2a & b). In fig. (8.2a) the fluctuations in fast readout speed are shown. It is seen that over a long period they can vary from 2 % to -2.5%. This can even happen in a short period of time. This means the bias level can vary about 30 ADU. In fig. (8.2b)) the fluctuations in slow readout speed are shown. The fluctuations here are less aggressive meaning not as abrupt as in fast readout speed. Still they vary from 1.5 % to -2 % over a period of 5 days. This would give a fluctuation of about 25 ADU.

The bias level fluctuations of the wide field camera of the Isaac Newton Telescope chip 1, 3 and 4 in fast readout speed are plotted in fig. (8.3 a, b & c). The fluctuation of chip 2 is not plotted

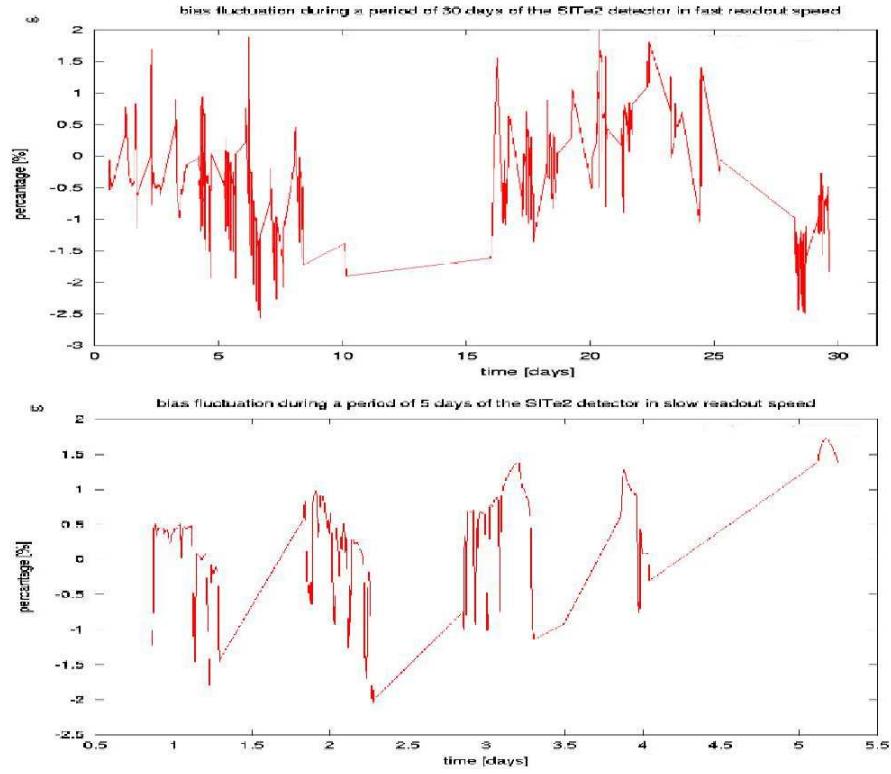


Figure 8.2: a) bias level fluctuations of the SITE2 detector in fast readoutspeed over a period of 30 days. b) bias level fluctuations of the SITE2 detector in slow readout speed over a period of 5 days

because there were problems which will be discussed later. It can be seen that the three plots of the different chips look similar. This is not surprising since all chips are located close to each other so the temperature variations are the same for each chip, although there are differences. The main difference is the amplitude of the fluctuation of the bias levels from the three chips. Chip 1 fluctuates from 1 % to - 1 %, chip 3 from 1 % to - 3 % and chip 4 from 3 % to - 1 %. Which would mean then measured in ADUs a fluctuation of chip 1: 30 ADU, chip 3: 60 ADU and chip 4: 70 ADU. This difference is explained by the minor differences in the chips electronics. They are all the same type of chip but minor differences in electronics will make them respond differently to the temperature fluctuations in small fashions. Above the fluctuations that are the same for every chip there are also fluctuations which are unique to each chip. These fluctuations are caused by the electronics or by the amount of light received close to the bias regions. The last reason is explained later.

In fig. (8.4) the data of the bias level measurement of chip 2 of the wide field camera is plotted. On this plot big spikes can be seen. These spikes remained after filtering all the for this measurement useless images. Some of the spikes are in the order of 100 % and some even as big as 1200 %. This required a closer inspection to find the cause of these spikes. After close examination of data the reason found was that the bias region which appeared in the image header was incorrect. It was partly located inside the image area so if it is used for bias level determination it would picked up signal from the image which could be stars or other bright objects. In the .dat file (the file where the DAS system gets the information to put in the image header) the correct region was provided. This means there was a problem in the transfer of the bias region information to the header. This was problem was not noticed until this time. Since the in the header specified bias regions are mostly used to measure the bias level the correct location of the bias region in of great importance and could affect measurements (as it did). The problem was noted to be rectified. The bias regions of the rest of the chips of the wide field camera were also examined and were correctly

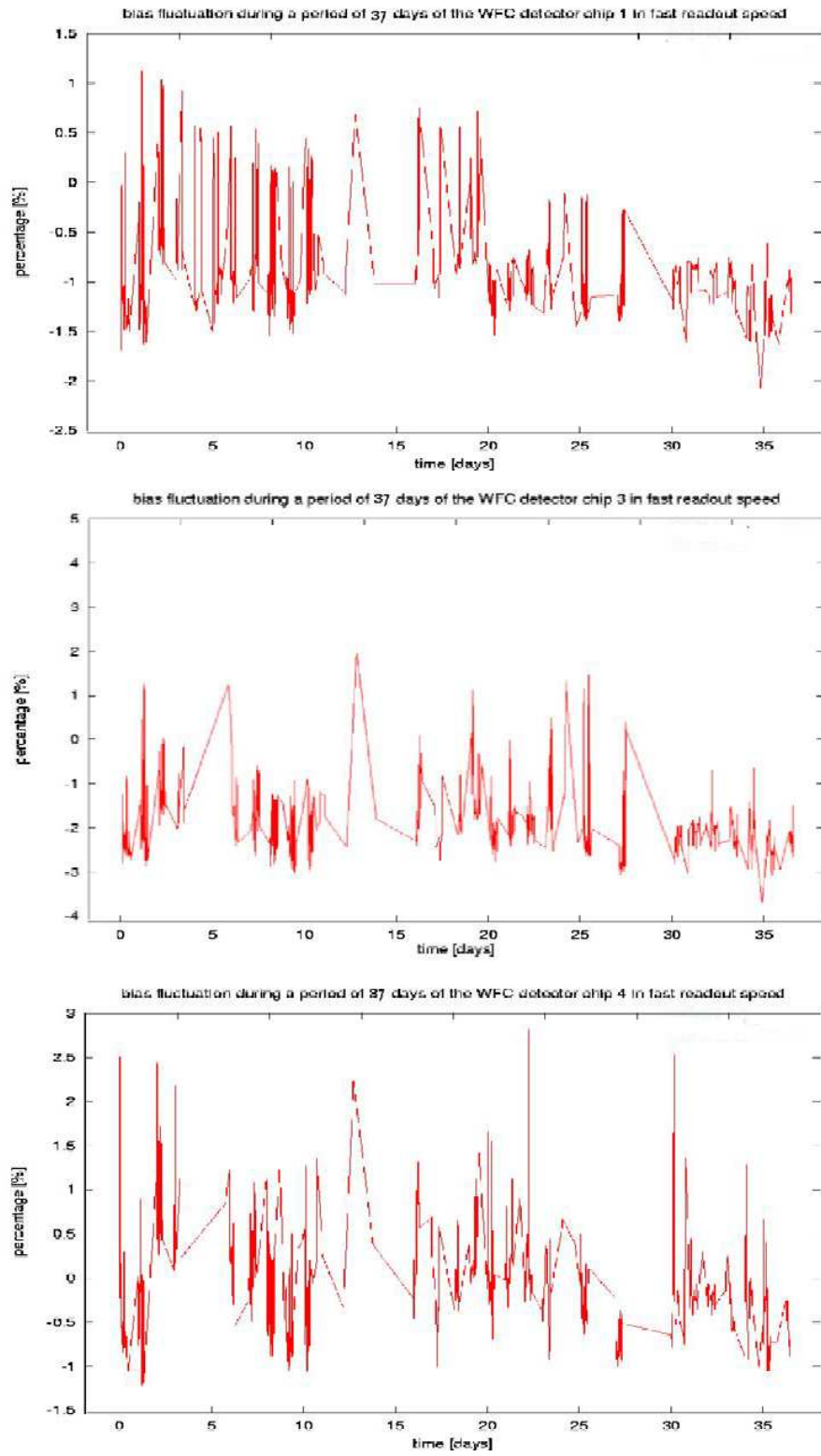


Figure 8.3: Bias level fluctuations of the wide field camera in fast readout speed over a period of 37 days. a) of chip 1. b) of chip 3. c) of chip 4.

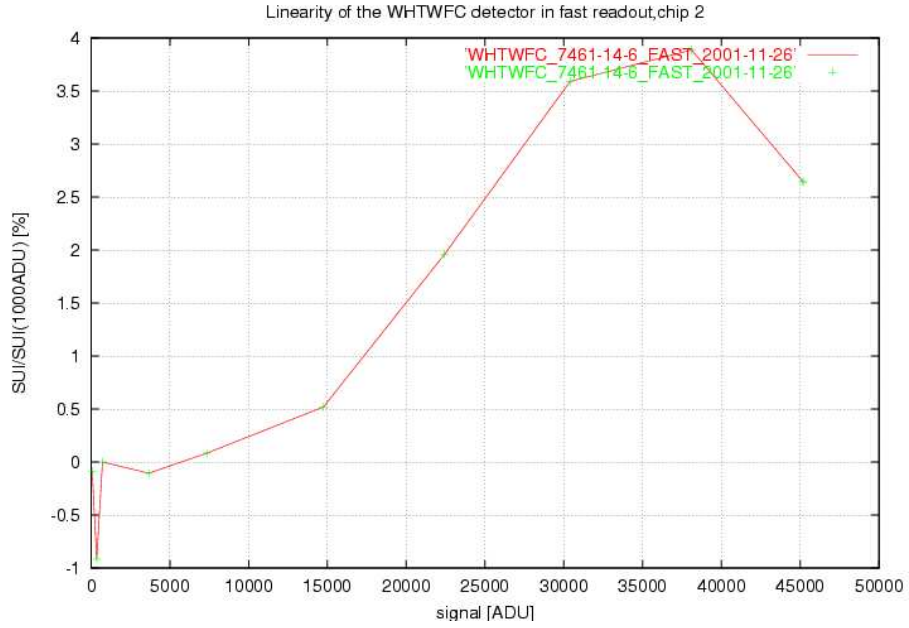


Figure 8.4: The bias level data of the chip 2 of the wide field camera of the Isaac Newton Telescope. Lots of spikes are seen which are too high. This indicates there is something not correct.

written to the image header.

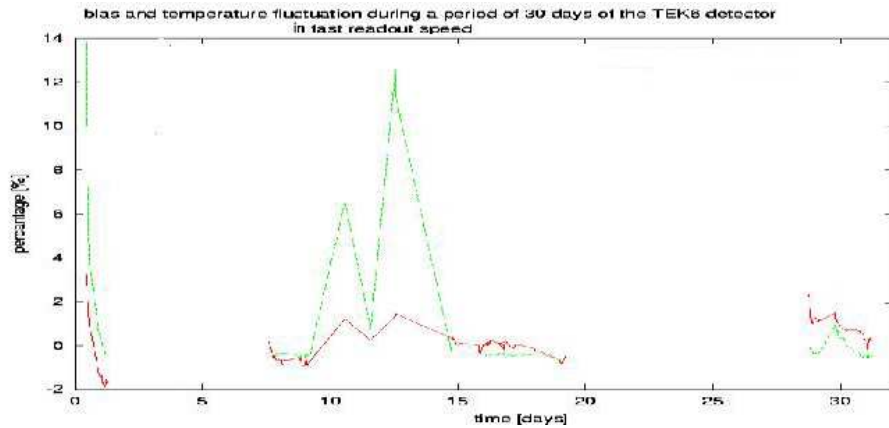


Figure 8.5: Bias level and temperature fluctuations of the TEK6 detector in fast readout speed over a period of 32 days.

In fig. (8.5) the bias fluctuations of the TEK6 detector are plotted. This camera was not used during the whole period it was monitored. The periods it was not used are excluded from the measurement since many things could have happened to the detector. All the data is still put in one graph to see how the bias level changed during this period. It seems that TEK6 is extremely sensitive to temperature changes. A change of 1 % in the temperature will result in a change of about 7 % in the bias level. The range over which the TEK6 detector changed is 3 % to -2 %; this is a variation of about 45 ADU.

In fig. (8.6) the biasfluctuations of the TEK4 detector are plotted. The detector was not used during a part of the observation as can be seen in the graph. The fluctuations of the TEK4 detector go from 1 % to -1 % which is a variation of 26 ADU.

In fig. (8.7a & b) the bias level fluctuations of the EEV12 detector in fast and slow readout

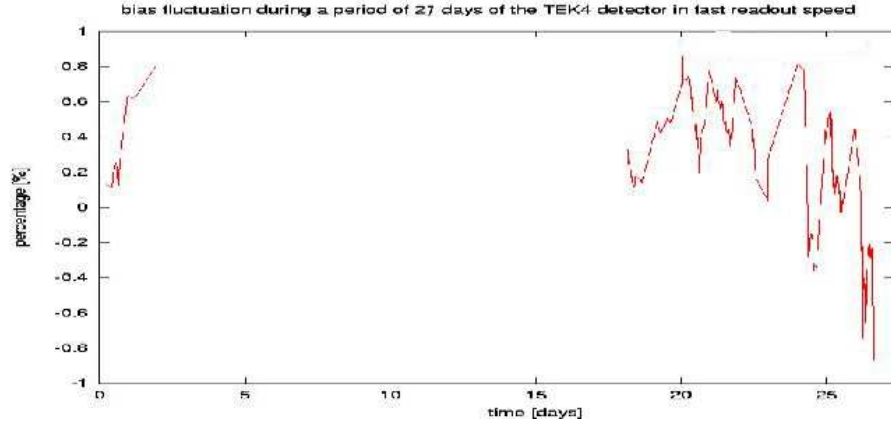


Figure 8.6: Bias level fluctuations of the TEK4 detector in fast readout speed over a period of 30 days.

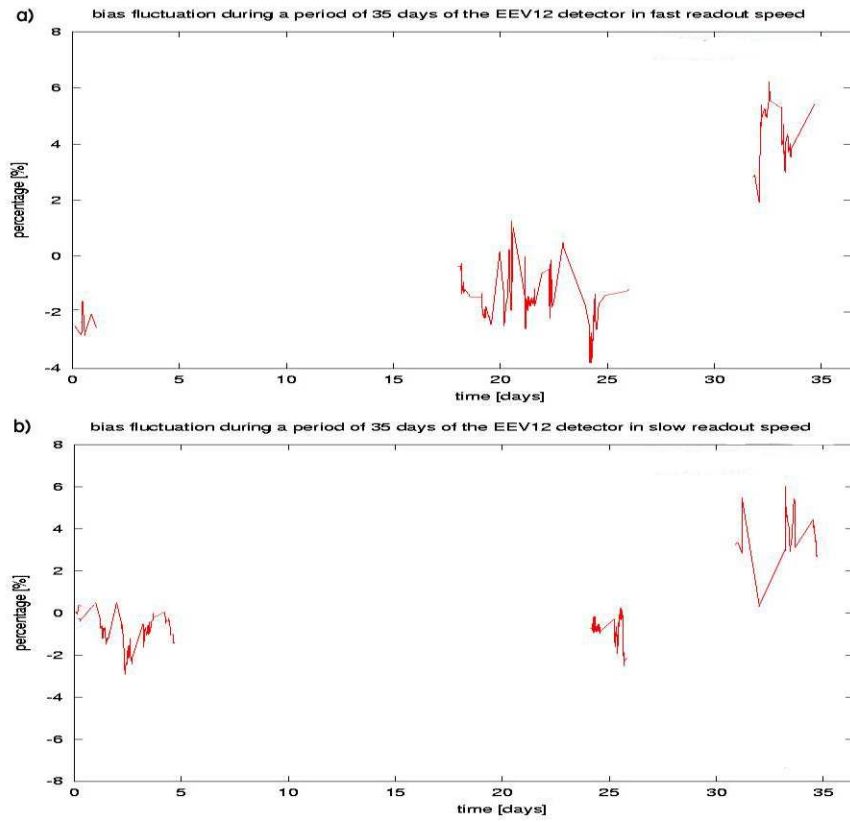


Figure 8.7: Bias level fluctuations of the EEV12 detector in fast readout speed over a period of 35 days.

speed are plotted. The fluctuations in fast readout speed go from -4 % to 6 %. This corresponds with a range of 75 ADU. In slow readout speed the fluctuations go from -3 % to 6 %. In this readout speed it corresponds to a range of 85 ADU. It seems that the EEV12 detector suffers a lot from fluctuations in the bias level.

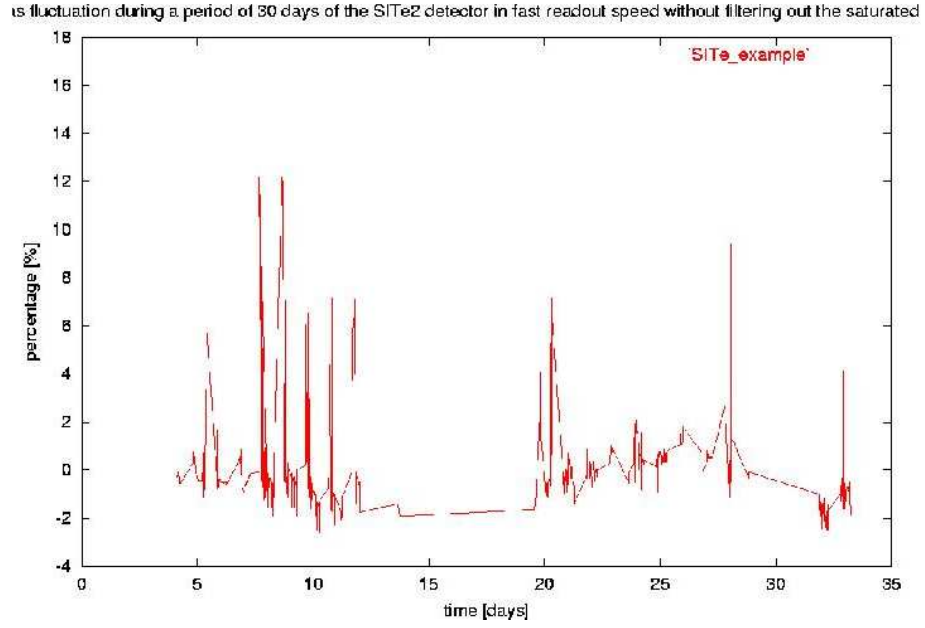


Figure 8.8: Bias level fluctuations of the SiTe2 detector in fast readout speed over a period of 30 days without filtering out the problem images.

### 8.3.4 Problems which came up during the measurements

During the long term measurements some problems in measuring the bias level turned up. In the biasfluctuations high spikes were observed (see fig. (8.8)). These spikes were too large to be real biasfluctuations and appeared with all of the detectors. After closer study of the images that produced these spikes three causes were found.

The first cause to be found was blooming on a large scale caused by saturated flat fields. When a flat field is exposed for a long period the chip can be saturated. This means that all of the wells of the pixels are full with electrons. Because full well is reached the excess electrons will flow over to the other pixels. These pixels can also be the pixels of the biasregion when the electrons flow out during readout. This produces extra charge in the bias regions which increases the signal in this area. What is measured at that point is the bias level plus an extra chargelevel produced by the excess electrons.

The second cause which was found was blooming on a small scale. If a star in the image is exposed to long the pixels where this star is located will saturate. Again this will produce full well and charge will leak into the nearby pixels. The bigger the saturation the more charge will leak into the nearby pixels producing a bigger area which is contaminated. Because the threshold in the vertical direction is lower than the threshold in the horizontal direction the charge will smear out in the vertical direction. This can produce long vertical trails which can reach into the biassection on top of the chip. Since this is also the biasregion which is put into the image header this is also the section which is mostly used in this experiment.

The third problem that turned up were stars close to the image edge (see fig (8.9)). As mentioned when there is a bright star on the image which is saturated charge can leak into the nearby pixels. If these stars are located close to the edge of the image area close to a biasregion it will not need much saturation to contaminate the biassection. The problem with this kind is that it is hard to see. Only a few pixels in the biassection are contaminated close to the bright star. But if the saturation is high enough it can affect the bias level to large extent. This kind of contamination can happen to all bias regions.

With all the graphs most of the spikes which are caused by one of these problems are filtered out. These problems can be of importance for further studies on the bias level. At Isaac Newton



Figure 8.9: A saturated star which is close to the biasregion. It is seen that the charge also leaks into the bias regions causing an increase in the average biassignal of this region.

Group the bias level measurements will become a part of the routine checks now. And also for observers these problems will be of importance while using the biassections to measure the bias level. As a precaution it is best not to saturate pixels on the chip. And to avoid the trail of the blooming stars it is best to use the bias regions which are on the sides of the chip.

## Chapter 9

# Wide Field Camera control on the Isaac Newton Telescope

### 9.1 Summary

Because the Wide Field Camera (WFC) on the Isaac Newton Telescope will be permanently on the telescope starting 2003, there should be some indication about the frequency that it is necessary to take the detector off for pumping. That is why the detector is monitored for a long period of time in this experiment. In this experiment the hold time of the cryostat pressure is measured by measuring it at least once a week. It seems that the pressure stays under tolerable levels for at least 44 days. Also the quantum efficiency of the LORAL type autoguider is measured every week. This is done because the quantum efficiency is enhanced with a coating which deteriorates in time. This enhancement is called thinning, (C.1) for more detail about the autoguider and the thinning process. Because of this deterioration it needs an air bath to restore the coating when it is worn off. During the period it was monitored no deterioration was observed.



## 9.2 Theory

### 9.2.1 Quantum efficiency

[WFCauto] Because the autoguider is mounted inside the cryostat next to the Wide Field Camera its quantum efficiency cannot be measured in the quantum efficiency rig with the photodiode. This is why the quantum efficiency is measured with a different procedure. This procedure uses the Wide Field Camera science chip #1 as a reference detector instead of the photodiode. This makes it more complicated to calculate the quantum efficiency of the autoguider then normal. Factors like differences in exposure time, pixel area and gain are to be taken into account. The way to derive the equations to calculate the gain is to find a constant factor for both chips. This is the light that falls on the detector per unit area and unit time calculated with eq. (9.1).

$$flux = \frac{S \cdot G}{QE \cdot A \cdot exp} \quad (9.1)$$

In this equation the QE is the quantum efficiency of the detector,  $A$  the area of the chip,  $exp$  the exposure time,  $S$  the signal measured in the images and  $G$  the gain of the chip.  $S$  is multiplied by the gain to get the electron count and it is divided by the quantum efficiency to change the light detected into the light received. This factor is constant for both chips and equal. When you set these equal and get the quantum efficiency of the autoguider to one side of the equation you get the formula to calculate the quantum efficiency of the autoguider which is (see eq. (9.2)):

$$QE_{ag} = \frac{QE_{science} \cdot A_{science} \cdot exp_{science} \cdot S_{ag} \cdot G_{ag}}{S_{science} \cdot G_{science} \cdot QE_{ag} \cdot A_{ag} \cdot exp_{ag}} \quad (9.2)$$

In this equation all the subscripts 'science' belong to the science chip and all the subscripts 'ag' belong to the autoguider.

## 9.3 Procedure

### 9.3.1 Quantum efficiency Wide Field Camera autoguider

The quantum efficiency of the autoguider on the Wide Field Camera is enhanced with a special coating (see (C.1)). This coating deteriorates over time. The coating can be restored with an oxygen flood. To make sure that the QE of the autoguider remains within tolerable levels the deterioration time of the coating must be known. This is measured by monitoring the QE of the autoguider. Because the Wide Field Camera autoguider does not fit into the quantum efficiency measurement rig quantum efficiency cannot be measured in the conventional manner. This is why another method has been developed. With the Wide Field Camera on the telescope a series of three 5.31 second dome flat field images are taken with the autoguider. Each of the dome flat field images is taken through a different filter. The U, B and V filter are used for this to cover the spectrum, with U = 360 nm, B = 430 nm and V = 542 nm. Because the filters have different pass bands, different intensities were necessary for each filter to get a sufficiently high ADU count. At the Isaac Newton Telescope these different intensities are achieved by using the different lamps in the dome. For the U filter all the bright lamps in the dome are switched on. For the B and V filter the dome lights are switched off and the lights in the corridors are switched on. These lamps need about 10 minutes to warm up to stabilize. With the science chip normal dome flats through each of the filters are taken and used as reference images. These are all taken with the same intensities as the autoguider flat field images and with an exposure time of 5 second. The chip #1 of the Wide Field Camera is used as the reference chip for this measurement because it is closest to the autoguider and will receive the same amount of light.

**Measurement script** A custom written IRAF script is used to analyze the images and calculate the quantum efficiency of the autoguider. It takes in a list of the images in the format:

filter:flat autoguider:flat science chip

It also asks for the number of days passed since the first of February since this is the day the experiment started. It starts a while-loop where it reads the data from the file. It takes the images and looks for the filter with which they are taken to set a different quantum efficiency of the science CCD, which is wavelength dependent. It then measures the signal from the autoguider image from a specified region and the signal from the science image from a specified region. Of course it also measures the bias level from the bias region which is declared in the image header. The specified image regions where it measures the signal are chosen in such a way that they are closest to the used bias region and defect free. This is done as a precaution so they receive the same amount of light. The regions are:

$$\begin{aligned}\text{signal region autoguider} &= [260:300,80:140] \\ \text{signal region science chip} &= [970:1500,3500:4000]\end{aligned}$$

After the bias is subtracted from the signal the quantum efficiency is calculated using eq. (9.2). Then the outputs are selected by the filter used with the image. The outputs of each filter and the quantum efficiency of the science chip are displayed in tab. (9.1).

Table 9.1: Filters with the quantum efficiency of the science chip and the output used by the script.

filter	quantum efficiency science chip	output
U	53	quantum efficiency_U_ag
B	81	quantum efficiency_B_ag
V	81	quantum efficiency_V_ag

After it has written the data it continues to the next line of the file. If all the files are done the program displays the quantum efficiency of the autoguider with each filter on the screen and thanks the user. The data from the files can then be plotted with the quantum efficiency of the autoguider of a specified wavelength versus time in days.

### 9.3.2 Pressure

Since the Wide Field Camera needs to be on the telescope for long periods of time the hold time of the cryostat must be known. During pumping of the detector it cannot be used on the telescope, since the WFC is the only detector of the Isaac Newton Telescope this should be done as efficient as possible. To measure the hold time the pressure of the detectors cryostat has been monitored for a period of two months. This pressure is plotted versus time to see the pressure decay with time.

## 9.4 Results

### 9.4.1 Quantum Efficiency Measurements

The quantum efficiency of the autoguider for the three wavelengths has been measured during a period of 42 days. The results are plotted in fig. (9.1).

In fig. (9.1) it is seen that the quantum efficiency of the autoguider stays nearly constant during the period it is observed. This means the quantum efficiency is stable and a normal dry flood when the detector is pumped is more than sufficient to keep the quantum efficiency of the autoguider at tolerable levels. The increase of quantum efficiency in the beginning in the U band is most likely due to temperature effects.

### 9.4.2 Pressure

The pressure of the Wide Field Camera cryostat has been monitored for a period of 44 days. The results are plotted in fig. (9.2).

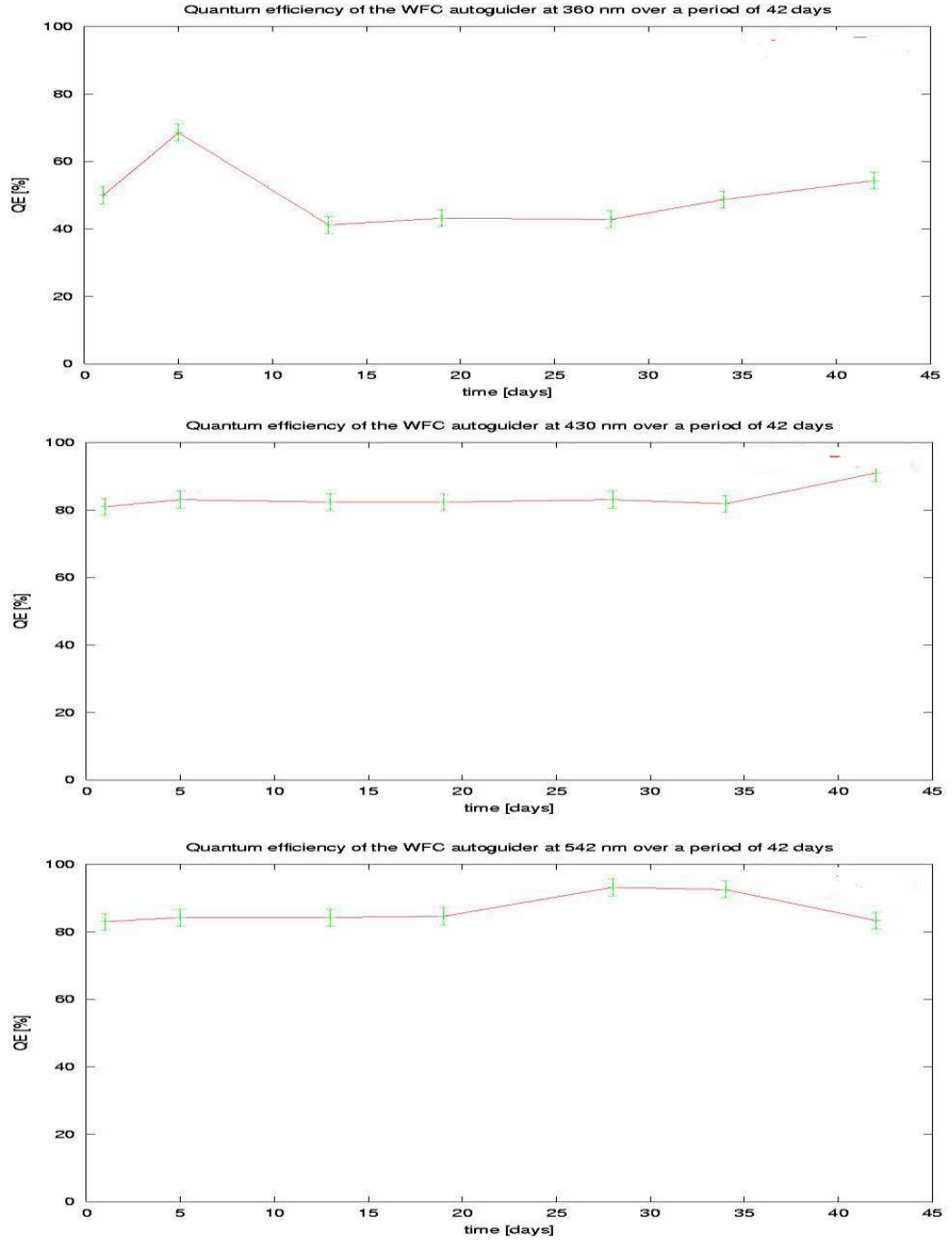


Figure 9.1: Quantum efficiency decay of the autoguider on the Wide Field Camera over a period of 42 days.

After 25 days the pressure begins to fluctuate and increases. But the cryostat pressure does not reach the critical pressure of  $1 \cdot 10^{-4}$  for at least 44 days. The fluctuations are most likely due to temperature changes and absorption of molecules by the getter. It is not explored further due to lack of time. As a conclusion it is possible to leave the Wide Field Camera on the telescope for 44 days. After this the pressure will reach the value of  $1 \cdot 10^{-4}$ . It is best to repump the detector each month but as an exception longer periods, up to 44 days, are possible.

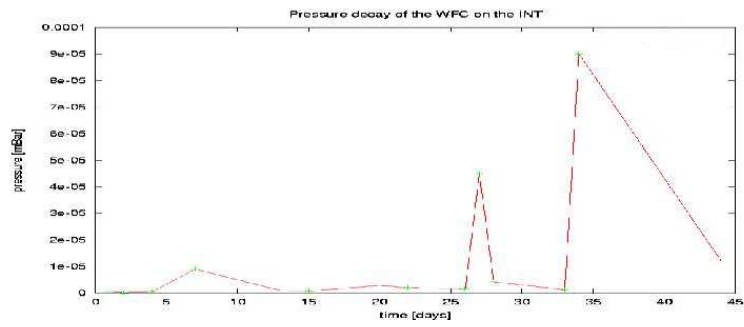


Figure 9.2: Pressure decay of the Wide Field Camera cryostat over a period of 45 days.

## 9.5 References

- [WFCauto] [http://www.ing.iac.es/~eng/detectors/intwfc\\_ag/int\\_wfc\\_auto.htm](http://www.ing.iac.es/~eng/detectors/intwfc_ag/int_wfc_auto.htm)
- [Jane] Scientific Charge-Coupled Devices, by James R. Janesick

## Chapter 10

# Temperature survey on the detectors of Isaac Newton Group

### 10.1 Summary

In this experiment the temperature control in the ULTRADAS system is calibrated for all of the detectors. The temperatures of the CCD detectors are monitored with a platinum resistor. This resistor changes its resistance with temperature. First the Pt resistor is calibrated with temperature to find the temperature coefficient of these devices. This is found to be  $0.41 [\Omega/K]$ .

Second the resistance of the Pt resistor inside the cryostat is measured to calculate the temperature inside the cryostat. This is then compared with the temperature provided by the system.

Third a temperature calibration unit is designed which simulates temperatures of 196 K and 152 K. This calibration unit is connected to the controller so these simulated temperatures are provided to it.

It seemed that the temperature of the cryostats were not monitored correctly. This was due to a design flaw in the measuring circuitry and a fault in the software. The design flaw in the circuitry is removed and the software is being changed. Luckily the faults were such that the detectors were still operating on efficient temperatures. So no increase in dark current should be visible in images taken earlier.

## 10.2 Electronics

### 10.2.1 Temperature electronics within the detector

A wire diagram of the electronics is shown in appendix (D.1). The most important part is the *Wheatstone bridge* which acts as a first order noise filter. With this circuit the temperature of the CCD chip is measured. The main part is the platinum resistor (Pt). This resistor changes its resistance with temperature. It is calibrated to have a resistance of  $100\ \Omega$  at  $273.15\ \text{K}$ . When the temperature goes down the resistance goes down. What the temperature coefficient is of the resistor depends on the kind of resistor is being used. There are two kinds, one with a temperature coefficient of  $0.38\ \Omega/\text{K}$  and one  $0.41\ \Omega/\text{K}$ . The relationship between resistance and temperature is linear in the range of  $30\ \text{K}$  to  $873\ \text{K}$ . The range in which the resistor is used inside the cryostat is well within this range.

The signal of the temperature circuitry inside the detector is send to the controller were it is amplified. This is done by the circuitry shown in appendix (D.1.2). This circuitry contains a non-inverting amplifier with a gain of 47.

## 10.3 Procedure

### 10.3.1 Calibrating the platinum resistor

For all the detectors the same kind of resistor is used to measure the temperature. To calibrate the resistors a spare resistor is used. This is possible because of the linearity and accuracy the resistors are operating at. And it is assumed that the difference in resistance of the wires is negligible. The resistor is first put in iced water, which is exactly  $273.15\ \text{K}$ , and the resistance is measured. This should be precisely  $100\ \Omega$  since the resistors are manufactured this way. Any offset of this value is caused by a bias caused by the resistance of the wires. Then the resistor is put in liquid nitrogen. Since the measurement is done at the observatory where the atmospheric pressure is  $750\ \text{mbar}$ , the boiling point of nitrogen ( $75.1487\ \text{K}$  [Kaye]) is lower than the boiling point at sea level. This difference should be taken into account in the measurement. In here the resistance it measured again and the bias value is subtracted. With these two points the temperature coefficient of the resistor can be calculated. When this value is known the gains of all of the Pt resistors are known since the same resistors are used in all cryostats.

### 10.3.2 Temperature measurement with the DVM

To see if the DAS gives a correct value of the temperature of the CCD chip while it is at the preferred operating temperature, the resistance of the Pt resistor inside the cryostat has to be measured when the detector is at this temperature. The DVM (or multimeter) has to be connected to the F and E pins of the temperature plug on the cryostat (see appendix (D.1)). For this a cable is designed which fits on the temperature plug and connects the DVM. The operating temperature inside the cryostat can then be calculated with the reading of the DVM and the temperature coefficient of which is measured in the previous measurement. This value should be compared with the value which is provided by the DAS.

### 10.3.3 Temperature test box

To measure the temperature coefficient and offset which is used by the controller to calculate a temperature a test box has to be built (see fig. (10.1)). This test box should have the same circuitry as with which the temperature is measured inside the cryostat. The only difference is that the platinum measurement resistor is replaced by two resistors with fixed values. With a button it is possible to switch between the two values. The temperature that correspond to the two resistor values can be calculated with the temperature coefficient that is measured in the previous section.

The test box is connected with the controller to simulate the thermometer inside the cryostat. With the switch on one of the two values of resistance the temperature given on the screen is

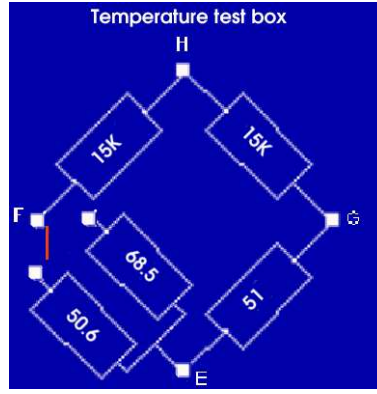


Figure 10.1: Temperature test box.

measured. This is also done for the second setting. Since the Pt resistor is linear the equation used in the software is also linear, so two points are sufficient.

## 10.4 Results

### 10.4.1 Calibrating the platinum resistor

The resistance of the Pt resistor has been measured in ice water which should give 100  $\Omega$ . The value measured was 100.3  $\Omega$  which gives a bias of 0.3  $\Omega$ . The resistance in liquid nitrogen was 19.8  $\Omega$ . The vapour pressure of nitrogen is 0.084 K/kPa [Kaye]. This gives at 750 mbar airpressure a boiling point of 75.1 K. With these numbers the calculated temperature coefficient of the used Pt resistor is 0.407  $\Omega/K$  with an offset of  $-11.05$  at  $T=0$  K. This gives:

$$T = 2.46 * R + 27.19 \quad (10.1)$$

### 10.4.2 Temperature measurements

Five detectors underwent the temperature measurements. SITe2, TEK4, wide field camera, EEV13 and EEV12. The offset at the operating temperature was measured with the DVM and the temperature coefficient and offset used by the DAS are measured with the temperature testbox. All results are shown in table (10.1).

Table 10.1: Offset between the real operating temperature and indicated temperature by the DAS.

detector	operating temperature DVM	operating temperature DAS	difference
SITe2	136.0 K	146 K	10 K
TEK4	149.2 K	147 K	-2 K
WFC	121.7 K	137 K	15 K
EEV13	137.4 K	144 K	7 K
EEV12	118.8 K	160 K	41 K

The temperature coefficient and offset that are used by the DAS are measured with the temperature test box. With that information the used equation by the DAS per detector is calculated. The results are tabulated in table (10.2)

Table 10.2: Equations used by the DAS to calculate the temperature of the CCD.

detector	equation $G[\Omega/K] * T + O[K]$	difference temperature coefficient $\Delta G[\Omega/K]$	difference in offset $\Delta O[K]$
SITe2	$T=2.6*T-44$	$0.2 K/\Omega$	-63 K
TEK4	$T=1.1*T+71$	$1.4 K/\Omega$	44 K
WFC	$T=2.4*T-12.5$	$0 K/\Omega$	-40 K
EEV13	$T=1.2*T+60.8$	$1.2 K/\Omega$	34 K
EEV12	$T=1.1*T+93.5$	$1.3 K/\Omega$	66 K

## 10.5 Consequences

Resulting from these measurements a closer look was taken to the circuitry of the temperature measurements by Simon Tulloch. He discovered that there was a design fault in the amplifier circuitry inside the controllers. Since the Op-Amp has too high a gain, fluctuations occur at the end of the amplifier circuit. These fluctuations are oscillatory and large in amplitude. The DAS takes a value in these fluctuations to calculate the temperature. This way there is no correlation between the actual temperature and the temperature displayed on the screen since it is measured from the noise rather than from the actual signal. To counter these fluctuations a 100 nF capacitor should be put in the negative feedback of the Op-Amp as shown in fig.(10.2)

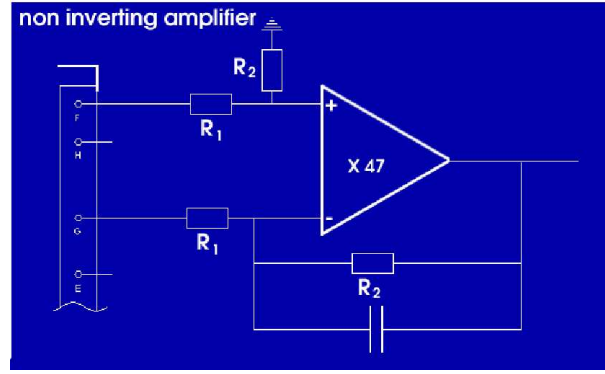


Figure 10.2: Changed temperature measurement circuitry inside the controller.

With this change in the circuit the fluctuations in the output voltage disappear. The DAS system still did not display the correct temperature but this was due to errors in the software. This still has to be repaired. It is a concern that the detectors have operated for so long with faulty temperature measurement systems. A reassuring fact is that the temperatures of the detectors were all operating at the preferred temperature or operating at a lower temperature. So there is no indication for high dark currents in the past.

## 10.6 References

- [temp] [www.ing.iac.es/~eng/detectors/temperature\\_sense/ccd\\_temperature\\_wiring.html](http://www.ing.iac.es/~eng/detectors/temperature_sense/ccd_temperature_wiring.html)
- [Horo]The art of electronics, Horowitz and Hill
- [Kaye] Tables of physical and chemical constants, Kaye & Laby



# Appendix A

## Useful reading

### A.1 Documents

- A beginner's guide to Using IRAF, Jeanette Barnes
- Learning Perl, by Randal L. Schwartz
- Programming Perl, by Larry Wall, Tom Christiansen & Randal L. Schwartz
- Solid State Image Sensors, Terminology, Eastman Kodak Company Microelectronics Technology Division, Rochester, New York 14650-2010
- gnuplot 3.5 User's Guide. Andy Liaw & Dick Crawford, Feb. 27, 1995

### A.2 Weblinks

- [www.ing.iac.es](http://www.ing.iac.es)
- [www.ing.iac.es/~smt/CCD\\_Primer/CCD\\_Primer.htm](http://www.ing.iac.es/~smt/CCD_Primer/CCD_Primer.htm)
- [vela.ing.iac.es/Engineering/engweb6a.htm](http://vela.ing.iac.es/Engineering/engweb6a.htm)
- [www.ing.iac.es/~eng/detectors/QC/qc.htm](http://www.ing.iac.es/~eng/detectors/QC/qc.htm)
- numerical recipes: [www.nr.com/](http://www.nr.com/)
- FTOOLS: [heasarc.gsfc.nasa.gov/docs/software/ftools/ftools\\_menu.html](http://heasarc.gsfc.nasa.gov/docs/software/ftools/ftools_menu.html)
- FITSIO: [heasarc.gsfc.nasa.gov/docs/software/fitsio/fitsio.html](http://heasarc.gsfc.nasa.gov/docs/software/fitsio/fitsio.html)
- Simbad: [simbad.u-strasbg.fr/sim-fid.pl](http://simbad.u-strasbg.fr/sim-fid.pl)
- IDL: [www.dfanning.com/documents/programs.html#toc](http://www.dfanning.com/documents/programs.html#toc)
- idlastro: [gsfc.nasa.gov/other\\_url.html](http://gsfc.nasa.gov/other_url.html)
- PGPLOT: [www.astro.caltech.edu/~tjp/pgplot/](http://www.astro.caltech.edu/~tjp/pgplot/)

# Appendix B

## IRAF scripts

### B.1 IRAF script to find the defect on the SITe2 detector

```
#October 4 2001
#Author:Richard Hijmering
#procedure to find and fale the defects in a flatfield.
#originaly designed for the sit2 defects

## This program maps the defects a CCD chip. It was initially designed for
## the SITe2 detector. It workes with the assupmtion that a defected pixel
## will reseave less light then a good pixel. This way the charge (and ADU
## value) of that pixel will be less then from the good pixels that surround
## the bad pixel. It look to every pixel seperately and measures the value,
## then it creates a 10X10 pixel box arround it and measures the mean value
## of that box. The two values are compaired. If the value of the examined
## is 10
## coordinates and the value is stored in a file. This file can that be used
## to plot a map of the defect. Programs as gnuplot or excel can be used for
## this task.
procedure finddefects(flat1a, outputa,x_starta,x_enda,y_starta,y_enda,xb1a,xb2a,yb1a,yb2a)

string flat1a {prompt="filename flatfield image 1"}
string outputa {prompt="filename output"}
int x_starta {prompt="put in the lower x-value of the image"}
int x_enda {prompt="put in the higher x-value of the image"}
int y_starta {prompt="put in the lower y-value of the image"}
int y_enda {prompt="put in the higher y-value of the image"}
int xb1a {prompt="give lower x coordinate in bias region"}
int xb2a {prompt="give higher x coordinate in bias region"}
int yb1a {prompt="give lower y coordinate in bias region"}
int yb2a {prompt="give higher y coordinate in bias region"}

#put in the file name of the image and the bounderies of the image so the bias
#will be excluded
#put in the output filename and the a box within the biasframe so the mean
#can be substracted from the whole image

begin

flat1=flat1a
```

```

string  flat1,flat1_temp,flat2_temp,output
string  coordin1,coordinb, coordinc,coordin2
int      x1,x2,y1,y2          # coordinates for the field around the pixel examined
int      x_start,x_end,y_start, y_end      # The boundaries of the image
int      x,y,xb1,xb2,yb1,yb2      # The pixel coordinates that is examined
                                           # n is number of defects recorded, av is average
                                           # value of depth
real      mn1,mnb1,mnpoin,av,p,q,rat,n,r  # q is number of pixels examined,
                                           # q is total depth defects
                                           # ratio is percentage of defects in ccd

output=outputa
x_start=x_starta
x_end=x_enda
y_start=y_starta
y_end=y_enda
xb1=xb1a
xb2=xb2a
yb1=yb1a
yb2=yb2a
flat1_temp = mktemp ("tmp$FG")
flat2_temp = mktemp ("tmp$FG")

coordinb=flat1+"{" + xb1 + ":" + xb2 + "," + yb1 + ":" + yb2 + "}"
imstatistics (coordinb,fields="mean", lower=INDEF, upper=INDEF,format=no) | scan(mnb1)
#calculates the bias of the flatfield

imarith (flat1, "-", mnb1, flat1_temp)      #subtracts the bias from the flat field

y=y_start      #sets y to the startpoint in the y direction
n=0
mn1=0
mnpoin=0
q=0
r=0
p=0
while (y≤y_end)      #while loop to go through the y coordinates
{
x=x_start      #sets x to the startpoint in the x direction
while(x≤x_end)      #while loop to go through the x coordinates
{clear
print ("point that is currently examined:")
print(" y=",y," x=",x)      #showes the program is running and the coordinates
x1=x-5      #makes a box around the examined coordinate
y1=y-5
x2=x+5
y2=y+5

if (x1≤x_start)      #makes shure no bias region is included
{x1=x_start      #if there is the 10X10 box is moved so
x2=x_start+10}      #the biasregion is excluded
if (x2≥x_end)
{x2=x_end
x1=x_end-10}
if (y1≤y_start)
{y1=y_start
y2=y_start+10}

```

```

if (y2≥y_end)
{y2=y_end
y1=y_end-10}

coordin1=flat1_temp+"{" + x1 + ":" + x2 + "," + y1 + ":" + y2 + "}"
coordin2=flat1_temp+"{" + x + ":" + x + "," + y + ":" + y + "}"

imstatistics (coordin1,fields="mean", lower=INDEF, upper=INDEF,format=no) | scan(mn1)
#calculates the mean of the area that surrounds the pixel
imstatistics (coordin2,fields="mean", lower=INDEF, upper=INDEF,format=no) | scan(mnpoint)
#calculates the mean of the pixel

if (mnpoint≤0.90mn1)      #looks if the value of the pixel comes under the threshold
{q=(mn1-mnpoint)/mn1
print(x," ",y," ",q,>>output)
n=n+1
r=r+q
}
p=p+1
x=x+1 }
y=y+1 }

rat = (100n)/p
av=r/n

imdelete (flat1_temp, ver-, >&"dev$null")
imdelete (flat2_temp, ver-, >&"dev$null")

clear
print (p,"pixels examined")
print (n,"defects found")
print (rat,"
print (av,"is the average value of the depth/signal")
print ("")
print ("Thank you for using this script")
print (" have a nice day")

end

```

## B.2 IRAF script to measure the darkcurrent

```

#procedure to measure the dark current after a light exposure
#original designed for the INT wfc
#author: Richard Hijmering
#23-11-2001

##
## As a input this script uses a file with a list of images that are taken
## after the dome flood. The first image in the list must be the image with
## wich the CCD is flooded. This is to get the preciese time the experiment
## is started. First the program prompts for the file of the list of
## images, number of chips in the detector and the name of the output
## file. After that it sets some of the variables to useable variables.
## From the first image it gets the time the experiment is started. From
## all of the other images it also gets the time that image was taken so
## the program can calculate the expired time after the domeflood. Then
## the program goes in a while loop where it first reads a line from the
## file. After this it goes in a while loop to do the calculations on each

```

```

## of the extension of the image file separately. In that while loop in sets
## the coordinates and preforms a imstatistics to measure the mean of the
## pixalvalue in the image region in the underscan region. These two values
## are subtracted from eachother to get the signal. From the image header
## it gets the gain of the chip so it can convert the measured value from
## ADU's into electrons. Together with the exposure time it calculates the
## number of electrons per hour measured all of this is saved to files.
## Every chip has his own file where the calculated data will be stored.
## At the end it plots a graph on the screen the last chip examined for
## the user to look if no problems have occured.
##

```

```

procedure fdwfc(filea,k,outputa)

```

```

real      k      {prompt="number of chips"}
string    outputa {prompt="output"}
string    filea
string    *list1
begin

#setting the parameters
int      x1,x2,y1,y2,n,i,l
real      mn,mnb,mna,time,min,exp,timeb
real      stddev,stddevb,factor
string    image,output,outputb,imageb,flood,floodb,file_name,img
string    coordin
string    coordinb,bias
file_name=filea
n=k
output=outputa
x1=300
x2=400
y1=300
y2=400
i=0

#getting the first image from the list.
#This is the images where the detector is flooded
list1=file_name
l=fscan(list1,img)
flood=img

#starting a while loop that goes through the images
while(fscan (list1,img) !=EOF)
{
image=img

#starting a while loop that goes through the different chips
while (i<n)
{ i=i+1

#setting some coordinate strings
imageb=image//"{"/i//"}"
print (imageb)

#getting the biasregion from the image header
imgget(image=imageb,param="BIASSEC")
bias=imggets.value
coordin =imageb//"{"/x1//":"/x2//",""/y1//":"/y2//"}"

```

```

coordinb=imageb//bias
outputb=output//"/i/"
floodb=flood//"/i/"

#measuring the value of the pixal and the mean of 10x10 box
imstatistics (coordin,field="mode,stddev", lower=INDEF, upper=INDEF,format=no) | scan(mn,stddev)
imstatistics (coordinb,field="mode,stddev", lower=INDEF, upper=INDEF,format=no) | scan(mnb,stddevb)

# getting some additional information from the image header
imget(image=imageb,param="UTSTART")
time=real(imgets.value)
imget(image=floodb,param="UTSTART")
timeb=real(imgets.value)
min=(time-timeb)*60
imget(image=imageb,param="EXPTIME")
exp=real(imgets.value)
imget(image=imageb,param="GAIN")

#calculating from ADU in the images to electrons per hour
factor=real(imgets.value)*(3600/exp)
mna=(mn-mnb)*factor

#Setting a boundery so the values can't be lower than 0 (for nice getting graphs)
if (mna<0)
{mna=0}

# printing to output
print(min,"",mna,"",sqrt(stddev*factor+stddevb),>>outputb)

#printing a message to standert output if a chip is below 10 e/hour
if (mna<10)
{print (imageb, "is finished")}
}
i=0
}

#plotting one of the graphs on the screen for a quick check
graph(input=outputb,logy=yes,xlabel="time {min}",ylabel="darkcurrent {e/hour}", title="darkcurrent
decay after a 2 min domeflood through a filter, on the ")

#thanks the user
print ("Thank you for using this script, have a nice day")

end

```

## B.3 IRAF script to find the maximum

```

#procedure to find a 10 by 10 box with the highest intensity
#original designed for the Linearity checks
#author: Richard Hijmering
#13-12-2001

## This procedure finds a 10 by 10 box where the pixel value is the largest.
## it was original designed to find the maximum intensity for the linearity
## checks.
##
## First it looks in wich quarter in the X direction of the image the brightest

```

```

## region is. Then it sweeps the image in the x-direction with a band 10 pixels
## wide to find the brightest band. After this it does the same in the
## y-direction. The crossection of the two band is the 10 by 10 region wich is
## the brightest. This region has an error of about 3 pixels from the real
## brightest region. But the mean of the region will have an error less then 1 ##

procedure fm(imagea)

string      imagea      {prompt="image"}

begin

string      image, coordin,region,x1string,x2string,y1string,y2string,time1
int         x_end, y_end, x, y, x1_old, x2_old, y1_old, y2_old,x1,x2,y1,y2,n,nr_runs
real        mn, mn_old,mn1,mn2

image=imagea

#####
#gets the size of the chip

imget(image=image,param="i_naxis1")
x_end=real(imgets.value)-1
imget(image=image,param="i_naxis2")
y_end=real(imgets.value)-1
#####
#here it searches in wich part the bright spot is in, in the x direction.
#At the first run it takes the half of the image.
#At the second run the quarter of the image.
#And so on.

nr_runs=2
mn_old=0
y1=1
y2=y_end
x=1
n=0

while (n<nr_runs)
{
#calculates the mean of the left part
x1=x
x2=x_end/2

coordin=image/"["//x1/" ":"//x2/" ","//y1/" ":"//y2/" "]"
imstatistics (coordin,field="mean", lower=INDEF, upper=INDEF,format=no) | scan(mn1)

#calculates the mean of the right part
x1=x_end/2
x2=x_end

coordin=image/"["//x1/" ":"//x2/" ","//y1/" ":"//y2/" "]"
imstatistics (coordin,field="mean", lower=INDEF, upper=INDEF,format=no) | scan(mn2)

if (mn1<mn2)      # |      |x|      |x|
{
x=x_end/2+x/2
}
}

```

```

if (mn1>mn2)      # |x|      |x|      |
{
x_end=x_end/2+x/2
}
n=n+1}

#####
#begins a while loop to searche the chip in the x direction

while (x < x_end)
{
x=x+5
x1=x-5
x2=x+5

if (x1<1)      #makes shure no bias region is included
{x1=1
x2=10}
if (x2>x_end)
{x2=x_end
x1=x_end-10}

coordin=image/"["//x1/" ":"//x2/" ","//y1/" ":"//y2/" "]"
imstatistics (coordin,field="mean", lower=INDEF, upper=INDEF,format=no) | scan(mn)
#checks if this mean is greater then all of the previous measured means.
if (mn>mn_old)
{
mn_old=mn
x1_old=x1
x2_old=x2
}

}

#####
x1=1
x2=x_end
y=1
n=0

#here it searches in wich part the bright spot is in, in the y direction.
#At the first run it takes the half of the image.
#At the second run the quarter of the image.
#And so on.

While (n<nr_runs)
{
y1=y
y2=y_end/2
#calculates the mean of the lower part
coordin=image/"["//x1/" ":"//x2/" ","//y1/" ":"//y2/" "]"
imstatistics (coordin,field="mean", lower=INDEF, upper=INDEF,format=no) | scan(mn1)

#calculates the mean of the higher part
y1=y_end/2
y2=y_end
coordin=image/"["//x1/" ":"//x2/" ","//y1/" ":"//y2/" "]"
imstatistics (coordin,field="mean", lower=INDEF, upper=INDEF,format=no) | scan(mn2)

```



```

if (mn1<mn2)      # |      |x|      |x|
{
y=y_end/2+y/2
}
if (mn1>mn2)      # |x|      |x|      |
{
y_end=y_end/2+y/2
}
n=n+1
}

#####
#begins a while loop to searche the chip in the y direction

mn_old=0
while (y < y_end)
{
y=y+5
y1=y-5
y2=y+5
x1=1
x2=x_end

if (y1<1)      #makes shure no bias region is included
{y1=1
y2=10}
if (y2>y_end)
{y2=y_end
y1=y_end-10}

coordin=image+"[/x1/":"/x2/"/","/y1/":"/y2/"/]"
imstatistics (coordin,field="mean", lower=INDEF, upper=INDEF,format=no) | scan(mn)
#checks if this mean is greater then all of the previous measured means.
if (mn>mn_old)
{
mn_old=mn
y1_old=y1
y2_old=y2

}

}

x1string=x1_old
x2string=x2_old
y1string=y1_old
y2string=y2_old

region="[/x1_old/":"/x2_old/"/","/y1_old/":"/y2_old/"/]"

print(region)

print ("Thank you for using this script, have a nice day")

end

#####

```

#### B.4 IRAF script to find the SUI value with a electron count nearest to 1000 electrons

```

#procedure to find the SUI at a 1000 ADU
#original designed for the Linearity checks
#author: Richard Hijmering
#13-12-2001

## This procedure find the value of SUI at a 1000 electrons. For that it
## needs a list of images and the region where the maximum value of the
## light source is. The program then calculates the mean of this region
## calculate the number of electrons excited. It does this for all the
## images in the image file It compares the calculated value of excited
## electrons with the value of the previous image. If it is nearer to nr_e
## electrons then the previous one then it will remember this value. So the
## closest value to 1000 electrons will be remembered.

procedure fsui1000(regiona,filea)

string      filea      {prompt="file"}
string      regiona    {prompt="region"}
string      *list1

#####
begin

real        mn1,mnb1,mn1a,expo,SUI1000a,gain,electron_old,nr_e
string      image
string      coordin1,coordinb1,bias,region
string      file_name,img,SUI1000
real        exposure

region=regiona
file_name=filea
nr_e=1000
electron_old=1000000000000000

#begins a while loop to read the images from a file and executes the calculations
list1=file_name
while(fscan (list1,img,exposure) !=EOF)
{
image=img
expo=exposure

#####
#imstatistics on the images to measure the mean

imget(image=image,param="BIASSEC", value="")
bias= imgets.value
imget(image=image,param="GAIN")
gain= real(imgets.value)

coordin1=image//region
coordinb1=image//bias

imstatistics (coordin1,field="mean", lower=INDEF, upper=INDEF,format=no) | scan(mn1)
imstatistics (coordinb1,field="mean", lower=INDEF, upper=INDEF,format=no) | scan(mnb1)

#####

```

```

#The calculations to get the SUI and the error

mn1a=(mn1-mnb1)

if (((mn1a/gain)-nr_e)*(mn1a/gain)-nr_e)<electron_old)
{
SUI1000a=(mn1a/expo)
electron_old=(mn1a/gain-nr_e)*(mn1a/gain-nr_e)
}
}

print(SUI1000a)
SUI1000=SUI1000a

print ("Thank you for using this script, have a nice day")
end

```

## B.5 IRAF script to measure the linearity

```

#procedure to measure the linearity of a detector
#original designed for the Linearity checks
#author: Richard Hijmering
#13-12-2001

## With this script the line arity of a CCD-detector can be measured. Three
## kinds of output can be selected, 1. output in ADU's, 2. output in SUI,3.
## output in SUI/SUI at 1000 ADU. This is going in the folwing way

#####

## It askses the user for two files. One with the images taken for the linearity
## measurement and one with the coordinates of the light spot and from the bias
## region. Then it askses for the name of the output file. As last it askses the
## user wich of the three kinds of output format he/she wants.

## After this the programs sets some parameters.

## The program reads the coordinates of the flash point from a file.
## Then it enters a while loop where it reads the image and the flashtime
## from a file one every cycle of the while loop ubntill no more images
## are left. The program uses imstatistics to measure the mean value and
## the standert deviation at flashpoint and in the underscanregion. When
## option 1 is choosen then these are the outputvalues (value in ADU's).
## If optios 2 is choosen then the mean value will be devided by the
## flashtime to give the output in SUI. The error is calculated then by
## error propargation If option 3 is choosen the SUI must be devided by the
## SUI value at 1000 adu's. To calculate this a nother while loop is started.
## This one goes through al of the calculated values again and devide them
## through the SUI value closest to the value at a 1000 ADU's. This value is
## then returned to the given output valuefile. The outputfilename is in the
## following format:

##          detector_chipname_readoutspeed_date

## After the calculations the program plots a graph on the screen and saves
## this plot as a detector_chipname_readoutspeed_date.ps file

```

```

procedure linearity(filea,regiona,SUI1000a)

string      filea      {prompt="file"}
real        SUI1000a    {prompt="SUI1000"}
string      regiona     {prompt="region"}
string      *list1

#####
begin

real        mn1,mnb1,mn1a,expo,SUI,SUI1000,SUIperc
real        stddev1,stddevb1,err,det
string      image,output,datafile,output_temp,title1
string      coordin1,coordin1a,coordinb1,coordinb1a
string      detector,date,speed,chipname,bias,region,psfile
string      file_name,img
real        exposure
int         l

#####
#declaring some variables
SUI1000=SUI1000a
region=regiona

file_name=filea
list1=file_name

#####
#Here it gets the information to name the output file

l=fscan (list1,img,exposure)
image=img
imget(image=image,param="DETECTOR", value="")
detector= imgets.value
imget(image=image,param="DATE-OBS", value="")
date= imgets.value
imget(image=image,param="CCDSPEED", value="")
speed= imgets.value
imget(image=image,param="CCDNAME", value="")
chipname= imgets.value

output_temp= detector/"_"//chipname/"_"//speed/"_"//date
print("#","Signal", " ", "Signal in SUI", " ", "error", " ", "flashtime", " ", "bias", " ", "image", >> output_temp)

#####
#starting a while loop through al the images. It is ended at the end of the file
list1=file_name
while(fscan (list1,img,exposure) !=EOF)
{
image=img
expo=exposure

#####
#imstatistics on the images to measure the mean

imget(image=image,param="BIASSEC", value="")
bias= imgets.value

coordin1=image//region

```

```

coordinb1=image//bias
imstatistics (coordinb1,field="mean,stddev", lower=INDEF, upper=INDEF,format=no) | scan(mn1,stddev1)
imstatistics (coordinb1,field="mean,stddev", lower=INDEF, upper=INDEF,format=no) | scan(mnb1,stddevb1)
#####
#The calculations to get the SUI and the error

mn1a=(mn1-mnb1)

SUI=mn1a/expo
SUIperc=100*(SUI-SUI1000)/SUI1000
err=0.2
#####
#Here it writes the information to a file

print(mn1a," ",SUIperc," ",err," # ",expo," ",mnb1," ",image,>>output_temp)
}

#####
#plots a graph on screen and in a .ps file

title1="linearity of the "//detector//" detector, chip "//chipname//", "//speed//", "//date
graph(input=output_temp,xlabel="exposure level {ADU}",ylabel="diviation from SUI _(1000ADU)
{
graph(input=output_temp,xlabel="exposure level {ADU}",ylabel="diviation from SUI _(1000ADU)
{
psfile=output_temp//".ps"

mv ("sgi*",psfile)

clear

#####
#print a message to the user about the outputfile format.
print ""
print "#####"
print ("all is done")
print ""
print ("the graph is names in the following sintext:")
print (" detector_chipname_speed_date.ps")
print "#####"
print ""

print ("Thank you for using this script, have a nice day")

end

#####

```

## B.6 IRAF script for the linearity measurements

```

#procedure to autmate the linearity checks.
#original designed for the Linearity checks
#author: Richard Hijmering
#13-12-2001

## This procedure will measure and calculate the linearity of the detectors.
## For that it needs a list of all the images taken with there flashtime.

```

```

## First it calles the procedure fm. This finds a box of 10 by 10 where the
## intensity of the pixels is the highest.

## Then it calles upon the procedure fsui1000, this finds the value of SUI
## at a 1000 ADU
## ##Then it calles upon the procedure linearity what calculates the linearity
## by a method sugested by Thomas Augustijne ##
procedure autolin(filea)

string      filea
string      *list1

begin

string      file_name,region,img
real        SUI1000
int         l

file_name=filea

#####
#Here it reads the file file_name and gives the value to fm. fm takes it and
#finds the region with the highest intensity

print ""
print ("finding 10X10 area where the intensity is the highest")

list1=file_name
l=fscan(list1,img)
fm(imagea=img) | scan(region)

print ("this area is:")
print(region)

#####
#here it calles upon fsui to find the SUI at 1000 ADU
#takes the file_name and the region
#the output is SUI at 1000

print ""
print ("finding the ADU value where the electroncount is 1000 electrons")

fsui1000(filea=file_name,regiona=region)|scan(SUI1000)

print ("this value is:")
print(SUI1000)

#####
#Here it calles upon linearity to calculate the linearity
#It takes the file the region and the SUI at 1000 ADU
#The output is a file with three columns. The mean (ADU), the SUI as a
#percentage of SUI at 1000 ADU and the exposuretime

print ""
print ("measuring the linearity of the CCD")

linearity(filea=file_name,regiona=region,SUI1000a=SUI1000)

#####

```

end

## B.7 An IRAF script to measure the biaslevels from the detectors.

```
#procedure to measure the biaslevels
#author: Richard Hijmering
#19-02-2002

procedure biaslevel(datuma)

real datuma {prompt="date of march"}
string
list1

#####
begin

string      file_name,img,image,value,bias,detector
string      output_temp1,coordinb1,coordin1,chipname,speed,date,cat
real        T,time1,time,totmean,mnb1,Ttot,stddevb1,datumb,datum
int         n

#####
# All fit files in the directory are written to the file "test"
!ls .fit>test

totmean=0
Ttot=0
file_name="test"
datumb=datuma
datum=datumb

#####
# Starting to read all the files from the file "test" one file per run
list1=file_name
while(fscan (list1,img) !=EOF)
{
n=1
image=img/"["/n/"]"
# getting the information from the image header
imget(image=image,param="OBSTYPE", value="")
value=imgets.value
# if the image has a target it is examined
if ( value == "TARGET" )
{
imget(image=image,param="DETECTOR", value="")
detector= imgets.value

imget(image=image,param="CAT-NAME", value="")
cat= imgets.value
# if image is a test image the loop is broken and started
# again with the next image
if (cat == "TEST")
{next}

imget(image=image,param="DATE-OBS", value="")
date= imgets.value
```

```

imget(image=image,param="CCDSPEED", value="")
speed= imgets.value
imget(image=image,param="CCDNAME", value="")
chipname= imgets.value
imget(image=image,param="CCDTEMP", value="")
T= real(imgets.value)
imget(image=image,param="UTSTART", value="")
time1= real(imgets.value)
imget(image=image,param="BIASSEC", value="")
bias= imgets.value
# if the image has no biasregion the loop is broken and started # again with the next image
if (bias=="[0:0,0:0]") {next}

if (time1>12)
{
time1=time1-24
}

#calculates the precise time in days
time=datum+time1/24
output_temp1= "/home/rh/scriptie/biaslevel/2month_check/"//detector//"- " //chipname//"- " //speed

coordinb1=image//bias
imstatistics (coordinb1,field="mean,stddev", lower=INDEF, upper=INDEF,format=no) |scan(mnb1,stddevb1)

totmean=totmean+mnb1
Ttot=Ttot+T

#prints information to the screen for the user to check
print ("With detector : ",detector,"-", n)
print ("on time: ",time)
print ("the biasvalue was: ",mnb1)
print("#","time"," ","mean"," ","error"," ","temp"," ","image",>>output_temp1)
print(time," ",mnb1," ",stddevb1," ",T," ",image,%%output_temp1)

# If the examined detector is the WFC all the other chips are also examined by this loop
if (detector=="WFC")
{
# a while loop to run through all the chips of the detector
while(n!=4)
{
n=n+1
image=img//"[n//]"
# getting the information from the image header
imget(image=image,param="OBSTYPE", value="")
value=imgets.value
# if the image has a target it is examined
if ( value == "TARGET" )
{
imget(image=image,param="DETECTOR", value="")
detector= imgets.value

imget(image=image,param="CAT-NAME", value="")
cat= imgets.value
# if image is a test image the loop is broken and started # again with the next image
if (cat == "TEST")
{next}

imget(image=image,param="DATE-OBS", value="")

```



```

date= imgets.value
imget(image=image,param="CCDSPEED", value="")
speed= imgets.value
imget(image=image,param="CCDNAME", value="")
chipname= imgets.value
imget(image=image,param="CCDTEMP", value="")
T= real(imgets.value)
imget(image=image,param="UTSTART", value="")
time1= real(imgets.value)
imget(image=image,param="BIASSEC", value="")
bias= imgets.value
# if the image has no biasregion the loop is broken and started # again with the next image
if (bias=="[0:0,0:0]") {next

if (time1>12)
{
time1=time1-24
}

#calculates the precise time in days
time=datum+time1/24
output_temp1= "/home/rh/scriptie/biaslevel/2month_check/"//detector/"_"//chipname/"_"//speed

coordinb1=image//bias
instatistics (coordinb1,field="mean,stddev", lower=INDEF, upper=INDEF,format=no) |scan(mnb1,stddevb1)

totmean=totmean+mnb1
Ttot=Ttot+T

#prints information to the screen for the user to check
print ("With detector : ",detector,"-", n)
print ("on time: ",time)
print ("the biasvalue was: ",mnb1)
print("#","time"," ","mean"," ","error"," ","temp"," ","image",>>output_temp1)
print(time," ",mnb1," ",stddevb1," ",T," ",image,>>output_temp1)

}
}
}
}

print("=====")
print ("")
print (" Thank you for using this script, ")
print (" have a nice day")
print ("")
print ("=====")

end

```

## B.8 IRAF script to measure the quantum efficiency of the auto guider of the wide field camera.

```

#procedure to measure the holdtime of the pt coating and QE of the WFC autoguider
#original designed for the WFC INT
#author: Richard Hijmering
#06-02-2002

```

```

procedure qeag(filea,days)

#####
# printing info for the user to the screen
#print ("#####")
#print ("Make shure the textfile is made in the following format:")
#print ("filter image_autoguider image_science_chip")
#print ("U image image")
#print ("B image image")
#print ("V image image")
#print ("#####")

#####
# setting variables
string      filea      {prompt="file_name"}
real        days      {prompt="day of february"}
string      *list1

#####
begin

string      file_name,image_ag,image_science,img1,img2
string      coordin_ag,coordin_agb,coordin_science,coordin_scienceb
string      filter,fltrQE_AG_V,QE_AG_B,QE_AG_U,output_U
string      output_B,output_V
real        mn_ag1,stddev_ag1,mn_agb,stddev_agb
real        mn_science1,stddev_science1,mn_scienceb,stddev_scienceb
real        mn_ag,mn_science,QE_ag,day,QE_U_ag,QE_B_ag,QE_V_ag
real        gain_ag,A_science,exp_science,A_ag,exp_ag,gain_science
real        QE_science

file_name=filea
day=days
#####
# declaring the outputfiles
output_U="/home/rh/scriptie/WFCcontrol/QE_AG_U"
output_B="/home/rh/scriptie/WFCcontrol/QE_AG_B"
output_V="/home/rh/scriptie/WFCcontrol/QE_AG_V"
gain_ag=1.08
A_science=13.5
exp_science=5
A_ag=15
exp_ag=5.31
gain_science=2.8

#####
# beginning a while loop to run through the images
list1=file_name
while(fscan (list1,filter,img1,img2) !=EOF)
{
  fltr=filter
  #####
  # setting the parameter with each filter
  if (fltr=="U")
  {
    QE_science=53
  }
  if (fltr=="B")
  {

```

```

        QE_science=81
    }
    if (fltr=="V")
    {
        QE_science=81
    }

#####
# setting right coördinates
image_ag=img1
image_science=img2

coordin_ag=image_ag/"{260:300,80:140}"
coordin_agb=image_ag/"{5:12,10:290}"
coordin_science=image_science/"{1}{970:1500,3500:4000}"
coordin_scienceb=image_science/"{1}{10:40,10:3900}"

#####
# measuring the signals
imstatistics (coordin_ag,field="mean,stddev", lower=INDEF, upper=INDEF,format=no) |
scan(mn_ag1,stddev_ag1)
imstatistics (coordin_agb,field="mean,stddev", lower=INDEF, upper=INDEF,format=no) |
scan(mn_agb,stddev_agb)
imstatistics (coordin_science,field="mean,stddev", lower=INDEF, upper=INDEF,format=no) |
scan(mn_science1,stddev_science1)
imstatistics (coordin_scienceb,field="mean,stddev", lower=INDEF, upper=INDEF,format=no) |
scan(mn_scienceb,stddev_scienceb)

#####
# subtracting the biaslevels
mn_ag=mn_ag1-mn_agb
mn_science=mn_science1-mn_scienceb

#####
# calculating the QE
QE_ag=QE_science*mn_ag*gain_ag*A_science*exp_science/(A_ag*exp_ag*mn_science*gain_science)

#####
# setting the right QE-value to the right filter variable
if (fltr=="U")
{
    QE_U_ag=QE_ag
}
if (fltr=="B")
{
    QE_B_ag=QE_ag
}
if (fltr=="V")
{
    QE_V_ag=QE_ag
}
}

#####
# printing QE-values tot he screen and to the files
print ""
print ("QE of the autoguider at 360 nm = ", QE_U_ag)
print(day," ",QE_U_ag," ",10",>>output_U)
print ("QE of the autoguider at 430 nm = ", QE_B_ag)

```

```

print(day," ",QE_B_ag," ", "10",>>>output_B)
print ("QE of the autoguider at 542 nm = ", QE_V_ag)
print(day," ",QE_V_ag," ", "10",>>>output_V)
print ""
#####
# printing information about the files to the screen for the user
print "The outputs are written in:"
print (output_U)
print (output_B)
print (output_V)
print ""

#####
# thanking the user
print ("=====")
print (" thank you for using this script,")
print (" have a nice day.")
print ("=====")

#####
# opening the files for public use
!chmod 777 /home/rh/scriptie/WFCcontrol/QE_AG_U
!chmod 777 /home/rh/scriptie/WFCcontrol/QE_AG_B
!chmod 777 /home/rh/scriptie/WFCcontrol/QE_AG_V

end

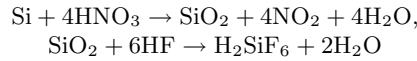
```

# Appendix C

## Autoguider coating

### C.1 Thinning process

[WFCauto] The autoguider chip of the wide field camera on the Isaac Newton Telescope is a frametransfer back side illuminated CCD chip. Since it is a back side illuminated chip it had to undergo certain processing to remove the substrate from the silicon chip. This process is called thinning. The wafers are first *backlapped* to remove some of the substrate. This can be done mechanically or chemically. After this proces an acid etch using a mixture of corrosive acids is employed. The mostly used mixtures are, nitric acid ( $\text{HNO}_3$ ), hydrolfluoric acid (HF) and acetic acid ( $\text{CH}_3\text{COOH}$ ). The reaction at the surface is an oxidation reduction reaction followed by the dissolution of the silicon dioxide formed according to the chemical equations:



When the etching process reaches the epitaxial layer it is slowed down drastically by a factor of roughly 100. The reason is that the oxydation rate and consumption is much greater for silicon than it is for highly doped material. Therefore the epitaxial interface is used as an etch stop.

After this thinning process a native  $\text{SiO}_2$  layer grows on the backside of the chip. This growth goes on for several months and reaches a thickness of approximately 25 Angström when it essentially stops. The properties of this oxide layer are disastrous for the quantum efficiency of the detector. The Si-SiO<sub>2</sub> interface has surface states that range in density from  $10^{11}$  to  $10^{13}$  /cm<sup>2</sup> depending on the growth. Some of these states are neutral when filled with an electron and positively charged when empty. This produces a positive electric field that forms a potential well near the Si-SiO<sub>2</sub> interface. This electric field is in the direction to attract the produced signal electrons into the backside well (see fig. (C.1)). The field attracts especially the photons in the blue region of the spectrum because these generate photo-electrons closest to the interface. This effect will lower the quantum efficiency in the blue region of the spectrum drastically.

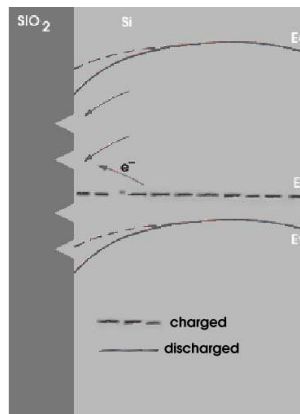


Figure C.1: Backside well induced by positive charge at the Si-SiO<sub>2</sub> interface.

The signal charge produced during an exposure will neutralize some of this positive field and so cause the quantum efficiency to rise again. During the readout the trapped electrons will recombine causing the field to rise and the quantum efficiency to lower again. This character is called the quantum efficiency-hysteresis.

This effect is also not temperature independent: it is more noticeable at low operating temperatures than at high ones. As said before the quantum efficiency hysteresis is caused by charging and discharging of states. These states have a vast range of emission time constants. These time constants for the traps can be much longer at lower temperatures. They can even be longer than the readout time of the detector producing a stable quantum efficiency performance. Effectively the traps remain filled during several exposures.

There are several remedies against this effect. The general purpose of these are to generate a negative field on the backside surface to counteract the positive field and repel the electrons to the gates. In this paper only one will be discussed. This is the one which is used mostly and is also used at the autoguider of the Isaac Newton Telescope Wide Field Camera. For further information please see [Jane]

**Chemosorption charging** [Jane] For this method the negative field is charged by dissociation of oxygen or other gases promoted by a catalyst action of the metal film. With oxygen the molecules form  $O^-$  ions that are chemisorbed to the film. This creates a negatively charged layer. The lifetime of the  $O^-$  ions is many years at room temperature, producing a permanent backside charging mechanism. The strong bond between the ions and the metal film accounts for the mechanism's immunity to environmental effects.

With the autoguider from the Wide Field Camera this method is used with a procedure *Passivated Platinum Film*. With this method oxygen ions are placed on the surface with a platinum layer on the backside of the CCD as a catalyst. The platinum layer provides no significant absorption because of the small thickness of the layer. This method introduces a very stable and uniform backside charging and hence a very stable and uniform quantum efficiency. Because hydrogen also reacts with platinum, this causes a weakness in the layer. After the coating has been exposed to  $H_2$  it might need recharging. Also exposing to water vapor can discharge the chip. The chip can then be easily restored by blowing pure oxygen or even dry air over the chip.

## C.2 References

- [WFCauto] [http://www.ing.iac.es/~eng/detectors/intwfc\\_ag/int\\_wfc\\_auto.htm](http://www.ing.iac.es/~eng/detectors/intwfc_ag/int_wfc_auto.htm)
- [Jane] Scientific Charge-Coupled Devices, by James R. Janesick

## Appendix D

# Temperature circuitry

### D.1 Wire diagram of the temperature measurement circuitry

#### D.1.1 Temperature electronics inside the detector

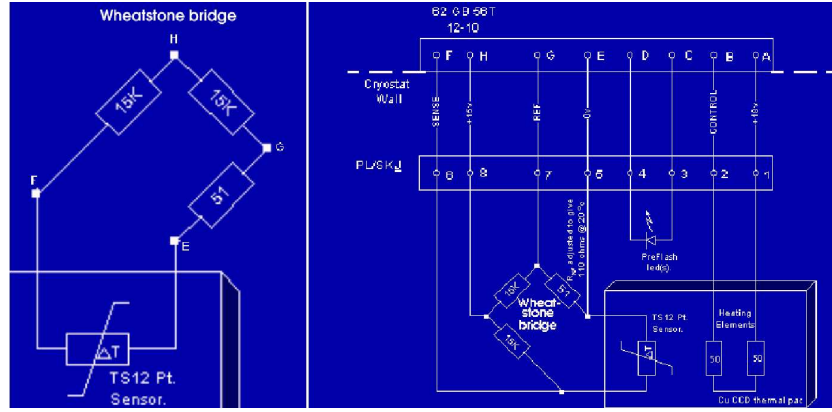


Figure D.1: Temperature measurement circuitry inside the cryostat.

[temp] In fig. (D.1) the circuitry inside the detector is shown. The letter designation shown in this blueprint is the same as which is used in the connections from the detector to the controller.

The Wheatstone bridge surrounding the Pt resistor is there to give a first order noise filter. The points H and E have a voltage of +15 V and 0 V. The resistance between F and G is measured. Because the top part of the bridge has large resistors in comparison with the resistance of the bottom these will be measured. This is the Pt and a 51  $\Omega$  is series from which the resistance of the Pt resistor can be calculated easily by normal subtraction. If there is noise in the signal between points H and E the voltage on points F and G will fluctuate with that noise in the same manner so the voltage difference between the two measured points will remain the same.

#### D.1.2 Temperature electronics inside the controller

Inside the controller the signal is amplified by the circuitry shown in appendix (D.1.2). It is a circuitry containing a non-inverting amplifier with a gain of 47. This gain is controlled by the resistors  $R_1$  and  $R_2$  according to equation (D.1) [Horo].

$$\frac{V_{out}}{R_2} = -\frac{V_{in}}{R_1} \quad (D.1)$$

In this equation,  $V_{in}$  equals the voltage difference between the two inputs (connections F and G). This gives a gain of (see equation (D.2)).

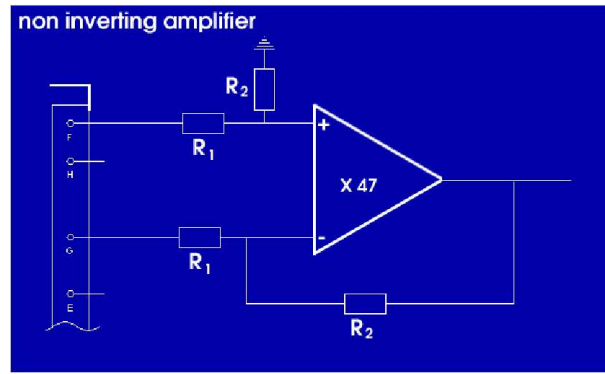


Figure D.2: Temperature measurement circuitry inside the controller.

$$Gain = \frac{V_{out}}{V_{in}} = -\frac{R_2}{R_1} \quad (D.2)$$

So the value of the two resistors are chosen to follow the rule  $\frac{R_2}{R_1} = 47$ .